NASA TN D-107

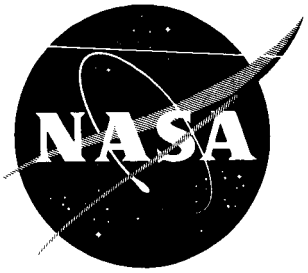

TECHNICAL NOTE
D-107

STUDIES OF SECOND- AND THIRD-ORDER CONTACTOR CONTROL SYSTEMS

By Irmgard Flügge-Lotz and Herbert E. Lindberg

Stanford University

NATIONAL AERONAUTICS AND SPACE ADMINISTRATION

WASHINGTON

October 1959

TABLE OF CONTENTS

NATIONAL AERONAUTICS AND SPACE ADMINISTRATION

TECHNICAL NOTE D-107

STUDIES OF SECOND- AND THIRD-ORDER CONTACTOR CONTROL SYSTEMS

By Irmgard Flügge-Lotz and Herbert E. Lindberg

SUMMARY

The majority of this paper is devoted to the study of the response of second- and third-order contactor systems with linear switching, that is, switching according to the sign of a linear combination of the error and its derivatives. The example chosen for the third-order system is a simplified equation of the pitching motion of a missile whose control surface takes on only two positions, full up or full down. The performance of these systems during chatter operation and during their response to step inputs is studied in great detail.

The results show that for certain rather wide ranges of combinations of natural damping of the controlled process and step input amplitude, there is very little difference between optimum and linear switching response. In order to extend the range of step inputs for which nearly optimum response can be obtained without using a complicated optimum switching function, a quasi-optimum switching function is suggested which requires only a two-dimensional function generator. Experiments showed that the response with this switching function was very nearly optimum for a wide range of step inputs.

INTRODUCTION

A control system containing one or more on-off devices is called a relay or contactor control system. In most cases, the use of a relay in the system is much less expensive and less complicated because a relay can control large amounts of power by rather simple means. On the other hand, the output of a relay is not proportional to the input; that is, the input-output relation is not linear, and the behavior of a relay control system cannot be analyzed by a linear theory. Also, the rapid type of operation of a contactor system makes it inferior to the smooth proportional action of a linear system. In many applications, however, the sudden accelerations and high-frequency chatter

caused by the relay are not objectionable because of the filtering action of the rest of the system. In fact, in recent years a great deal of work has been done on "optimum" contactor systems which give the fastest possible response to step inputs, and in this respect the contactor system becomes superior to a linear system with the same saturation values.

Earlier work (ref. 1) reported investigation of the practical use of adding discontinuous feedback to a second-order control system. This feedback provided a means of discontinuously varying the coefficients of the differential equation of the uncontrolled process so that an ensemble of eight linear differential equations was obtained. The present paper compares such a scheme with the more conventional discontinuous control systems in which the forcing term of the differential equation is switched discontinuously. In making this comparison, the similarities of contactor systems designed by phase-plane and frequency-response methods are pointed out.

A well designed contactor system chatters during a large part of the operation because of imperfections in the switching device. Two types of error that arise during this chatter operation are studied in detail for second- and third-order systems with linear switching, that is, switching according to the sign of a linear combination of the error and its derivatives. The first type of error is the high-frequency chatter error itself. Approximate equations for this error as a function of the input and of the relay imperfections are derived for small relay-time delays or thresholds occurring separately. Analog-computer experiments, made to check these expressions under various conditions, agreed very well with the theory. The second type of error occurs at the same frequency as the input and is caused by the filtering delays encountered in forming the error derivatives used in the switching function. A simple theory is given to explain these errors and again analog-computer experiments give good agreement with this theory. In Laplace transform notation, this theory gives an equivalent linear transfer function for the system operating in the presence of relay chatter. Therefore, although most of the experiments were made with sinusoidal inputs, the resulting theory is valid for general inputs because the law of superposition holds. This approach is somewhat similar to the method of Lozier (see ref. 2), who replaced the relay with an equivalent amplifier during chatter operation. However, the equivalent transfer function given here is for a system with a different type of feedback and is essentially different from Lozier's solution in that this transfer function depends mainly on the linear switching function and its associated filters, while the differential equation of the controlled process determines only the range of inputs for which this theory applies.

The main bulk of the work above was done on systems with linear switching, which were found to give quite good response. However, a

great deal of work has been done by various people in recent years on what is called optimum contactor systems. These systems give the minimum response time for step inputs and are therefore superior to systems with linear switching. The hardware necessary to form the optimum three-dimensional switching surface (for a third-order system) is a great deal more complicated than the simple differentiation circuits required for linear switching. The obvious question is, how much is lost in performance if one chooses to use the more economical linear switching function? To give a partial answer to this question, the step response of a third-order system with two complex roots and linear switching is compared with that of the same system operating with optimum switching, using an analog-computer simulation.

This investigation was conducted at Stanford University under the sponsorship and with the financial assistance of the National Advisory Committee for Aeronautics. The authors wish to thank Dr. A. M. Peterson of the Electrical Engineering Department, Stanford University, for his continued interest and his most helpful advice on the electronic problems which were encountered during this investigation.

SYMBOLS

Some symbols have different meanings in different sections. The context of the section will give the reader the correct choice.

A	amplitude of sinusoidal input
A_K	amplitude of sinusoidal input to relay (Kochenburger)
A,B,C,A_1,B_1,C_1	constants in equations (131) and (134)
a,a_1,a_2,b_1,b_2	driving terms for second-order systems
C,C_1,C_2,C_3	integration constants
a_y	computer scale factor on controlled variable, third-order system
c	output of compensation network
D	damping factor of second-order controlled process
E	error (used in appendix A), $y - x$
e	error (used throughout the text), $x - y$

e_{max_ϵ} peak value of symmetrical chatter error due to relay threshold imperfection

e_{max_T} peak value of symmetrical chatter error due to relay time delay imperfection

e_o integration constant

e_{peak_ϵ} peak value of unsymmetrical chatter error due to relay threshold imperfection

e_{peak_T} peak value of unsymmetrical chatter error due to time delay imperfection

F argument of switching function

G_C compensation network transfer function

G_D relay describing function

G_S controlled process transfer function

h vertical distance to peak error plotted in inclined coordinates

H used to simplify expressions, $\frac{1}{2}\sum_n (T_i\omega)^2$

$i = \sqrt{-1}$

k parameter in linear switching function of a second-order system; generally, coefficient of e'

k_1, k_2 coefficients of e' and e" respectively in linear switching function of a third-order system

L distance (see fig. 9)

$m = a_1/a_2$

N, N_1, N_2 absolute values of driving terms of third-order system

$n = N_1/N_2 < 1$

$2\Delta n$ distance existing between switching lines due to a relay time delay imperfection

p operator, $\frac{d}{d\tau}$

R output of relay (Kochenburger)

r radius from origin of inclined phase-plane axes to spiral trajectory

r_0 r for $\tau = 0$

T half period of symmetrical chatter oscillations

T_1 duration of application of a_1 (second-order system) or N_1 (third-order system) per cycle of chatter

T_2 duration of application of a_2 (second-order system) or N_2 (third-order system) per cycle of chatter

T_c time delay of Padé derived circuit

T_i, T_{1i}, T_{2i} time constants of x' and x" filter circuits

$$T_{mm} = \sum_{m} T_{2i}$$

$$T_{nn} = \sum_{n} T_{1i}$$

T_R relay time delay imperfection

$T_{R_{cr}}$ critical relay time-delay imperfection

$T_{x'}, T_{y'}$ time lags of derivatives used in switching function

t real time

V_{ra} runaway velocity of third-order controlled process in computer units

v_{ra} runaway velocity of third-order controlled process in problem units

x input variable, computer units

x_o ramp input

x'_o slope of ramp input

y controlled variable in computer or dedimensionalized units

α_K constant of compensation network (Kochenburger)

$\alpha, \alpha_1, \alpha_2$ phase angle lags of filtered quantities

W 1 1 0

$\beta_m = -_1\beta \operatorname{sgn}(y'e) - {}_2\beta \operatorname{sgn}(y'e')$

$\beta, \gamma, {}_1\beta, {}_2\beta, {}_1\gamma, {}_2\gamma$ constants

$\gamma_n = -_1\gamma \operatorname{sgn}(ye) - {}_2\gamma \operatorname{sgn}(ye')$

ϵ relay threshold imperfection

ϵ_{cr} critical threshold imperfection

ζ damping ratio of third-order controlled process

η angle between switching line and e' axis using inclined coordinates

θ aircraft pitching angle, measured from level flight

λ_1, λ_2 scale factors for error phase-plane axes

μ_1 phase angle (see eq. (82))

$\nu = \sqrt{1 - D^2}$

ξ_1, ξ_2 error in distorted phase planes

ρ radius of curvature of spirals at origin, $a/\sqrt{1 - D^2}$

σ angle between inclined error phase-plane coordinates, arc cos(-D)

τ	dedimensionalized or computer time
τ_{cr}	computer time from start of interval T_1 to point of maximum chatter error, third-order system
τ	constant of compensation network (Kochenburger)
τ^*	coefficient of filtered error derivative (Kochenburger), $\left(1 - \frac{1}{\alpha_K}\right)\tau$
τ_m	τ for e_{max}
τ_s	time of travel on zero trajectory
ϕ	switching function, takes on only values ± 1
Ψ	controlled variable from reference 3
Ψ_A	Ψ for $t = 0$
ω_a	undamped natural frequency of rapid incidence adjustment made by aircraft, 1/sec
Ω	natural frequency of undamped third order controlled process, computer units
ω	radian frequency, usually of input, computer units
ω_c	breakdown frequency, computer units
ω_ϵ	frequency of chatter oscillations due to relay threshold imperfection, computer units
ω_0	scale factor in equation (C3)
ω_T	frequency of chatter oscillations due to relay time-delay imperfection, computer units
sgn( )	algebraic sign of a real quantity; sgn $f = \frac{f}{\lvert f \rvert}$
$( )', ( )'', ( )'''$	differentiation with respect to τ

$(\tilde{\ })$ filtered or delayed quantity

$\approx$ approximately equal to

CONSIDERATIONS FOR DESIGNING AND COMPARING CONTACTOR SYSTEMS

There have been a great number of papers written in recent years about different types of contactor systems, but very little has been written about the relative merits of these various systems. In this section several different nonoptimum systems developed by very different techniques will be compared in order to point out their similarities and to determine which can be classified as the best system.

W 1 1 0

Similarities of Contactor Control Systems

Phase-plane method.- One method of studying a contactor control system is to look directly at its transient response in the phase space. Consider, for example, the second-order system studied by Flügge-Lotz (ref. 3). This is a zero-seeking device whose differential equation in a dedimensionalized form is

$$\psi'' + 2D\psi' + \psi = -\operatorname{sgn}(\psi + k\psi') = \phi \tag{1}$$

Notice that, in this system, the switching function is simply minus the sign of $\psi + k\psi'$; that is, it takes on the values -1 or 1 depending on whether $\psi + k\psi'$ is plus or minus. There are systems with more complicated switching functions that give optimum response (ref. 4) but for the moment only those with linear switching functions will be considered because they are more easily realized in an actual application.

Since equation (1) describes a second-order system, the phase space becomes a phase plane as shown in figure 1(a) for $k > 0$ and in figure 1(b) for $k < 0$. If $k < 0$, the trajectories do not converge to the origin, and limit cycles of oscillatory motion as shown in figure 1(b) exist even for the ideal system. The ideal system is one in which the device performing the operation $\operatorname{sgn}(\psi + k\psi')$ has no time delays, hysteresis, or threshold imperfections. Figure 1 shows this type of operation. In all of the phase-plane drawings for this system the ψ axis is inclined to the ψ' axis by the angle $\sigma = \arccos(-D)$ as shown. Using such properly inclined axes, the authors of reference 5 show that the phase-plane trajectories become logarithmic spirals of the form

$$r = r_0 e^{-\frac{D}{\nu}\nu\tau} \tag{2}$$

where r is measured from the point $(0,\pm 1)$ depending on the sign of ϕ, $\nu\tau$ is the angle between two radii extending from $(0,\pm 1)$, and $\nu = \sqrt{1 - D^2}$.

The curve shown in figure 1(a) is a typical response to an initial error and error rate represented by point P_i (since this is a zero-seeking device, the error is identical with the controlled variable). Notice in figure 2, which is essentially an enlarged view of part of figure 1(a), that for the ideal system of the type $k > 0$ no motion is defined beyond point A. That is, only two trajectories pass through this point, namely, arc PAB for $\phi = 1$ and arc CAD for $\phi = -1$; and the only paths leading out of point A are those toward B and D. Motion cannot proceed along the path toward B because above the switching line $\psi + k\psi' = 0$ equation (1) dictates that the switching function ϕ is -1; also, motion cannot proceed along the path toward D because below the switching line $\phi = 1$. Any point such as A is called an end point and occurs when a trajectory such as arc PAB intersects the switching line twice in succession on the same side of the origin. Every path such as the one shown in figure 1(a) has an end point.

If the device which forms the switching function ϕ is allowed to have an imperfection such as a time delay, then the motion does not stay at point A but proceeds to point E. Here ϕ can change to -1 then back to 1, etc., and the motion proceeds toward the origin as shown by the solid path. The average path is along the switching line and the differential equation of this average motion is

$$\psi + k\psi' = 0 \tag{3}$$

whence

$$\psi = \psi_A e^{-\frac{1}{k}t} \tag{4}$$

Equation (4) shows that in the "end motion" ψ tends toward zero exponentially. A consideration of this motion alone would indicate that k should be chosen small and positive. However, if motion is to proceed quickly from a point such as P_i in figure 1(a) to an end point, then it is advantageous to increase k. Depending on the position of the expected P_i, a compromise selection of k can be made.

For study of response to step inputs, much of the theory developed for equation (1) can be extended to a followup system as shown in figure 3. The equation of this system is

$$y'' + 2Dy' + y = \operatorname{sgn}(e + ke') \tag{5}$$

which can be written by substituting $y = x - e$ as

$$e'' + 2De' + e = x - \operatorname{sgn}(e + ke') \tag{6}$$

for a step input where $x'' = x' = 0$. The presence of x affects the position of the foci of the phase-plane spirals indicated in figure 1(a).

Kochenburger method.- Another method of approaching nonoptimum relay systems is presented by Kochenburger (ref. 6). This technique is entirely different from the phase-plane method. The study of the phase plane gives a pictorial view of the exact transient response, whereas the method presented by Kochenburger provides an extension of the frequency-response stability criterion of Nyquist. The basic assumption is that, if a sinusoidal signal is impressed on the relay coil, the periodic square-wave output of the relay can be replaced by its first harmonic. This assumption becomes more and more acceptable as the complexity (degree of the differential equation) of the system being controlled increases (G_S in fig. 4) because of the filtering action of these components.

With this assumption the action of the relay can be expressed in terms of a "describing function" which gives the amplitude and phase shift of this harmonic in terms of the amplitude of the impressed sinusoidal input A_K and the relay characteristics. The block diagram is shown in figure 4 where G_D is the describing function and G_C is a compensation network added for obtaining good response and stability. In order to determine the compensation network, Kochenburger uses the standard frequency-response techniques that are used for linear systems with the exception that the system must be examined for each value of G_D since it is amplitude dependent. Absolute stability means, for example, that the polar plot of $1/G_C(i\omega)G_S(i\omega)$ must completely enclose the locus of $-G_D(A_K)$ rather than merely the point -1 (see fig. 5).

Kochenburger found that if $G_S = 1/(p^2 + 2Dp)$ the compensation network should be a lead network of the form $G_C = (1 + \tau p)/\left(1 + \frac{\tau}{\alpha_K} p\right)$

where α_K is made as large as possible without allowing too much noise to be transmitted. As an interesting comparison between this result and the conclusions of reference 3, consider the output c of the compensation network:

$$c = e\left(\frac{1 + \tau p}{1 + \frac{\tau}{\alpha_K} p}\right) = e\left[1 + \frac{\left(1 - \frac{1}{\alpha_K}\right)\tau p}{1 + \frac{\tau}{\alpha_K} p}\right] \tag{7}$$

In the time domain, this can be written as

$$c = e + \tau * \tilde{e}' \tag{8}$$

where $\tilde{e}'$ is the time derivative of e filtered by the network whose transfer function is $1\Big/\left(1 + \frac{\tau}{\alpha_K} p\right)$. If the system equations are reduced to a nondimensional form, the output of an ideal relay is simply

$$R = \operatorname{sgn} c = \operatorname{sgn}(e + \tau * \tilde{e}') \tag{9}$$

and Kochenburger's differential equation of the complete system is

$$y'' + 2Dy' = \operatorname{sgn}(e + \tau * \tilde{e}') \tag{10}$$

A direct comparison of this equation with equation (5) shows that what Kochenburger refers to as a "series compensation network" is referred to as a "control function" by Flügge-Lotz and coworkers. The only difference is that $\tilde{e}'$ appears in the first and e' appears in the latter. This is merely an academic difference because in any physical application of the latter work the error derivative e' must be filtered by some means. The left-hand sides of the equations differ because Flügge-Lotz and coworkers studied the more general case in which the output itself appears in the equation, that is, a system with restoring force.

If one examines other examples given by Kochenburger, an extension of this comparison can be made. For $G_S = 1\Big/p(p + 1)^2$ he found that

the lead network required for compensation must be quadratic. The network he used had a transfer function of

$$G_C = \frac{1 + ap + bp^2}{1 + dp + fp^2} \tag{11}$$

where a, b, d, and f are constants. For the required phase lead, he made d and f as small as possible, again without transmitting too much noise. In the ideal case where d and f are both zero, the compensator-relay combination gives an output of

$$R = \operatorname{sgn}(e + ae' + be'') \tag{12}$$

which is the same form of control function which Flügge-Lotz and coworkers found necessary for good performance with a differential equation of third order.

Varied-coefficient scheme.- What at first appears to be a completely different scheme for synthesizing a contactor system is presented in reference 1. The block diagram for this system is shown in figure 6. The differential equation of this system in a dedimensionalized form is

$$y'' + 2D\left(1 + \beta_m\right)y' + \left(1 + \gamma_n\right)y = x \tag{13}$$

where

$$\left.\begin{aligned} \beta_m &= -{}_1\beta \operatorname{sgn}(y'e) - {}_2\beta \operatorname{sgn}(y'e') \\ \gamma_n &= -{}_1\gamma \operatorname{sgn}(ye) - {}_2\gamma \operatorname{sgn}(ye') \end{aligned}\right\} \tag{14}$$

with ${}_1\beta$, ${}_2\beta$, ${}_1\gamma$, and ${}_2\gamma$ being constants. Notice that the coefficients of the differential equation are varied discontinuously, whereas in the two previous examples a lumped forcing constant was switched.

The switching functions for β_m and γ_n are each broken into two parts, one which changes with e and one which changes with e'. It is shown in appendix A that it is more advantageous to switch single quantities β and γ according to the following equations

$$\left.\begin{aligned} \beta_m &= -\beta \operatorname{sgn}\left[y'(e + ke')\right] \\ \gamma_n &= -\gamma \operatorname{sgn}\left[y(e + ke')\right] \end{aligned}\right\} \tag{15}$$

where β and γ are positive constants. If equations (15) are substituted into equation (13), the complete equation becomes

$$y'' + 2Dy' + y = x + \left(2D\beta|y'| + \gamma|y|\right) \operatorname{sgn}(e + ke') \tag{16}$$

Notice that this differential equation is somewhat similar to equations (5) and (10). However, in equation (16) the coefficient of the switching function is a variable whereas in equations (5) and (10) it is a constant. The input x is also present in equation (16) but it will be shown in the next section that this has the same sort of effect as the varying switching-function coefficient.

Differences in Contactor Control Systems

Although the contactor control systems previously discussed are similar, there are differences that warrant investigation. Can it be said, for example, that equation (16) will give better response to a random input than will equation (5)? To answer this, it is first necessary to write equation (16) in terms of the error e by substituting $y = x - e$:

$$e'' + 2De' + e = x'' + 2Dx' - \left(2D\beta|y'| + \gamma|y|\right) \operatorname{sgn}(e + ke') \tag{17}$$

Consider now that this system is operating in a region where input velocities and accelerations are small, or $|x'' + 2Dx'| < 2D\beta|y'| + \gamma|y|$. In fact, if this inequality is not true, the output will soon begin to diverge from the input x. This is discussed in great detail in reference 7. If the inequality does hold, then the terms governed by the switching function $\operatorname{sgn}(e + ke')$ predominate and determine the sign of the entire right-hand side of the differential equation. Under these conditions the error is soon driven to zero and it has been shown both analytically (ref. 3, p. 29) and experimentally by Lindberg (see ref. 1) that the error "chatters" about zero with a small amplitude and very high frequency relative to x or y due to relay imperfections. (Appendix B gives a detailed study of the chatter error of control

systems whose switching function is of the form used in equations (5) and (16). Reference 1 contains a study of the chatter error of equation (13) using equation (14).) Because the frequency is high and the amplitude very small, quantities such as x', x'', and y may be regarded as constants during a few error cycles, $2D\beta|y'|$ can be considered small compared with $\gamma|y|$, and the equation of motion becomes

$$\left.\begin{aligned} e'' + 2De' + e &= a_1 \quad \text{if} \quad e + ke' < 0 \\ e'' + 2De' + e &= -b_1 \quad \text{if} \quad e + ke' > 0 \end{aligned}\right\} \tag{18}$$

where a_1 and b_1 are positive constants.

Similarly, equation (5) can be transformed into

$$e'' + 2De' + e = x'' + 2Dx' + x - \operatorname{sgn}(e + ke') \tag{19}$$

Again, if the error is not to diverge, $|x'' + 2Dx' + x| < 1$ and the equation of motion becomes

$$\left.\begin{aligned} e'' + 2De' + e &= a_2 \quad \text{if} \quad e + ke' < 0 \\ e'' + 2De' + e &= -b_2 \quad \text{if} \quad e + ke' > 0 \end{aligned}\right\} \tag{20}$$

Notice that these equations are identical to equations (18), except for the values of a_1, a_2, b_1, and b_2 and perhaps the value of k. In fact, these equations would result even if the switching function were something more complicated such as $\operatorname{sgn}\left(e + k_1 e'|e'|\right)$ because the chatter response is close enough to the origin of the e,e' phase plane that any complicated switching function can be replaced by a straight line, and hence the switching function reduces to $\operatorname{sgn}(e + ke')$ (see fig. 7).

The parameters of these equations could conceivably be very different between the two systems and within each system itself at different times depending on the instantaneous values of x, y, and their derivatives. It will be shown later that the amplitudes of the chatter errors for equations (18) and (20) are approximated by

$$|e|_{max_\epsilon} = \frac{1}{2a}\left(\frac{\epsilon}{k}\right)^2 \tag{21}$$

for a relay threshold imperfection of ϵ and

$$|e|_{max_T} = \frac{aT_R^2}{2}\left(\frac{k - \frac{1}{2}T_R}{k - T_R}\right)^2 \tag{22}$$

for a relay time-delay imperfection of T_R if each occurs separately. In each of these expressions, a represents the driving-force amplitude appearing on the right-hand sides of equation (18) or (20), such as a_1 and b_1.

Equation (22) is a simplified version of the complete expression for the chatter error due to a relay time-delay imperfection which is discussed later. This simplified version is valid only when the positive and negative driving-force amplitudes are of equal magnitude (e.g., $a_1 = b_1$ in eq. (18)). All the arguments concerning equation (22) that follow here would apply equally well if the complete expression were used. Equation (21) for a threshold imperfection is complete and is valid for any value of a_1 and b_1.

In an actual system, both threshold and time-delay imperfections occur together and since a appears in the denominator of equation (21) and in the numerator of equation (22), the error amplitude tends to depend only slightly on a. The error depends a little more on k, but even this dependence is secondary to the dependence on relay characteristics because k has a strong influence in only one of the two expressions for error. It must then be concluded that during chatter response, that is, when the input is varying slowly as indicated by the inequalities that were necessary for the formulation of equations (18) and (20), the system response depends much more strongly on the relay characteristics than on the controlled-process equation, feedback, and switching function.

Design Criterion

How, then, should one compare different system equations to determine which gives the best response to an undefined input? First, recall that the errors during chatter operation are very small. As was mentioned earlier, there is a large class of applications where this type

of operation is very satisfactory, and the range of inputs for which chatter occurs might be called the "region of satisfactory response." Hence, one measure of merit for a system is that it have the largest region of satisfactory response consistent with its saturation values. From this standpoint equation (5) can be considered to be a better system than equation (16). To see this, first recall that the region of satisfactory response for equation (5) is defined by

$$|x'' + 2Dx' + x| < 1 \tag{23}$$

where the saturation value of this system is unity for the units chosen.

To find the region of satisfactory response including saturation effects for equation (16) all of the variables that are produced by the component whose saturation value is under consideration must be gathered together. For equation (16) this means the quantities that exist at point m in figure 6 where a motor or amplifier, for example, would saturate. Equation (17) is now written

$$e'' + 2De' + e = x'' + 2Dx' + x - \left[x + \left(2D\beta|y'| + \gamma|y|\right)\operatorname{sgn}(e + ke')\right] \tag{24}$$

where the terms in the brackets are the same terms as those on the right-hand side of equation (16) and are the quantities at point m. The inequality to insure chatter operation for this system is defined by

$$|x'' + 2Dx' + x| < \left|x + \left(2D\beta|y'| + \gamma|y|\right)\operatorname{sgn}(e + ke')\right| \tag{25}$$

This must necessarily give the same or (usually) a smaller region of satisfactory response than that defined by equation (23) because the right-hand side of equation (25) is a complicated expression which must be equal to or less than unity if the systems of equations (5) and (16) are to have the same saturation values. Therefore, from the standpoint of providing the widest region of satisfactory response, the system of equation (5) is superior to that of equation (16).

Nothing has been said yet about what control function would give better response to a random input. During chatter operation the choice of different control functions is equivalent to changing k. In the discussion of equations (21) and (22), however, it was seen that changing k had a secondary effect on an already small error. Thus to compare or design a control function it is necessary to examine responses to

inputs which fall in part, at least, outside the region of satisfactory response. Also, the test input must fall largely within the region of satisfactory response in order to insure that the test will not degenerate into a simple examination of saturation operation. The most easily produced inputs that satisfy these requirements are discontinuities, the simple step function being the most commonly used.

Therefore, after a system has been designed to take full benefit of its saturation values, a rational approach to designing it to follow random inputs is to arrange the system to follow a step input in spite of the fact that superposition does not hold.

W
1
1
0

APPROXIMATE EXPRESSIONS FOR RELAY CHATTER ERRORS

It was mentioned several times previously that for slowly varying inputs the error of a contactor system chatters about zero at a frequency which is very high compared with the input frequency. Two main causes for this high-frequency oscillation are relay threshold and time-delay imperfections. Exact expressions for the amplitude and frequency of these oscillations would be cumbersome to the point of being useless. Approximate expressions for small imperfections are quite simple for second- and third-order systems, however, and give a good indication of how these errors depend on the system parameters.

Second-Order Systems

Consider first the second-order systems of equations (18) and (20). For concreteness, let $b_1 = 0.8$, $a_1 = 2.1$, $b_2 = 0.2$, and $a_2 = 1.2$. The e,e' phase-plane trajectories for $e'' + 2De' + e = a$ are spirals with their focus at a. Figure 8 shows a sketch of the phase-plane meshwork for each of the chosen examples. The top two sketches in figure 8 show a good portion of the phase-plane portrait and show well the difference in curvature effected by the various values of a and b. If one confines his attention only to that portion of the phase plane very close to the origin, as shown in the bottom sketches of figure 8, the differences in curvature are not nearly so important. Experimental evidence indicates that the error and error rates are small enough that an error study could indeed be confined to the area of the phase plane close to the origin.

In fact, the radius of curvature of the trajectories near the origin is so large compared with the error resulting from a relay threshold or time delay that it becomes difficult to draw an error limit cycle to scale. Figure 9(a) is a sketch of an error limit cycle caused by a

switching-function threshold and figure 9(b), of an error cycle caused by a time delay. In both figures the angle between the switching line $e + ke' = 0$ and the e' axis is given by Flügge-Lotz (ref. 3) as

$$\eta = \arctan \frac{k\sqrt{1 - D^2}}{1 - kD} \tag{26}$$

Relay threshold imperfection.- For threshold errors the single switching line is replaced by two lines parallel to it which intersect the e axis at $\pm\epsilon$ (fig. 9(a)) where ϵ is the threshold. These lines intersect the e' axis at $\pm\frac{\epsilon}{k}$. The very small arcs of the phase-plane spirals are replaced by arcs of circles with a radius equal to the radius of curvature of the spirals at the origin, namely $\rho = a/\sqrt{1 - D^2}$. The requirement that the spirals intersect the e axis with a tangent parallel to the e' axis (i.e., where the error velocity is zero, the error must have an extremum) is very nearly satisfied if the circles are drawn with their centers on a line which is perpendicular to the e' axis and which passes through the origin. This approximation makes the arcs intersect the switching lines at the same points that the switching lines intersect the e' axis, which is consistent with the statement (ref. 3) that these two types of intersections do occur very close to one another. Because these arcs are so flat, the maximum error can be taken as $h/\cos(\sigma - 90^\circ) = h/\sqrt{1 - D^2}$. From the geometry of the construction

$$h \approx \frac{L^2}{2\rho} = \frac{L^2\sqrt{1 - D^2}}{2a} \tag{27}$$

and the maximum error due to a threshold imperfection is

$$e_{max} = \frac{1}{2a}\left(\frac{\epsilon}{k}\right)^2 \tag{28}$$

Relay time-delay imperfection.- The arguments for a time-delay error are similar except that the new switching lines are inclined at an angle $\eta - \nu T_R$ from the e' axis and the distance between them is given by Flügge-Lotz (ref. 3, p. 96) as

W
1
1
0

$$2\Delta n \approx 2aT_R \sin \eta \tag{29}$$

for a small time delay. The distance L becomes

$$L = \frac{aT_R \sin \eta}{\sin\left(\eta - \nu T_R\right)} \approx aT_R \tag{30}$$

and the error due to a time delay is

$$e_{max_T} = \frac{aT_R^2}{2} \tag{31}$$

Notice that for threshold errors a appears in the denominator while for time-delay errors it appears in the numerator. This is to be expected since the magnitude of a represents the amount of correcting force being applied discontinuously. For a threshold imperfection it is reasonable to expect that, if the correcting force is larger, the resulting error will be smaller because the high forces will hold the error close to the band of error caused by the threshold of measurement. On the other hand, if the error is caused by a time delay it would be desirable to keep the forces at a low level because they are acting through a given time in an undesired direction, and hence the error increases as the forces increase. In either case the effect is small relative to the squared time delay or threshold. Also, in an actual system both time delay and threshold occur together thus making the effect of the value of a still less important.

Alternate derivation.- Although the above derivation gives one a good graphical picture of the nature of the approximations made to find a simple expression for chatter errors, the procedure was rather lengthy and is not easily extended to higher order systems. The same results are obtained if one makes the approximations by neglecting terms in the differential equation itself. Because the chatter frequency is quite high, it is possible to neglect terms containing e and e' and retain those containing e". This reduces

$$e'' + 2De' + e = -a \operatorname{sgn}(e + ke') \tag{32}$$

to

$$e'' = -a \operatorname{sgn}(e + ke') \tag{33}$$

To see that this approximation is the same as the geometrical approximations made above, recall that the differential equation which gives circles as trajectories in the phase plane (one of the assumptions made) does not contain an e' term. Therefore, the assumption that the phase-plane trajectories are circles near the origin is equivalent to dropping the e' term. But, neglecting higher harmonics, e is related to e' by the same factor (namely, the frequency) that relates e' to e''; thus, if one is to neglect e' and retain e'', one can certainly neglect e at the same time. This, of course, yields equation (33).

By inspection of the differential equation, the chatter error for equation (33) for a threshold or time-delay imperfection is symmetrical; that is, the negative half cycle is merely the reverse of the positive half cycle as shown in figure 10(a). The initial and final conditions for the positive half cycle with a relay threshold imperfection (assuming the imperfection is also symmetrical) are

$$(e + ke')_{\tau=0} = \epsilon \tag{34a}$$

$$e(T) = -e(0) \tag{34b}$$

$$e'(T) = -e'(0) \tag{34c}$$

Also, the equation of motion for the first half cycle is

$$e = -\frac{1}{2} a\tau^2 + C_1\tau + C_2 \tag{35}$$

where C_1 and C_2 are constants of integration. Substituting equations (34) into equation (35) gives the maximum error for the positive half cycle, an expression which is identical to equation (28).

Figure 10(b) shows the actual waveform resulting from equations (34) and (35). It is interesting to notice that the switch points occur at $e = 0$, which is consistent with the way in which the switch points were drawn in the phase-plane study of figure 9. This is due to the quarter-cycle symmetry of the chatter error resulting from equation (33). That

is, the homogeneous solutions to this equation are parabolas which have a line of symmetry through their vertices. In a similar fashion it can be shown that the chatter errors for the equation

$$e'' + e = -a \operatorname{sgn}(e + ke') \tag{36}$$

also have quarter-cycle symmetry and again the switch points occur at $e = 0$. This is because the homogeneous solutions to equation (36) are sinusoids, which, of course, have a line of symmetry. The exact chatter errors for equation (32) would not have this type of symmetry, however, because the damping term $2De'$ does not allow any symmetry in the homogeneous solution.

For a symmetrical relay time-delay imperfection T_R the chatter error for equation (33) is again symmetrical as shown in the sketch given in figure 10(c). For the positive half cycle the switching function passes through zero at $T - T_R$ (indicated by a cross in the figure):

$$(e + ke')_{\tau=T-T_R} = 0 \tag{37}$$

This condition must be applied at $\tau = T - T_R$ rather than at $\tau = -T_R$ because the latter value of τ does not fall within the interval for which equation (35) applies. Equations (34b), (34c), and (35) are the same for both threshold and time-delay imperfections. Combining these with equation (37) the maximum error for a time-delay imperfection is found to be

$$e_{max_T} = \frac{1}{2} a T_R^2 \left(\frac{k - \frac{1}{2} T_R}{k - T_R} \right)^2 \tag{38}$$

Again, the actual switch points occur at $e = 0$ as shown in figure 10(d). Notice that the term in parentheses in equation (38) did not appear in equation (31). For very small values of T_R this term approaches unity so that in this case it might be neglected. This would correspond to the approximations made in equations (29) and (30). The error maximum given by equation (38) therefore is more complete and accurate than equation (31) because fewer approximations were made in deriving it.

A rough indication of the range over which these approximate expressions (based on eq. (33)) for error apply can be given if the chatter error is replaced by its first harmonic. Its frequency for a threshold imperfection is

$$\omega_\epsilon = 2\pi \frac{1}{2T} = \frac{\pi ak}{2\epsilon} \tag{39}$$

Also, for the first harmonic,

$$(e'')_{peak} = (\omega e')_{peak} = (\omega^2 e)_{peak} \tag{40}$$

Recall that the basic assumption made in deriving equations (28) and (38) was that $e'' \gg 2De' \gg e$. It might then be expected that the approximate expressions for error would be accurate to about 10 percent if

$$\frac{\pi ak}{2\epsilon} > 10(2D) = 20D \tag{41}$$

Similarly, for a time delay

$$\omega_T = \frac{\pi}{2T_R}\left(\frac{k - T_R}{k - \frac{1}{2}T_R}\right) > 20D \tag{42}$$

Solution for unequal driving terms.- In all of the preceding discussions it was implicitly assumed that the positive and negative driving forces were equal in magnitude. It is only a very special case when they are equal because the relative magnitudes of these terms are continuously changing because of terms which appear on the right-hand side of the error differential equation, such as $x'' + 2Dx' + x$ in equation (19). In the case of a threshold imperfection, equation (28) applies even if the positive and negative driving terms differ; that is, the error for each half cycle can be found by applying this equation for each value of the driving force. This procedure is valid because the initial conditions for any half cycle are merely the negative of the final conditions independent of the driving term; that is, $C_2 = 0$ and $C_1 = \epsilon/k$ in equation (35) for threshold imperfections.

For time-delay imperfections, however, this is not true because

$$C_1 = aT_R\left(\frac{k - \frac{1}{2}T_R}{k - T_R}\right)$$

and depends directly on a. In this case then, the error must be computed on the basis that it repeats itself every cycle rather than every half cycle. This can be done by setting up equations similar to equation (34) that match the end conditions at both the positive and negative switch points. However, in the third-order case this same sort of problem will come up and it will be found that a semigraphical method of finding the error is easier to apply and visualize. To acquaint the reader with this method, it is also used to solve the second-order problem (see appendix B). This method follows very closely the procedure used in finding shear, moment, slope, and deflection diagrams for simple beams. Appendix B shows that the maximum error in each interval is

$$\left.\begin{aligned} e_{peak_{T_1}} &= -\frac{1}{8}a_1T_R^2\left(\frac{1+m}{m}\right)^2\left(\frac{k - \frac{1}{2}T_R}{k - T_R}\right)^2 - \frac{a_1T_R}{2}\left(\frac{1-m}{m}\right)\left(k - \frac{1}{2}T_R\right) \\ e_{peak_{T_2}} &= \frac{1}{8}a_1T_R^2\frac{(1+m)^2}{m}\left(\frac{k - \frac{1}{2}T_R}{k - T_R}\right)^2 - \frac{a_1T_R}{2}\left(\frac{1-m}{m}\right)\left(k - \frac{1}{2}T_R\right) \end{aligned}\right\} \quad (43)$$

where $m = a_1/a_2$. For $m = 1$ these equations reduce to equation (38). Notice that in addition to an oscillatory error, represented by the first terms of equations (43), there is a bias error represented mainly by the second term. In fact, for the small values of T_R that are being considered, the bias error is larger than the oscillatory error. The value of k is usually much larger than T_R because k must be chosen large enough that the system will respond well to a good range of step inputs ($k = 0.3$ is a typical value used in the experiments). This same type of error will be found to occur even more generally in third-order systems.

It is rather curious to note that while a change in the level of the driving forces (i.e., both a_1 and a_2 are changed by the same factor) has the opposite effect on the overall chatter amplitudes for threshold and time-delay imperfections, the ratio between the positive

and negative peak errors is the same for either threshold or time-delay errors (neglecting the bias term in the time-delay case). That is,

$$\left(\frac{e_{peak_{T_1}}}{e_{peak_{T_2}}}\right)_{\text{Oscillatory part}} = -\frac{a_2}{a_1} \tag{44}$$

in either case. This observation has rather dubious meaning because the presence of the bias term seriously affects what one means by "positive" and "negative" peaks. But it does aid in picturing the motion because the level of the bias line can be observed by the change from negative to positive curvature, or vice versa, at this point. Thus in figure 11, which shows the response of equation (5) (or, more properly, eq. (45)) to an input of $x = A \sin \omega\tau$, the effect of the continuously changing m is clearly evident, and also one can picture where the bias line (which is approximately a sinusoid at the input frequency in this case) lies. This error at the input frequency is not caused entirely by the bias error discussed here and the additional error is discussed in the section "Simple Theory for Low-Frequency Errors That Occur in Presence of High-Frequency Relay Chatter."

W
1
1
0

Analog-computer simulation of relay time delay.- An analog-computer simulation was made of the second-order system given by

$$y''(\tau) + 2Dy'(\tau) + y(\tau) = a\ \operatorname{sgn}\left[e\left(\tau - T_R\right) + ke'\left(\tau - T_R\right)\right] \tag{45}$$

The circuit for this simulation is shown in figure 12. Notice that the time delay T_R was effected with the Padé type circuit discussed in reference 1. In order to take into account the inherent delay of the relay used, a study was first made of the equation

$$y''(\tau) = a\ \operatorname{sgn}\left[e\left(\tau - T_R\right) - ke'\left(\tau - T_R\right)\right] \tag{46}$$

for which the exact expression for chatter error is available. With the input x held at zero, experimental results of peak errors were found for a series of Padé circuit time delays T_c. These results were then compared with the curve of peak error versus time delay given by equation (38) and it was found that if an inherent relay delay of 0.015 second (computer time was the same as actual time for the units chosen) is

added to the Padé time delay T_c, the experimental results agree very closely with the errors given by this equation for $k = 0.5$ and 0.25.

These experiments were repeated using the more complete equation (45) with $D = 0.5$ and $x = 0$, again for $k = 0.5$ and 0.25. The results are tabulated in table I along with the error calculated using equation (38) with $T_R = T_c + 0.015$. The agreement between theory and experiment is quite good except for large values of T_R. Also, a plot of theoretical and experimental errors versus time delay in figure 13 shows that the theory diverges from the computer results in a manner predicted by equation (42). For example, at $T_R = 0.120$, equation (42) indicates that the difference between the approximate error of equation (38) and the actual error should be about 9 percent while figure 13 shows this difference to be 10 percent.

Third-Order Systems

Relay threshold imperfection.- Consider the third-order differential equation

$$y''' + 2\zeta\Omega y'' + \Omega^2 y' = N \operatorname{sgn}\left(e + k_1 e' + k_2 e''\right) \tag{47}$$

which is not reduced to the minimum number of parameters as was done in the second-order case; however, the units are carefully considered and fully discussed in appendix C. Equation (47) might be considered a simplified differential equation for the longitudinal motion of an aircraft or missile with natural frequency Ω and damping ratio ζ, where y is the missile angle with respect to some average flight path. In this case the coefficient N would represent the effect of some control surface on the motion of the missile. The position of the control surface is reversed discontinuously as dictated by the linear switching function in equation (47) which can be made into a differential equation in the error e by substituting $y = x - e$ as was done for equation (5):

$$e''' + 2\zeta\Omega e'' + \Omega^2 e' = x''' + 2\zeta\Omega x'' + \Omega^2 x' - N \operatorname{sgn}\left(e + k_1 e' + k_2 e''\right) \tag{48}$$

As was the case for second-order systems, if the error is not to diverge, $\left|x''' + 2\zeta\Omega x'' + \Omega^2 x'\right| < N$. When this inequality holds, equation (48) can be written

$$\left.\begin{aligned} e''' + 2\zeta\Omega e'' + \Omega^2 e' &= N_1 \quad \text{if} \quad e + k_1 e' + k_2 e'' < 0 \\ e''' + 2\zeta\Omega e'' + \Omega^2 e' &= -N_2 \quad \text{if} \quad e + k_1 e' + k_2 e'' > 0 \end{aligned}\right\} \tag{49}$$

where N_1 and N_2 are positive.

To find the amplitudes of the chatter errors of equation (49), first consider the very special case in which $N_1 = N_2 = N$ (i.e., x = Constant). Also, assume that the frequency of the chatter errors is much higher than the natural frequency Ω of the missile (the subsequent derivation verifies this to be a valid assumption) so that $e''' \gg 2\zeta\Omega e'' \gg \Omega^2 e'$. Equation (49) can then be approximated by

$$e''' = -N \operatorname{sgn}\left(e + k_1 e' + k_2 e''\right) \tag{50}$$

As for the second-order system, in the case where the positive and negative driving terms are of equal magnitude, the error during application of the negative term is just the negative of the error during application of the positive driving term as shown in figure 14. This is because nothing in the differential equation gives preference to either a positive or negative error. Thus one needs to consider only one-half cycle in order to determine the motion. The initial and final conditions for the half cycle for which a negative driving term is applied are

$$\left.\begin{aligned} \left(e + k_1 e' + k_2 e''\right)_{\tau=0} &= \epsilon \\ e(T) &= -e(0) \\ e'(T) &= -e'(0) \\ e''(T) &= -e''(0) \end{aligned}\right\} \tag{51}$$

The equation of motion for this interval is

$$e = -\tfrac{1}{6} N\tau^3 + \tfrac{1}{2} C_1\tau^2 + C_2\tau + C_3 \tag{52}$$

where C_1, C_2, and C_3 are constants of integration. If equations (51) are substituted into equation (52), these integration constants and T can be found. The maximum error for this half cycle is then found to be

$$|e|_{max_\epsilon} = \frac{NT^3}{24} = |C_3| \tag{53}$$

where T is to be found from

$$-\frac{T^3}{12} + k_2 T = \frac{2\epsilon}{N} \tag{54}$$

If one would like to have an explicit expression for $|e|_{max_\epsilon}$, notice that, since ϵ is very small, T as solved from equation (54) will also be very small. But if T is very small, the first term in this equation can be neglected relative to the second. Hence one can take $T \approx 2\epsilon/k_2 N$ and

$$|e|_{max_\epsilon} = \frac{1}{3N^2}\left(\frac{\epsilon}{k_2}\right)^3 \tag{55}$$

The magnitude of the discrepancy that results from neglecting the first term of equation (54) is very conveniently seen if one plots the two terms on the left-hand side against T as shown in figure 15. A value of $k_2 = 0.10$ was taken for this plot. This is a realistic value as is seen in the section "Step Response of Third-Order Contactor System With Two Complex Roots." If T is to be a solution, then the difference between these curves must be equal to $2\epsilon/N$. In the figure, this means that the height measured from the $T^3/12$ curve to the k_2T curve must be equal to $2\epsilon/N$. If one chooses to neglect the cubic term, this height is measured from the T axis instead. Inspection of the curves shows that this approximation gives very little error in T for values of $2\epsilon/N$ up to 0.02, and the error at $2\epsilon/N = 0.035$ is still not too large. It is even more interesting to notice that figure 15 shows very clearly that equation (54) has a positive root for T only for values of $2\epsilon/N$ less than a certain "critical" value. That is, since $2\epsilon/N$ is always measured from the $T^3/12$ curve to the k_2T curve, the only positive values for $2\epsilon/N$ lie in the shaded area between the origin and the intersection of the two curves. The maximum value of $2\epsilon/N$ in this area is the "critical" value. For larger values, equation (54) has no real positive root for T and no periodic motion exists. A similar situation arises for a time-delay imperfection and it was observed experimentally that for

time delays greater than some critical value the error diverged. For the threshold-imperfection case, it can easily be shown that the critical value for ϵ is

$$\epsilon_{cr} = \frac{2}{3} N k_2^{3/2} \tag{56}$$

The half period T at this critical condition is simply

$$T_{cr} = 2\sqrt{k_2} \tag{57}$$

This means that, no matter what the other parameters are, the lowest possible chatter frequency $f_{cr} = \frac{1}{2T_{cr}}$ is determined solely by the choice of k_2. This frequency is rather low; therefore, it can be applied only to equation (50) from which it was derived and not to equation (49) because the lower error derivatives are no longer negligible, although it was observed in an analog simulation that a critical time delay also exists for equation (49).

Returning to the discussion of the chatter error for small values of ϵ, figure 14(b) shows the shape of the error cycle during the interval just considered as found by actually solving equations (51) and (52). Notice that the initial values at the beginning of each half cycle, that is, C_1 and C_3 (where $C_2 = 0$) in equation (52), depend on the value of N as shown in equations (53) and (54). Hence when $N_1 \neq N_2$ one cannot use equation (55) to find the error of each half cycle separately in the same manner as was done in the second-order system with a threshold imperfection.

Without the symmetry argument that was used in the case where $N_1 = N_2$, conditions must be matched at both switch points and eight equations with eight unknowns would result, two of the equations being cubic. This is the point where the semigraphical method, presented in the second-order system with time delay, will very definitely be an aid by providing a systematic method of solving these eight equations. Again, the details are presented in appendix B and only a rough outline will be given here. In essence, the method involves finding the ratio of time intervals during application of positive and negative driving force and the constants of integration for e" and e' by imposing the

condition of periodicity on e'', e', and e, respectively. The period of the motion and the integration constant for e are then found by imposing the switching conditions

$$\left(e + k_1 e' + k_2 e''\right)_{\tau=0} = -\epsilon \tag{58}$$

and

$$\left(e + k_1 e' + k_2 e''\right)_{\tau=T_1} = \epsilon \tag{59}$$

at the beginning and end of interval T_1, respectively. Figure 16 shows a plot of e''' and the resulting error. The equation for T_1 that results from equations (58) and (59) is

$$-\frac{N_1^2}{12N_2} T_1^3 + k_2 N_1 T_1 = 2\epsilon \tag{60}$$

which, of course, is just a more general form of equation (54), and it is to be expected that the "critical threshold" consideration will apply here also. The procedure is identical to that used for equation (54) and the critical threshold is

$$\epsilon_{cr} = \frac{2}{3} \frac{N_1}{\sqrt{n}} k_2^{3/2} \tag{61}$$

where

$$n = \frac{N_1}{N_2} \qquad 0 < n < 1 \tag{62}$$

As it stands, equation (61) might lead one to believe that making the driving terms N_1 and N_2 more different, that is, making n smaller (see appendix B), has a stabilizing influence because this tends to make ϵ_{cr} larger. This is misleading because from equations (48) and (49)

$$N_1 + N_2 = 2N \tag{63}$$

so that equation (61) can be more properly expressed by

$$\epsilon_{cr} = \frac{2\sqrt{n}}{1 + n}\frac{2}{3}Nk_2^{3/2} \tag{64}$$

This form is more easily interpreted because none of the other parameters in the equation change when n changes. It shows that making n less than 1 makes ϵ_{cr} smaller and therefore does have the destabilizing effect that one might expect, but the reduction in ϵ_{cr} occurs very slowly at first. For instance, at $n = 0.49$, ϵ_{cr} is reduced from its value at $n = 1$ by a factor of only 1.40/1.49.

As in the case for $n = 1$, it is reasonable to neglect the first term in equation (60) for small values of ϵ so that an explicit expression for peak error can be obtained. With this approximation, it is shown in appendix B that the peak errors are expressed by

$$e_{peak_\epsilon} = \mp\left(\frac{1 + 2n}{3}\right)^{3/2}\left(\frac{1 + n}{2n}\right)^2\frac{1}{3N^2}\left(\frac{\epsilon}{k_2}\right)^3 - \left(\frac{1 - n^2}{6n}\right)\frac{k_1}{N}\left(\frac{\epsilon}{k_2}\right)^2 \tag{65}$$

There are several interesting features to this motion. First, both of the peak errors given by equation (65) occur in the interval of the driving term of smaller magnitude, regardless of whether it is applied as a positive or a negative term. In the derivation of this equation, N_1 was taken as the smaller driving term. As shown in figure 16, N_1 was applied as a positive term. Therefore, if one wishes to find the error in the case where the smaller N is applied as a negative term, then a negative sign must be attached to the error that is given by equation (65). Also, this equation shows that, as in the case for second-order time delays when $n \neq 1$, a bias error exists in addition to an oscillatory error. There are three distinguishing features to this bias error: (1) It takes on the sign of the driving term of larger magnitude, (2) for the small thresholds considered here, it is considerably larger than the oscillatory error, and (3) it is not equal simply to the integration constant for e as was found for a second-order system, because part of this constant is absorbed into the first or oscillatory term.

Relay time-delay imperfection.- For the special case where $N_1 = N_2$, the solution for peak errors for a time-delay imperfection follows, as for the second-order system, quite closely to the error derivation for a threshold imperfection. The maximum error is again given by equation (53) except that the half period T is now to be solved from

$$-\frac{T^3}{12} + \left(\frac{1}{2} T_R^2 - k_1 T_R + k_2\right) T = 2T_R\left(\frac{1}{6} T_R^2 - \frac{1}{2} k_1 T_R + k_2\right) \tag{66}$$

For very small values of T_R the peak error is given approximately by

$$e_{max_T} \approx \frac{1}{3} N T_R^3 \tag{67}$$

There is a critical time delay for equation (66) just as there was a critical threshold for equation (54). It is not difficult to show that the equation for this critical time delay $T_{R_{cr}}$ is

$$\frac{2}{3}\left(\frac{1}{2} T_{R_{cr}}^2 - k_1 T_{R_{cr}} + k_2\right)^{3/2} = \left(\frac{1}{6} T_{R_{cr}}^2 - \frac{1}{2} k_1 T_{R_{cr}} + k_2\right) T_{R_{cr}}$$

but finding a solution to this equation is reasonable only for specified values of k_1 and k_2, and even then a sixth-order polynomial must be solved.

For the case where $N_1 \neq N_2$ it will be assumed at the outset that a time delay can be considered as a variable threshold. This in itself is not an approximation, but it provides a means of making an approximation that greatly simplifies the error derivation. This restricts the solution to very small imperfections, but then equation (49) approximates equation (48) for only small imperfections. Denoting by F the argument of the switching function, its time derivative is

$$F' = e' + k_1 e'' + k_2 e''' \tag{68}$$

At the instant before a switch point from $-N_2$ to N_1 (just before the start of interval T_1 in fig. 16) this becomes

$$F' = \frac{N_1 T_1}{12}\left(T_1 - T_2\right) - k_1\left(\frac{1}{2} T_1 N_1\right) - k_2 N_2 \approx -k_2 N_2 \tag{69}$$

so that the equivalent threshold at this switch point is

$$\epsilon_{eq} \approx -k_2 N_2 T_R \tag{70}$$

The equivalent threshold at the other switch point is similarly approximated by this same expression with $-N_2$ being replaced by N_1 in equation (70). Using these thresholds, the equation for T_1 is

$$-\frac{N_1^2}{12N_2} T_1^3 + k_2 N_1 T_1 = k_2 N_2 T_R\left(1 + \frac{N_1}{N_2}\right) \tag{71}$$

The computation of a critical time delay using this complete cubic equation would not be too profitable because, for time delays large enough that the cubic term becomes important, none of the other approximations already made are reasonable. Neglecting the cubic term, this equation can be solved explicitly for T_1 and the peak error becomes

$$e_{peak_T} = \mp\left(\frac{1 + 2n}{3}\right)^{3/2}\left(\frac{1 + n}{2n}\right)^2 \frac{1}{3} NT_R^3 - \left(\frac{1 - n^2}{6n}\right) k_1 NT_R^2 - \left(\frac{1 - n}{1 + n}\right) k_2 NT_R \tag{72}$$

Notice that terms such as $\dfrac{k - \frac{1}{2} T_R}{k - T_R}$ that appeared in the second-order time-delay case do not appear here. These terms are absent because of the approximation made in equation (69). However, if this approximation is not made, the expression for the peak errors becomes quite lengthy, and for small values of T_R unnecessarily lengthy. If one desires to find the effect of the neglected terms for larger values of T_R, then he can go back to equation (66) for the case where $N_1 = N_2$ and no approximations are made. This will give the trend of the effect of T_R becoming large relative to k_1 and k_2 even in the case where $N_1 \neq N_2$.

Analog-computer simulation of relay time delay.- Equation (47) was set up on the computer as shown in figure 17 with the exception that the Padé time-delay circuit was inserted between the output of amplifier 19 and the relay. The first series of tests were run with $N_1 = N_2 = 40$ and the results are tabulated in table II along with the peak error predicted by equation (72). The agreement is quite poor except that a logarithmic plot of the experimental error showed that it can be expressed as a constant times the third power of the time delay. The inherent delay of the relays was again taken as 0.015 second for this comparison. These experiments were repeated using the third-order system described by equation (49) with $N_1 = N_2$ and the resulting errors were compared with the error predicted by the exact equations (53) and (66). The agreement was again poor and it was concluded that these errors were so small and depended so strongly on the time delay that considerable computer error crept in.

The bias errors for experiments where $N_1 \neq N_2$ were relatively large, however, and the agreement with equation (72) was quite satisfactory. Table III lists the experimental bias error and the bias error predicted by this equation for several values of the various parameters. Figure 18 shows an example of the bias error resulting from changing n. In running this test N_2 was changed back and forth from 10 to 40 $\left(N_1 = 40 \text{ throughout the test}\right)$ so as to reduce the effect of the computer drift.

SIMPLE THEORY FOR LOW-FREQUENCY ERRORS THAT OCCUR IN PRESENCE OF HIGH-FREQUENCY RELAY CHATTER

In the previous sections the only error mentioned is the high-frequency chatter error that exists because of relay imperfections. A closer study of the response of these contactor systems for slowly varying (slowly, that is, with respect to the chatter frequency) inputs for which chatter occurs shows that another error very different in origin and nature exists at the same time. This additional error is at the frequency of the input and can, in fact, be found by the consideration of an equivalent linear system.

Second-Order System

Error equation.- First consider the second-order system of equation (5). For a study of the low-frequency error (this is referred to as a low-frequency error because the chatter error is at a much higher frequency), assume that the relay imperfections are so small that

chatter errors become unimportant. Instead, take into account the delays that are encountered in forming the error derivative e'. Recall also that $e' = x' - y'$. If in obtaining this difference more delay is encountered in obtaining x' than y' or vice versa, it can be shown that a noticeable error will occur.

Suppose, for example, that y' is available with no appreciable delay but that filtering is necessary on x'. The analog-computer setup used (see fig. 12) gave a transfer function for $\tilde{x}'$ of the form

$$\frac{\tilde{x}'}{x} = \frac{p}{(1 + T_1 p)(1 + T_2 p) \cdot \cdot \cdot (1 + T_n p)} \qquad (73)$$

W
1
1
0

where $\tilde{x}'$ is the filtered x'. Values of n from 1 to 3 were found satisfactory, depending on the device used to provide the input x. It should be mentioned that figure 12 is a circuit used in later studies in which both x' and y' were filtered by the same amount.

The basic assumption to be made in order to find the low-frequency errors is that, since the system is chattering, the argument of the switching function is oscillating about zero and can be set equal to zero for the purpose of finding the low-frequency solution. For equation (5) this means that

$$e + k\tilde{e}' = 0 \qquad (74)$$

where

$$\tilde{e}' = \tilde{x}' - y' \qquad (75)$$

The delayed-error derivative $\tilde{e}'$ is given in equation (74) because this is the quantity that the system actually uses. Rewriting this equation in terms of the actual error e, it becomes

$$e + ke' = -k(\tilde{x}' - x') \qquad (76)$$

Considering sinusoidal inputs $x = A \sin \omega\tau$, the phase lag between $\tilde{x}'$ and x' is

$$\alpha = \sum_n \arctan(T_i \omega) \qquad (77)$$

which for small values of $T_i\omega$ (in forming x', the filter time constants T_i are made as small as possible without transmitting too much noise) is simply

$$\alpha \approx \sum_n T_i\omega \tag{78}$$

The attenuation between $\tilde{x}'$ and x' for small values of $T_i\omega$ is

$$\left|\frac{\tilde{x}'}{x'}\right| \approx 1 - \frac{1}{2}\sum_n \left(T_i\omega\right)^2 \tag{79}$$

The difference between $\tilde{x}'$ and x' is then

$$\tilde{x}' - x' = A\omega\left[1 - \frac{1}{2}\sum_n \left(T_i\omega\right)^2\right]\cos\left[\omega\tau - \sum_n \left(T_i\omega\right)\right] - A\omega\cos\omega\tau \tag{80}$$

Defining H by

$$H \equiv \frac{1}{2}\sum_n \left(T_i\omega\right)^2 \tag{81}$$

equation (80) can be written

$$\begin{aligned}\frac{\tilde{x}' - x'}{A\omega} &= (1 - H)\cos(\omega\tau - \alpha) - \cos\omega\tau \\ &= \left[(1 - H)\cos\alpha - 1\right]\cos\omega\tau + \left[(1 - H)\sin\alpha\right]\sin\omega\tau \\ &= \sqrt{(1 - H)^2 + 1 - 2(1 - H)\cos\alpha}\,\cos\left(\omega\tau - \mu_1\right) \\ &= \sqrt{1 - H}\sqrt{2(1 - \cos\alpha) + \left[H^2/(1 - H)\right]}\,\cos\left(\omega\tau - \mu_1\right)\end{aligned} \tag{82}$$

If H is small, this equation reduces to

$$\frac{\tilde{x}' - x'}{A\omega} \approx \left[1 - (H/2)\right] 2 \sin(\alpha/2)\cos\left(\omega\tau - \mu_1\right) \tag{83}$$

or

$$\tilde{x}' - x' \approx A\omega\left[1 - \frac{1}{4}\sum_n \left(T_i\omega\right)^2\right] 2 \sin\left[\sum_n \left(T_i\omega\right)/2\right] \cos\left(\omega\tau - \mu_1\right) \tag{84}$$

In fact values of $\sum_n \left(T_i\omega\right)^2$ consistent with the rest of the system are so small that the effect of attenuation between $\tilde{x}'$ and x' will be neglected. Making this approximation and noting that $\sum_n \frac{1}{2} T_i\omega$ is small, equation (84) becomes

$$\tilde{x}' - x' \approx A\omega^2 \sum_n T_i \cos\left[\omega\tau - \frac{\pi}{2} - \frac{1}{2}\sum_n \left(T_i\omega\right)\right] \tag{85}$$

Substituting equation (85) into equation (76) gives

$$e + ke' = -kA\omega^2 \sum_n T_i \cos\left[\omega\tau - \frac{\pi}{2} - \frac{1}{2}\sum_n \left(T_i\omega\right)\right] \tag{86}$$

Notice that this is merely the differential equation of a linear forced vibration problem and it can be solved very simply by a number of standard methods. The steady-state solution is

$$e = \frac{-kA\omega^2 \sum_n T_i}{\sqrt{1 + k^2\omega^2}} \cos\left[\omega\tau - \frac{\pi}{2} - \frac{1}{2}\sum_n \left(T_i\omega\right) - \theta\right] \tag{87}$$

where

$$\theta = \arctan(k\omega)$$

Computer simulation for sinusoidal inputs.- In order to check equation (87), the second-order simulation of figure 12 (without the time-delay circuit and with no y' filtering) was run using sinusoidal inputs generated in the computer. The agreement between computer results and the equation were within computer and instrumentation accuracy as shown in table IV. A typical computer response is shown in figure 19.

Third-Order System

Error equation.- An example of a third-order system, taking into account the filtering delays, can be written

$$y''' + 2\zeta\Omega y'' + \Omega^2 y' = N \operatorname{sgn}\left(e + k_1\tilde{e}' + k_2\tilde{e}''\right) \tag{88}$$

In a manner analogous to the second-order example, consider the case where y' and y'' are available directly and filtering is required on x' and x''. The analog-computer circuit of equation (88) is shown in figure 17. The broken-line y' input shown in figure 17 was used for these experiments and the filtering capacitors C_2 and C_4 across amplifiers 4 and 18 were set to zero. This circuit gives a transfer function for $\tilde{x}'$ of the form

$$\frac{\tilde{x}'}{x} = \frac{p}{\left(1 + T_{11}p\right)\left(1 + T_{12}p\right) \cdots \left(1 + T_{1n}p\right)} \tag{89}$$

Similarly, $\tilde{x}''$ is defined by

$$\frac{\tilde{x}''}{x} = \frac{p^2}{\left(1 + T_{21}p\right)\left(1 + T_{22}p\right) \cdots \left(1 + T_{2m}p\right)} \tag{90}$$

As for the second-order system, during chatter operation the argument of the switching function oscillates about zero and for very small relay imperfections

$$e + k_1\tilde{e}' + k_2\tilde{e}'' = 0 \tag{91}$$

Also, the actual error derivatives e' and e'' are related to $\tilde{e}'$ and $\tilde{e}''$ by

$$\left.\begin{aligned} \tilde{e}' &= e' + \tilde{x}' - x' \\ \tilde{e}'' &= e'' + \tilde{x}'' - x'' \end{aligned}\right\} \tag{92}$$

so that equation (91) becomes

$$e + k_1 e' + k_2 e'' = -k_1(\tilde{x}' - x') - k_2(\tilde{x}'' - x'') \tag{93}$$

The procedure for finding the terms on the right-hand side of this equation for $x = A \sin \omega\tau$ is identical to the procedure used in the second-order case so that

$$\tilde{x}' - x' \approx A\omega^2 \sum_n T_{1i} \cos\left(\omega\tau - \frac{\pi}{2} - \frac{1}{2}\sum_n T_{1i}\omega\right) \tag{94}$$

and

$$\tilde{x}'' - x'' \approx -A\omega^3 \sum_m T_{2i} \sin\left(\omega\tau - \frac{\pi}{2} - \frac{1}{2}\sum_m T_{2i}\omega\right) \tag{95}$$

If equations (94) and (95) are substituted into equation (93), the resulting differential equation is again merely a linear forced vibration problem. The resulting error is a sinusoid at the input frequency. This agrees very closely with the observations of the following experiments.

Computer simulation for sinusoidal inputs.- Experimental verification of the theory discussed in the preceding section was made using the analog-computer circuit of figure 17. The sinusoidal input was generated by solving the equation

$$x'' + \omega^2 x = 0 \tag{96}$$

on amplifiers 7, 8, and 9. This was done rather than using an external-function generator in order to reduce the noise on x and its derivatives. Generating these sine waves in the computer gave the additional advantage that x' and x'' were available as outputs of integrators. This allowed the effect of x' and x'' filtering delays to be studied separately because these integrator outputs could be used directly with no filtering. (Such techniques could usually not be used in an actual system, of course, because input derivatives are not always directly available.)

The first experiments were made using integrator outputs for both x' and x'' with no delays and the results are shown in figure 20(a). Notice that the error is very small but is roughly a sinusoid at the input frequency. This error is only 0.1 percent of the input amplitude and is small enough that it was attributed to computer error. Also, in this and the following experiments the chatter error was too small to be noticeable in the figures because no intentional relay delays were introduced and the inherent delay was very small.

Only x' filtering: To study the effect of x' filtering delay alone, x' was derived by actually differentiating x in amplifier 17

and filtering it as shown in figure 17. The second derivative x'' was again taken directly from an integrator.

Solving equation (93) with $\tilde{x}'' - x'' = 0$ and taking $\tilde{x}' - x'$ from equation (94), the error (neglecting chatter amplitude) is

$$e = \frac{-Ak_1\omega^2 \sum_n T_{1i}}{\sqrt{\left(1 - k_2\omega^2\right)^2 + k_1{}^2\omega^2}} \cos\left(\omega\tau - \frac{\pi}{2} - \frac{1}{2}\sum_n T_{1i}\omega - \theta\right) \qquad (97)$$

where

$$\theta = \arctan\left(\frac{k_1\omega}{1 - k_2\omega^2}\right)$$

Experiments were run using various values for A, k_1, ω, and T_{1i} and the error amplitude was measured and compared with the values given by equation (97). A typical computer response is shown in figure 20(b) and the results are tabulated in table V(a). The "normal" values of k_1 and k_2 used gave optimum response to a 20-volt step input. Notice that the agreement between theory and experimental results is very close. The widest gap of 11-percent difference occurs in run 9 with $k_2 = 0.588$ (the large 11-percent error of run 5 can be discounted because the error was so small that it was difficult to measure and was comparable to the computer error of figure 20(a)). This rather significant difference is not too surprising because a very large change (by a factor of 7.5 to 1) had to be made in k_2 in order to make an appreciable effect on the error amplitude. This means that any dependence that the error might have on k_2 other than as taken into account in equation (97) would have a good opportunity to affect the result. For example, the presence of only a very small unintentional time delay T_{2m} in the x'' circuit could account for the discrepancy of run 9, because the error with T_{2m} present depends strongly on k_2.

Only x'' filtering: Using an integrator output to obtain x' with no filtering and finding x'' by actually differentiating x twice in amplifiers 3 and 4 and filtering as shown in figure 17 with condensers C_3 and C_4 and resistors R_2 and R_3, the effect of x'' delay alone was studied.

Solving equation (93) with $\tilde{x}' - x' = 0$ and using $\tilde{x}'' - x''$ from equation (95), the theoretical error is

$$e = \frac{-Ak_2\omega^3 \sum_m T_{2i}}{\sqrt{\left(1 - k_2\omega^2\right)^2 + k_1{}^2\omega^2}} \sin\left(\omega\tau - \frac{\pi}{2} - \frac{1}{2}\sum_m T_{2i}\omega - \theta\right) \qquad (98)$$

Experimental results are again compared with the amplitudes given theoretically and the results are tabulated in table V(b). The results agree quite well.

Both x' and x'' filtering: Both x' and x'' were found by differentiation of x as indicated above, and experiments were run to find the effect of x' and x'' delays occurring simultaneously.

In this case, the theoretical error is found by substituting both equations (94) and (95) into equation (93) where the right-hand side then becomes

$$-k_1A\omega^2 \sum_n T_{1i} \cos\left(\omega\tau - \frac{\pi}{2} - \frac{1}{2}\sum_n T_{1i}\omega\right) + k_2A\omega^3 \sum_m T_{2i} \sin\left(\omega\tau - \frac{\pi}{2} - \frac{1}{2}\sum_m T_{2i}\omega\right)$$

$$= -k_1A\omega\alpha_1 \cos\left(\omega\tau - \frac{\pi}{2} - \frac{\alpha_1}{2}\right) - k_2A\omega^2\alpha_2 \cos\left(\omega\tau - \frac{\alpha_2}{2}\right) \qquad (99)$$

where $\alpha_1 = \sum_n T_{1i}\omega$ and $\alpha_2 = \sum_m T_{2i}\omega$.

Considering these two terms as vectors rotating at angular velocity ω and displaced from each other by the angle $\frac{\pi}{2} + \frac{\alpha_1}{2} - \frac{\alpha_2}{2}$, they can be added into a single vector by using the law of cosines and the magnitude of the summation vector is

$$M^2 = \left(k_1A\omega\alpha_1\right)^2 + \left(k_2A\omega^2\alpha_2\right)^2 - 2\left(k_1A\omega\alpha_1\right)\left(k_2A\omega^2\alpha_2\right)\cos\left(\frac{\pi}{2} - \frac{\alpha_1}{2} + \frac{\alpha_2}{2}\right) \qquad (100)$$

also

$$\cos\left(\frac{\pi}{2} - \frac{\alpha_1}{2} + \frac{\alpha_2}{2}\right) = \sin\left(\frac{\alpha_1}{2} - \frac{\alpha_2}{2}\right) \approx \frac{1}{2}(\alpha_1 - \alpha_2) \tag{101}$$

Using this summation vector as the forcing term on the right-hand side of equation (93), the error in this case is

$$e = \frac{A\omega\sqrt{k_1^2\alpha_1^2 + k_2^2\alpha_2^2\omega^2 + k_1k_2\omega\alpha_1\alpha_2(\alpha_2 - \alpha_1)}}{\sqrt{(1 - k_2\omega^2)^2 + k_1^2\omega^2}}\cos(\omega\tau - \mu_2) \tag{102}$$

The comparison of experimental error amplitudes with those predicted by equation (102) is given in table V(c). The results are consistent within about 6 percent.

Verification of theory for other inputs.- The analog-computer experiments of the previous paragraphs demonstrate that equation (93) is valid for sinusoidal inputs; that is, for sinusoidal inputs, at least, the nonlinear control system of equation (88) can be replaced by an equivalent linear control system as given by equation (93) during a region of chatter operation. But for a linear system, the law of superposition holds; therefore, equation (93) should be applicable to any input as long as chatter operation is maintained. A verification of this reasoning was made with the analog-computer simulation.

The inputs chosen to demonstrate superposition were two sinusoids at different frequencies and amplitudes. The experiments were conducted so that the only essential filtering delay was 0.10 unit of machine time in the x' circuit. It should be mentioned that this delay was made intentionally large so that the error would be large and easy to analyze. Figure 21(a) shows x and e for $x = 15\cos(0.446\tau)$ and figure 21(b), for $x = 1.00\cos(2.83\tau)$. As taken from these experimental results, the error amplitudes are 0.15 volt and 0.2 volt, respectively. Computation of the theoretical error for these inputs using equation (97) gave error amplitudes of 0.15 and 0.20, respectively. Figure 21(c) shows x and e for $x = 15\cos(0.446\tau) + 1.00\cos(2.83\tau)$. The resulting error is seen by inspection of the figure to be a simple superposition of the errors for the separate inputs. Notice that the error for $x = 1.00\cos(2.83\tau)$ is larger than that for $x = 15\cos(0.446\tau)$ even though the input amplitude is much smaller. This is because the error is proportional to the square of the input frequency. A similar example of superimposed inputs is shown in figures 21(d) to 21(f).

Range of inputs that give chatter response.- It is rather curious to notice that, so far in this discussion of response to slowly varying

inputs, no mention has been made about the coefficients of the differential equation of the system being controlled. The entire response during chatter operation has been determined by the coefficients in the switching-function argument and the delays required to measure input and output derivatives. At this point the nature of the differential equation being controlled is important and will be used to determine the range of inputs for which chatter operation is insured. For the case where the input is a simple sinusoid, the limit at which chatter operation ceases will be called the "breakdown frequency." Frequencies below this breakdown frequency are what have been referred to as slowly varying inputs. This frequency depends on the amplitude of the sinusoidal input and on the coefficients of the differential equation of the system being controlled, and only very slightly on the coefficients of the switching function.

Before going into the procedure for predicting the breakdown frequency, some mention should be made about operation around this frequency. When the breakdown frequency is reached, the system truly breaks down in that the error amplitude suddenly becomes very large; it becomes larger than the input amplitude. When operating just below the breakdown frequency, only a small disturbance is required to make the system break down. Because of this, care had to be taken to insure that $e = e' = e'' = 0$ at the start of each computer run. At lower frequencies it was not necessary to make the initial error and its derivatives zero because the system would "pull in" to chatter operation quite easily. Near the breakdown frequency the system pulls in more quickly if k_1 and k_2 are increased, but chatter operation continues if k_1 and k_2 are then decreased, except for a very narrow range of frequencies near breakdown. It should be at least mentioned here that depending on the magnitude of the initial error and the values of k_1 and k_2, the system may never pull in, even if the input frequency is zero. Such possibilities are treated in chapter 5 of reference 3 where chatter response is referred to as "after end point motion." This type of consideration is also discussed later in the present report.

It is also interesting to notice that right up to breakdown, the expressions developed to predict the error amplitudes give quite good correlation with experimental results (see fig. 22).

The explanation of breakdown is, of course, that with a finite value of N the system can reproduce only a finite frequency band before saturation occurs. This saturation is best seen if figure 23 is developed as follows:

The differential equation is

$$y''' + 2\zeta\Omega y'' + \Omega^2 y' = -\phi(e,e',e'')N \tag{103}$$

where $\phi(e,e',e'')$ is the switching function (in the previous examples $\phi = -\text{sgn}(e + k_1 e' + k_2 e'')$). A general switching function ϕ is specified here because what follows applies for any function ϕ. Integrating equation (103) once gives

$$y'' + 2\zeta\Omega y' + \Omega^2 y = -\phi(e,e',e'')N\tau + C \tag{104}$$

W
1
1
0

The purpose of the control function is to drive the process in such a way that $e = e' = e'' = 0$; that is, so that $y = x$, $y' = x'$, and $y'' = x''$. In particular, it is desired that

$$y'' + 2\zeta\Omega y' + \Omega^2 y = x'' + 2\zeta\Omega x' + \Omega^2 x \tag{105}$$

This particular expression is chosen for comparison because the left-hand side is given by equation (104) and the right-hand side can be computed for a given input. For a simple sinusoidal input of the form $x = A \sin \omega\tau$ the right-hand side, indicated by q_2 in figure 23, becomes a sinusoid at the input frequency as shown in the figure. The saw-tooth-type function in this figure is the left-hand side of equation (105) as given by equation (104) (designated q_1 in the figure). It is built up of a series of straight lines of slopes $\pm N$ and must be continuous because each term on the left-hand side of equation (104) must be continuous.

During chatter operation the system has the power capacity to make $e = e' = e'' = 0$ because it does chatter. A more convenient way of looking at this is to state that during chatter operation the system is capable of making $q_1 \approx q_2$ in figure 23; but, by inspection, this is possible only when the slope of q_1 is greater than the maximum slope of q_2. That is, the limit of chatter operation is defined by

$$N > \left| x''' + 2\zeta\Omega x'' + \Omega^2 x' \right|_{max} \tag{106}$$

Notice that equation (106) is identical to the inequality found in discussing equation (47) in the section "Relay threshold imperfection" of third-order systems. For $x = A \sin \omega\tau$ equation (106) becomes

$$N > A\sqrt{\left(\omega^3 - \omega\Omega^2\right)^2 - 4\zeta^4\Omega^2\omega^4} \tag{107}$$

In the limit where equation (107) is an equality, it can be solved for ω_c, the breakdown frequency. This was done for various values of the

equation parameters and the results compared favorably with experiments as shown in table VI. Notice that, in all cases, the experimental breakdown frequency is greater than the theoretical breakdown. This occurs because experimental breakdown was defined by the chatter completely ceasing, the error becoming extremely large, and only two switchings occurring per input cycle. At frequencies slightly below this the error was reasonably small (as approximately given by equations (97) and (98)) and breakdown was not thought to have occurred even though chatter operation occurred for only part of each input cycle. Such operation is beyond the frequency limit given by equation (107), but it is very difficult to observe experimentally at just what point "partial chatter" begins. One could preassign some arbitrary time between switchings such that when this time interval is exceeded complete chatter operation is said to have stopped, but this would be cumbersome and would not give the same physical significance as complete breakdown, which is, after all, what is being investigated. This also explains why the theoretical error agrees quite well with experiment only until the theoretical breakdown frequency is reached (see fig. 22).

W 1 1 0

Reduction of Errors Due to Filter Lags for Both Second- and Third-Order Systems

It was mentioned earlier that the reason for the errors discussed here is that the lags encountered in finding x' and x'' are not the same as those encountered in finding y' and y''. The validity of this statement can be seen by investigating the lags in x' and y', for example. Consistent with the notation already used, let $\tilde{x}'$, $\tilde{y}'$, and $\tilde{e}'$ be the actual delayed terms which are available for use in some switching function. Then by definition

$$\tilde{e}' = \tilde{x}' - \tilde{y}' \tag{108}$$

$$= x'\left(t - T_{x'}\right) - y'\left(t - T_{y'}\right) \tag{109}$$

Further manipulation of this expression yields

$$\tilde{e}' = x'\left(t - T_{y'}\right) - x'\left(t - T_{y'}\right) + x'\left(t - T_{x'}\right) - y'\left(t - T_{y'}\right)$$

or

$$\tilde{e}' = e'\left(t - T_{y'}\right) - x'\left(t - T_{y'}\right) + x'\left(t - T_{x'}\right) \tag{110}$$

which for $T_{y'} = 0$ reduces to the first of equations (92).

Substituting equation (110) into equation (91) and assuming for the moment that $\tilde{e}'' = e''$

$$e(t) + k_1 e'\left(t - T_{y'}\right) + k_2 e''(t) = k_1 x'\left(t - T_{y'}\right) - k_1 x'\left(t - T_{x'}\right) \qquad (111)$$

or

$$e(t) + k_1 e'(t) + k_2 e''(t) = k_1\left[x'\left(t - T_{y'}\right) - x'\left(t - T_{x'}\right)\right] + k_1\left[e'(t) - e'\left(t - T_{y'}\right)\right] \qquad (112)$$

But even in the case when undesirable errors do occur they are always quite small as compared with the amplitude of the input and the second term on the right-hand side of equation (112) can be neglected as compared with the first term. (Although e' and e'' due to chatter oscillation may become larger than x' and x'' because the chatter frequency is very high, the values of e' and e'' averaged over several chatter cycles are much smaller than those of x' and x'', respectively. It is this "average" error that is being considered here.) If this is done, it can be seen by inspection that the magnitude of the driving term in equation (112) depends very strongly on the difference between $T_{y'}$ and $T_{x'}$ and disappears if $T_{x'} = T_{y'}$. In this case it is necessary to reconsider the second term on the right-hand side, but this would still give a very small error as compared with the errors when $T_{y'} \neq T_{x'}$.

An identical argument can be used to demonstrate how different lag times for $\tilde{x}''$ and $\tilde{y}''$ affect the error in the same way.

In many cases some of these delay times can be adjusted to be very nearly equal so as to minimize the error. In the analog-computer setup this involved forming $x' - y'$ and then filtering the difference rather than filtering just the noisy x'. This gave the same delay on both x' and y' and reduced the error considerably. For a third-order system this procedure can only be used to a very small extent in the e'' circuit because y'', the highest derivative in the switching function, is fluctuating to a considerable amplitude at the chatter frequency. This means that any delay on y'' acts to a large extent as a relay delay. The first derivative of the output y' also oscillates at the chatter frequency, but the amplitude of this oscillation is much smaller than the y'' chatter oscillation (see fig. 24 noting that $y_{chatter} = -e_{chatter}$). In general, the delay on the highest derivative output feedback should be delayed as little as possible (the $(n - 1)$st derivative for an nth-order system) while the other derivatives should be delayed by as close to the same amount as the corresponding input derivative as possible. It was noticed that, for the third-order system simulated here, the errors caused by x'' filtering

lags were quite small because the value of k_2 that gave good response to step inputs was small ($k_2 = 0.10$) and ω^3 was usually small and never very large before breakdown occurred.

Third-Order Theory in Laplace Notation

The equivalent linear system of equation (93) can easily be put into Laplace transform notation, which for many engineers is a more useful form. Equation (93) is then written

$$e\left(1 + k_1 p + k_2 p^2\right) = -k_1 p x\left(\frac{1}{1 + T_{nn}p} - 1\right) - k_2 p^2 x\left(\frac{1}{1 + T_{mm}p} - 1\right) \quad (113)$$

for the case where x' and x'' are given by equations (89) and (90) with the approximation

$$\frac{p}{\left(1 + T_{11}p\right)\left(1 + T_{12}p\right) \cdots \left(1 + T_{1n}p\right)} \approx \frac{p}{\left(1 + T_{nn}p\right)} \quad (114)$$

where

$$T_{nn} = \sum_{n} T_{1i} \quad (115)$$

and similarly for T_{mm}. This approximation will not give exactly the same results as the previous approximations but very nearly the same results for small values of T_{1i} and T_{2i}.

Simplifying equation (113), it becomes

$$e\left(1 + k_1 p + k_2 p^2\right) = x\left(\frac{k_1 T_{nn} p^2}{1 + T_{nn}p} + \frac{k_2 T_{mm} p^3}{1 + T_{mm}p}\right) \quad (116)$$

For the case where $T_{mm} = 0$ (only x' filtering), the closed-loop transfer function of the equivalent linear system is

$$\frac{y}{x} = \frac{\left(1 + T_{nn}p\right)\left(1 + k_1 p + k_2 p^2\right) - k_1 T_{nn} p^2}{\left(1 + T_{nn}p\right)\left(1 + k_1 p + k_2 p^2\right)} \quad (117)$$

For the case where $T_{nn} = 0$ (only x" filtering), the closed-loop transfer function of the equivalent linear system is

$$\frac{y}{x} = \frac{\left(1 + T_{mm}p\right)\left(1 + k_1p + k_2p^2\right) - k_2T_{mm}p^3}{\left(1 + T_{mm}p\right)\left(1 + k_1p + k_2p^2\right)} \tag{118}$$

STEP RESPONSE OF THIRD-ORDER CONTACTOR SYSTEM WITH TWO COMPLEX ROOTS

In the section entitled "Considerations for Designing and Comparing Contactor Systems" it was shown that contactor systems which at first might appear to be quite different are actually quite similar. It was also shown that a large part of the response of a contactor system is chatter response in which the driving term rapidly changes sign at a frequency determined by the imperfection of the relay or similar nonlinear device. The period and amplitude of these chatter errors were then determined in considerable detail and a further consideration of chatter response, but from the standpoint of finding the errors that result from filtering delays rather than from relay imperfections, followed in the next sections. A more complete study of the response of a contactor system must include response in which chatter does not occur. Unless specific information is available as to the nature of the expected input, discontinuities of the error and its derivatives are the most satisfactory choices of situations for which the response is not entirely chatter response. That is, if a system gives a chatter response with small error and is able to recover from input or error discontinuities quickly, then, within its saturation limitation, it will respond very well to a random input.

Optimum Response

In recent years there has been a great deal of work done on the response of contactor systems to step inputs. Most of this work is centered around the study of optimum response, which has been defined as the response that reduces the error and its derivatives to zero in the minimum time after a step command. A more complete definition of optimum response can be given in terms of the error phase space.

For a system described by an nth-order differential equation, the coordinates of this error phase space are the error and its derivatives up to the (n - 1)st. The information given by the coordinates of any point in this phase space is sufficient to define completely the state

or phase of the error motion. As the motion of a system proceeds in time, the error-state point traces out a path in the phase space. For any given system, this path or trajectory is defined by the system differential equation. The phase space is completely filled with possible trajectories for each system, each trajectory depending on the initial conditions of the motion. If a system is to be optimum, it must be capable of taking the error-state point from any location in the error phase space into the origin along the system's trajectories in the minimum time, within the limitation of the system's saturation values.

Second-order example.- A simple second-order example will demonstrate the definition of the error phase space. One of the equations studied by Bushaw in reference 4 is

$$y'' = -a\phi(e,e') \tag{119}$$

where a represents the saturation value of the system and ϕ is a switching function which takes on the values 1 or -1 and is to be determined to give optimum response. Physically, this equation may be interpreted as the equation of a frictionless motor whose shaft position is y. The saturation constant a would then be the ratio of the saturation torque of the motor to the rotor inertia. The block diagram for this simple system is given in figure 25. The differential equation for the error is found by substituting $y'' = x'' - e''$ into equation (119), and for a step input, where $x'' = 0$, it is

$$e'' = a\phi(e,e') \tag{120}$$

To find the error-phase-plane trajectories, this equation can be written

$$e' \frac{de'}{de} = a\phi(e,e') \tag{121}$$

which for $\phi = 1$ or -1 (one cannot integrate over a discontinuity in ϕ, of course) can be integrated immediately to

$$e'^2 = 2a(e - e_o)\phi \tag{122}$$

where e_o is the integration constant. This equation gives two families of parabolas with their vertices on the e axis, one family concave upward for $\phi = 1$ and the other family concave downward for $\phi = -1$, as shown in figure 26. All motion must be along one or more of these parabolas.

If the shaft position is at $y = 0$ and a step input command of $x = x_o$ is suddenly applied, the corresponding initial value in the error

phase plane is at a point x_o units out from the origin along the e axis, as indicated by the point e_o. Bushaw shows that to reduce this error to zero with no overshoot (that is, to move into the origin) in the minimum time, the motion should move along the $\phi = -1$ trajectory that passes through point e_o (path $\overline{e_oQ}$) until the $\phi = 1$ trajectory that passes through the origin (arc $\overline{OS}$) is intersected. At this point, ϕ should change to 1 and the motion will proceed along this "zero trajectory" until the error is zero. Similarly, for a negative step input, ϕ should change from 1 to -1 at the zero trajectory $\overline{OV}$. The line $\overline{SOV}$ is called the optimum switching line. For any point above this line ϕ is to be taken as -1 and below it, $\phi = 1$. Thus for this example

$$\phi_{opt} = -\text{sgn}(2ae + e'|e'|) \tag{123}$$

In this example, the above procedure intuitively gives the proper optimum response. In order to move the motor shaft through an angle x_o in the minimum time with no overshoot, one simply applies full torque until half of the step is recovered and then applies full reverse torque so that the system will be at rest when the error is zero. Bushaw further shows, however, that no matter what the initial conditions are, that is, no matter at what point the motion originates in the e,e' plane, optimum response is obtained by switching according to equation (123) as one can easily see by starting at arbitrary points and following acceptable trajectories into the origin. Therefore equation (123) gives optimum response for this system also for a ramp input $x' = x'_o$ with any initial conditions.

Bushaw also discusses optimum response for the equation

$$y'' + Dy' = -a\phi(e,e') \tag{124}$$

The optimum switching line for this equation is a curve quite similar in nature to the parabolas found for equation (119). It is again formed by the two halves of the two zero trajectories of the differential equation on which motion proceeds toward the origin (see appendix D). Again, this switching line is optimum for motion originating from any point in the error phase plane, but it is not optimum for a ramp input $x' = x'_o$. This is because y' is present in the differential equation so that when the differential equation in e is formed, an x' term appears on the right-hand side, thus

$$e'' + De' = x'' + Dx' + a\phi(e,e') \tag{125}$$

This means that although $x'' = 0$ for a ramp input, a bias of Dx'_o exists on the forcing side of equation (125), thus making invalid the

considerations that were made in finding the optimum switching line assuming $x'' = x' = 0$. This difficulty could be avoided by feeding x'_o into the device that forms the switching line in such a way as to change the scale factors in the upper and lower half planes as a function of x'_o. This would provide optimum response for ramp inputs even with the Dy' term present in the system equation (see appendix D). The authors have, however, found no reports of the use of such a scheme.

Discussion of third-order system.- In the second-order examples of optimum response just given, only one switching is required to go from any point in the error phase plane into the origin unless, of course, the initial point happens to lie on a zero trajectory in which case no switching is required. If the homogeneous equation has a restoring force term, more than one switching may be required (see ref. 8, p. 155). Bogner and Kazda, in reference 9, show that for the nth-order equation

$$\frac{d^n e}{dt^n} = A\phi \tag{126}$$

The number of switchings required to return the error and its derivatives to zero in the minimum time from any point in the error phase space is $n - 1$. Therefore, for a third-order system of this type, two switchings are usually required in order to give optimum response. This holds for a more general type of third-order system also, but no proof of this statement will be given here. Another example will serve to show how these switchings occur and what sort of switching function ϕ is required to give optimum response. A simplified description of the pitching motion of a missile or aircraft is given by a third-order equation and has received a great deal of attention in recent years. In terms of analog-computer units where y is a voltage (the conversion from problem to computer units is given in appendix C) such an equation can be written

$$y''' + 2\zeta\Omega y'' + \Omega^2 y' = -\Omega^2 V_{ra}\phi \tag{127}$$

The procedure for finding the optimum switching function for a third-order system is merely an extension of that used for second-order systems. There is considerably more difficulty in the third-order case, however, because one must work in a three-dimensional error phase space rather than a phase plane, and the switching function must depend on e'' as well as on e' and e. To begin with, equation (127) must be changed into an equation for the error e by substituting $y = x - e$:

$$e''' + 2\zeta\Omega e'' + \Omega^2 e' = x''' + 2\zeta\Omega x'' + \Omega^2 x' + \Omega^2 V_{ra}\phi \tag{128}$$

To find the optimum response to a step input, one can take $x''' = x'' = x' = 0$ so that equation (128) becomes

$$e''' + 2\zeta\Omega e'' + \Omega^2 e' = \Omega^2 V_{ra}\phi \qquad (129)$$

The first step in finding the optimum switching function for such an equation is to notice that only two space curves which are a solution to equation (129) pass through the origin of the error phase space, one for $\phi = 1$ and the other for $\phi = -1$. This means that when the error-state point passes from some initial position into the origin (i.e., the error and its derivatives are reduced to zero) its last bit of motion must be along one of these zero trajectories. Therefore, the motion must be such that the path of the error-state point intersects one of these curves and furthermore, it must intersect one of the two branches that goes toward the origin. It can be proven (see ref. 10) that, in order for the response to be optimum, the system must switch when the zero trajectory is intersected.

This indicates that the last (or second for this third-order example) switch point is on the zero trajectory. Figure 27 shows two views of the zero trajectories for equation (129) with $\zeta = 0$. The broken lines are the branches of the zero trajectories that lead away from the origin for positive time and the solid lines lead toward the origin. Notice that the solid lines are symmetrical about the origin, one side being with $\phi = 1$ and the other with $\phi = -1$. For this example, the second switch point would occur on one of the solid branches. In order to find the first switch point, notice that motion between the first and second switch points must be along a trajectory which terminates on the solid zero trajectories. It is not difficult to visualize that the sum total of all the possible trajectories that terminate on the solid zero trajectories defines a surface in the error phase space, because only one trajectory that is a solution of the differential equation can pass through any given point on the zero trajectory. There is only one rather than two because the trajectory that terminates on the solid zero trajectory must have ϕ of the opposite sign of the zero trajectory, since a switching occurs at the intersection. Again, this surface is symmetrical about the origin, one half of it terminating on each branch of the solid zero trajectory. Also, in order to get off this surface (i.e., to go away from the origin in negative time), one must again follow a path with opposite ϕ, that is, return to the same sign of ϕ that the corresponding solid zero trajectory has. This means that the first switch point occurs on this "switching surface." It is not difficult to visualize that the sum total of all trajectories that terminate on this surface fills the entire phase space.

The sequence of events, then, in driving the state point from any position in the phase space into the origin is as follows: The motion proceeds with $\phi = 1$ or $\phi = -1$ (depending on which side of the

switching surface the initial point lies) until the switching surface is intersected; here ϕ changes sign and the motion proceeds along the switching surface until the solid zero trajectory is intersected; and at this point another switching occurs and the motion proceeds into the origin. No rigorous proof is given here that this sequence indeed gives optimum response. For more details see the paper by Rose, reference 10.

Bypassing this point of rigor, the next step is to find the equation of the switching surface. Returning to the example of equation (129) with $\zeta = 0$, the differential equation is

$$e''' + \Omega^2 e' = \Omega^2 V_{ra} \phi \tag{130}$$

W
1
1
0

The general solution of this equation is

$$e = A + B \cos \Omega\tau + C \sin \Omega\tau + \phi V_{ra} \tau \tag{131}$$

To find the zero trajectories, the condition to be imposed is that the state point must pass through the origin at the end of the motion which, for convenience, will be defined by $\tau = 0$, that is, $e(0) = e'(0) = e''(0) = 0$. Imposing these conditions, the parametric equations of the zero trajectories are

$$\left.\begin{aligned} e &= \phi\left(V_{ra}\tau - \frac{V_{ra}}{\Omega} \sin \Omega\tau\right) \\ e' &= \phi\left(V_{ra} - V_{ra} \cos \Omega\tau\right) \\ e'' &= \phi V_{ra} \Omega \sin \Omega\tau \end{aligned}\right\} \tag{132}$$

In order to find the initial conditions for the trajectories that intersect these zero trajectories, that is, for the trajectories that carry the state point from the first to the second switch point, one merely proceeds out from the origin along the zero trajectory in negative time until the second switch point is reached. If the time of travel on the zero trajectory is τ_s, then the "initial" conditions desired are found by substituting $-\tau_s$ into equations (132):

$$\left.\begin{aligned} e\left(-\tau_s\right) &= \phi\left(-V_{ra}\tau_s + \frac{V_{ra}}{\Omega} \sin \Omega\tau_s\right) \\ e'\left(-\tau_s\right) &= \phi\left(V_{ra} - V_{ra} \cos \Omega\tau_s\right) \\ e''\left(-\tau_s\right) &= -\phi V_{ra} \Omega \sin \Omega\tau_s \end{aligned}\right\} \tag{133}$$

To avoid confusion, only half of the switching surface will be found, the other half being symmetrical about the origin. Consider the half that terminates on the $\phi = 1$ zero trajectory. Then the general solution for the next to last trajectory is

$$e = A_1 + B_1 \cos \Omega\tau + C_1 \sin \Omega\tau - V_{ra}\tau \tag{134}$$

Using this equation with $\tau = 0$ at the second switch point (i.e., when $\tau = -\tau_s$ in eqs. (132)) the constants A_1, B_1, and C_1 are found by imposing equations (133) at $\tau = 0$. The parametric equations of the next to last trajectory are then

$$\left.\begin{aligned} e &= -V_{ra}(\tau_s + \tau) + \frac{V_{ra}}{\Omega} \sin \Omega(\tau_s - \tau) + \frac{2V_{ra}}{\Omega} \sin \Omega\tau \\ e' &= -V_{ra} - V_{ra} \cos \Omega(\tau_s - \tau) + 2V_{ra} \cos \Omega\tau \\ e'' &= -V_{ra}\Omega \sin \Omega(\tau_s - \tau) - 2V_{ra}\Omega \sin \Omega\tau \end{aligned}\right\} \tag{135}$$

with parameter τ. If one considers the entire family of such trajectories, one trajectory for each value of τ_s, the result is the optimum switching surface. Equations (135) can be considered, then, as the parametric equations of half of the optimum switching surface, with parameters τ_s and τ. As the equations are set up, τ_s takes on positive values (negative time) and τ takes on negative values (also negative time). These parameters could be eliminated to find a single equation between e, e', and e'' that would represent the optimum switching surface, but this will not be done here because the authors wish only to give the reader a visual picture of an optimum switching surface and to outline the steps involved in finding one.

The use of such a switching surface gives optimum response for equation (127) only for a step input although there is no restriction on the initial conditions; that is, the initial state point can assume any position in the error phase space. If x' and x'' were fed into the device which forms the switching surface, and operations corresponding to the scale factor changes suggested for a second-order system were made, this system could be made optimum for step inputs of velocity and acceleration as well as for step inputs of position.

Comparison of Optimum and "Linear" Switching

The problem of finding the optimum switching surface for equation (129) is not too difficult. Perhaps the most convenient way of doing it would

be to actually go through all the steps outlined above (using eq. (130) rather than eq. (129)) with the problem set up on an analog computer. Negative time could be simulated by changing the signs of the appropriate terms in the differential equation, and the resulting trajectories could be recorded. The problem of building a device which forms this complicated switching function, however, is considerably more difficult. Three-dimensional function generators are complicated and cumbersome and considerable cost would be involved in developing one small enough to be carried in an aircraft. "Linear" switching as used in equation (47) is, on the other hand, quite easy to obtain in an actual installation as can be seen by the simple circuits involved in figure 17. The obvious question is, just how much is lost in using linear switching? To answer this question, step response times for optimum and for linear switching were found using an analog-computer simulation.

Optimum response time.- Fortunately, it was not necessary to create an optimum switching surface in order to find optimum response times because linear switching gives optimum response if the switching coefficients k_1 and k_2 are set to specific values for each step. For any single optimum response, only two points on the optimum switching surface are used for switching so that all that is required for optimum response for a specific input is a surface which passes through these two points. Since linear switching gives switching on a plane through the origin of the error phase space, one merely adjusts the angle of this plane so that it passes through the two optimum switch points for each input.

The values of k_1 and k_2 that give optimum response for each step were found very quickly by trial and error. The value of e versus e' was observed on an oscilloscope and k_1 was adjusted after each computer response to a step input until after two switchings the error was reduced to very nearly zero. Then e versus e'' was observed and k_2 was adjusted until e'' was also reduced to zero after two switchings. After this, only small changes in k_1 and k_2 had to be made to insure that e, e', and e'' were all reduced to zero after two switchings. Figure 28(a) shows plots of k_1 and k_2 versus step height for $\Omega^2 = 2.79$ and $\Omega^2 V_{ra} = 47.3$ volts with ζ as a parameter. Figure 28(b) is a similar plot for $\Omega^2 = 1.35$ and $\Omega^2 V_{ra} = 23.2$ volts.

Figure 28(a) shows very clearly that k_1 and k_2 repeat after a certain step height for $\zeta = 0$. The value of the step height at which the repetition begins is equal to the voltage through which the error passes during one period of the system's natural frequency. In figure 27, of the zero trajectory for $\zeta = 0$, this corresponds to the error spanned by one loop of the trajectory spiral of $2\pi \frac{V_{ra}}{\Omega}$. The calculated value of 65.5 volts checks very well with the experimental value of 67 volts. The

reason for the repetition in k_1 and k_2 is that for step inputs larger than this value the error-state point comes in on a spiral, path a in figure 27, on which no switchings are required until the error is within the first loop of the zero trajectory. Somewhere within this loop, the error-state point comes to rest with $e' = e'' = 0$ as shown by point R. This occurs because all of the step-response experiments were made with $e''(0) = e'(0) = 0$, that is, the motion always started at rest. Motion from this point on is the same as if the motion had started at point R, hence the switching requirements are the same. Also, all the trajectories that are solutions to equation (130) with $e'(0) = e''(0) = 0$ are cycloids identical to the zero trajectories except that they are displaced in the error phase space, so that the exact repetition of k_1 and k_2 results. That no switchings are required until the error is less than $2\pi \frac{V_{ra}}{\Omega}$ follows because the differential equation is such that, providing the error starts at rest, the error velocity is always less than $2V_{ra}$, and this velocity can always be built up or reduced to zero within one loop of the spiral. The acceleration is similarly bounded.

For $\zeta \neq 0$, k_1 and k_2 do not repeat but rather damp out to constants for large inputs. This occurs because, for large inputs, the oscillatory motion damps out due to the presence of the damping and the system travels toward the origin at the runaway velocity V_{ra}. This means that no matter how large the input step was, and no matter what the initial conditions were, by the time the error-state point is close enough to the origin for switching to be required the state point comes in on the same line, namely, path b in figure 27, defined by $e' = V_{ra}$ and $e'' = 0$ for a negative step input. For a system with damping then (the damping need not be very large, as seen in fig. 28(a)) if $2\pi \frac{V_{ra}}{\Omega}$ is rather small relative to the magnitude of the expected step inputs, there is no particular advantage in using optimum switching over linear switching because optimum response results for these inputs in either case.

Figure 29 gives a plot of optimum response times versus step height, again with ζ as a parameter. These response times were found using the analog computer. A quick one-point check of the accuracy of these plots can be made by checking the response time for the case where $\zeta = 0$ to a step input of $2\pi \frac{V_{ra}}{\Omega}$ volts. For this particular situation, the response time is merely the period of the natural vibration or $2\pi/\Omega$. For figure 29(a), $2\pi/\Omega = 3.76$ seconds which checks very well with the response time of 3.75 seconds shown in the plot. For figure 29(b) the comparison is 5.40 to 5.45 seconds, respectively.

Response time with linear switching.- Figure 30 shows the response times with linear switching for the same system discussed above. Each curve of response times for linear switching in these figures is for a fixed pair of values of k_1 and k_2. The parameter shown on the curves is the step voltage for which the specific combination of k_1 and k_2 gives optimum response, hence the linear switching curves are tangent to the optimum response time curve at these values of step height. In determining the response time with linear switching, time was measured from the instant the step was imposed to the time when e and e' were zero and e'' was less than a small value. In some respects this criterion might have made the figures somewhat misleading because many times the error was very small and was approaching zero asymptotically or in an oscillatory fashion some time before e, e', and e'' all became zero. An example of this, figure 31(a), shows the response to a step input of 60 volts for linear switching optimized at a step input of 30 volts. In this response, the error was quite small a few tenths of a second before the optimum response time had elapsed, although e, e', and e'' were not all zero until about a second later, and during this second the error never did become very large.

Two combinations of k_1 and k_2, one which gave optimum response for a 15-volt step input and the other for a 30-volt step input, are shown in figure 30(a). Also shown is the curve of optimum response times for $\zeta = 0$. In general, for step inputs greater than the step for which k_1 and k_2 were optimized, the response was first oscillatory (before chatter) and then sluggish (chatter operation, as exemplified in fig. 31(a)). For inputs less than the optimized step, the response was sluggish as shown in figure 31(b). For the linear switching optimized at 30 volts, the largest difference between the response time of this system and optimum response time occurs at 60 volts for the range of inputs studied. But recall that the error in the linear switching response to a 60-volt step passed very close to zero before the optimum switching time had elapsed and it became only slightly greater before it was reduced to zero (see fig. 31(a)). Therefore, if this small undershoot is not detrimental for the system application, the large difference in response times indicated in figure 30(a) is not a good comparison.

In figure 30(b) for $\zeta = 0.3$ the difference between optimum response and response with linear switching optimized at 30 volts is so small that for many practical purposes it could be neglected.

Quasi-Optimum Response

Between optimum switching with its complicated switching surface and linear switching which is optimum for motion originating only from special points in the error phase space there would seem to be much room for a compromise switching function. For lack of a better name, such a

compromise system will be called "quasi-optimum" switching. The possible number of such schemes that can be tried has no end, but all of them are merely attempts to form a switching function which approaches the shape of the optimum switching surface without the necessity of using a three-dimensional function generator. (One significant example of what might be called quasi-optimum response is treated in detail by Schmidt and Triplett in ref. 11.)

Figure 28(a), which shows how k_1 and k_2 must vary with step height in order to obtain optimum response, gives an insight as to one possibility for a quasi-optimum switching function. Notice that the percent change in k_2 required for a given change in step height is much greater than the percent change required in k_1. This observation suggests that one might use a variable rather than constant k_2 so that the switching function takes on the form

$$\phi = -\text{sgn}\left[e + k_1 e' + k_2(e,e')e''\right] \qquad (136)$$

As it stands, this switching function is no improvement over optimum switching as far as reducing complications is concerned because a three-dimensional function generator would be required to form $k_2(e,e')$. Therefore k_2 may be made a function of either e or e', but not of both, or the purpose would be defeated.

Recall now that in the brief discussion of optimum versus linear switching it was concluded that, if the system has natural damping present, the gap between optimum and linear switching is not very wide (see fig. 30(b)). In discussing quasi-optimum switching, then, it will be most beneficial to concentrate first on the case where $\zeta = 0$. For this case, experiments were made by taking k_2 as a function of e, but not much success was obtained. Experiments with k_2 taken as a function of e' were considerably more successful. An explanation of the determination of the function $k_2(e')$ will immediately show why this function worked well while k_2 as a function of e was unsatisfactory.

In forming k_2 either as a function of e or as a function of e', the data in figure 28(a) obviously had to be modified so that k_2 could be plotted against e or e' at switching rather than against initial step height, because, once the motion is in progress, a switching function has no way of knowing what the initial conditions were. To make this modification, e and e' at the first switch point were determined for each step input with optimum response, using the computer. The desired k_2 as a function of e'_s, for example, was then plotted point by point by taking the value of k_2 for a given step input from figure 28(a) and plotting this against the e' at switching found for the same step height. The resulting function is shown in figure 32.

The values of k_2 shown in figure 28(a) give optimum response only if k_2 remains constant throughout the response. If k_2 is taken as a function of e' or e, then it will vary continuously throughout the response. If this is the case, how can the function found by the above procedure be expected to give optimum response? In the case of $k_2(e)$ as determined above, the response is indeed not optimum, but for $k_2(e')$ the response was found to be optimum or very nearly so for any step in the test range of from 0 to 60 volts. This optimum response results because of the symmetry of the optimum response trajectory for $\zeta = 0$ as shown in figure 33. The lower curve is the e,e' projection of a typical optimum-response trajectory and the upper curve is the e,e'' projection. The sharp corners in the e,e'' projection occur, of course, at the switch points. Notice that, since the e,e' projection is symmetrical about an error equal to half of the step height and the switch points are similarly symmetrical, the value of e' at both switch points is the same. Therefore, even though k_2 varies continuously throughout the motion, it always repeats itself at the switch point so that as far as the switching is concerned, k_2 might just as well have been a constant equal to the value of k_2 at the first switch point. But in the above procedure, k_2 was chosen such that at this first switch point it takes on the proper value to give optimum response if it were allowed to remain constant. The motion resulting from using this function for k_2 is not exactly optimum except for selected step values because k_1 was not made a function of e', but, since k_1 does not change much with step height, the motion was very close to optimum.

The circuit used to form the product $k_2(e')e''$ is shown in figure 34. The function $k_2(e')$ was formed with a diode function generator whose break points are indicated by crosses in figure 32. The circles are data points taken from figure 28(a). In order to utilize a wider range of the function generator, the input to it was taken as $2e'$ rather than e'. The scale factor on the output $\overline{k_2}$ of the function generator was taken as 50 volts/sec^2, that is, $\overline{k_2} = 50k_2$. Unfortunately, the multipliers available for these experiments had a considerable degree of drift and nonlinearity, but slight modifications of the function $k_2(e')$ compensated for the nonlinearity, and the drift was not serious enough to affect general conclusions about the experiments.

As was mentioned earlier, this switching scheme gave very good response for step inputs. The value of k_1 used for these experiments was an average value of $k_1 = 0.66$ which gives optimum response for a step of 30 volts. For steps different from 30 volts, the response was not optimum but very nearly so. The derivatives e' and e'' were properly reduced to zero after two switchings, but there was a small undershoot, of the order of 1/2 volt, depending on the step. This residual

error was reduced to zero in a short time by chatter operation, just as in the case of linear switching. For practical purposes then, it seems that for step inputs this switching scheme is just as effective as optimum switching.

If the motion does not originate on the e axis in the error phase space (i.e., $e'(0) = e''(0) = 0$), however, the response with this scheme is not necessarily optimum. It is usually oscillatory and sometimes even unstable. This instability was eliminated by adding a constant to the function $k_2(e')$ given in figure 32. But adding this constant made the response to motions originating on the e axis sluggish as in the example with linear switching shown in figure 31(b). That is, in this respect the present scheme is no improvement over linear switching. This result might have been expected, however, because with only one free coefficient in the switching function, namely k_2, one can hope to find nearly optimum response only for points originating on a given surface. In this case, this surface is defined by the trajectories that pass through the e axis.

If the features of the system inputs are such that the expected disturbances usually give motion that originates near the e axis, then a scheme such as this represents a reasonable answer to the problem of finding a relatively simple switching function which gives quasi-optimum response. Similarly, if the inputs have another region in the phase space where nonchatter motion is expected to originate, a different function $k_2(e')$ may be developed. Quasi-optimum response then, seems to have meaning and application mainly when some type of information about the input is available.

CONCLUSIONS

The following results and conclusions were obtained from this investigation of second- and third-order contactor control systems:

1. A detailed examination of a great variety of system configurations shows that during chatter operation, that is, when the output is varying slowly enough that there is a high-frequency hunting due to relay imperfections, the resulting error is quite small and depends much more strongly on the relay imperfections than on the system configuration. In order to make a comparison among several control solutions to a given problem, one must therefore study responses for which chatter does not occur, the step input being the most commonly used. That is, the required tolerances on the relay imperfections for a contactor system are found by studying chatter operation, and the determination of a control scheme or switching function is made on the basis of step response.

2. The chatter errors due to relay imperfections were found to have two basic components for the second- and third-order systems studied. One component is a high-frequency oscillatory error, and the other is a direct-current bias error which exists when the driving forces for positive and negative error are unequal. The ratio of these driving-force magnitudes is a function of the input. For small time-delay or threshold imperfections occurring separately, the oscillatory component of error is proportional to the square of the imperfection for a second-order system and to the cube of the imperfection for third-order systems. The bias errors depend on lower powers of the imperfections.

3. In addition to these errors that are closely associated with the relay imperfections, another error exists during chatter operation. It is caused by the filtering lags that result in forming the error derivatives used in the switching function. For sinusoidal inputs to a system with linear switching (i.e., switching according to a linear combination of the error and its derivatives) it was found to be at the input frequency and was explained by using an equivalent linear system. Applying the law of superposition to this equivalent linear system, the equivalent transfer function becomes valid for general inputs that give chatter operation. This linear transfer function depends only on the filter circuit constants and the coefficients in the linear switching function, while the coefficients of the differential equation of the controlled process determine the input limitations for which chatter occurs.

4. Most of the work mentioned above was done on systems with linear switching, which were found to give quite good response. However, a great deal of work has been done by various people in recent years on optimum contactor systems. These systems give the minimum response time for step inputs and are therefore superior to systems with linear switching for such inputs. For a second-order system, the optimum switching function is a curve in the error phase plane which is relatively easy to build into a system. For a third-order system, however, the switching function required to give optimum response determines a surface in the three-dimensional phase space and its realization would be quite expensive and cumbersome in an actual installation. To determine how much is lost by going to linear switching in order to avoid this difficulty, the step response of a third-order system with two complex roots was studied in detail with an analog-computer simulation. The results show that, for certain rather wide ranges of combinations of natural damping of the controlled process and step input amplitude, there is very little difference between optimum and linear switching response. For example, with a natural damping ratio of $\zeta = 0.3$, the maximum difference between linear and optimum switching response time over a wide range of step inputs was about 10 percent. Also, the error during this last 10-percent interval of time is very small so that, in many practical applications, there is no significant difference between linear and optimum switching response.

For the case where $\zeta = 0$, the difference between optimum and linear switching response is more significant, but in this case it is possible to form a quasi-optimum switching function which requires a function generator using one rather than two independent variables. This function gives very nearly optimum response for a wide range of step inputs but is unsatisfactory for step responses that start with large initial velocity or acceleration. It is suggested that other quasi-optimum schemes be investigated in the future which give nearly optimum response for motion not starting at rest.

W
1
1
0

Stanford University,
Stanford, Calif., December 14, 1957.

APPENDIX A

COMPARISON OF TWO SWITCHING-FUNCTION ARRANGEMENTS

Consider two control systems whose equations are

$$y'' + 2Dy' + y = 0.625 \operatorname{sgn} e + 0.375 \operatorname{sgn} e' \tag{A1}$$

and

$$y'' + 2Dy' + y = \operatorname{sgn}(e + ke') \tag{5}$$

It will be shown here that during chatter operation and in response to step inputs, equation (5) gives a response which is superior to that of equation (A1). From this, it can be concluded that it is more advantageous to switch according to equation (15) than (14). Full-saturation values are used as coefficients on the right-hand sides of equations (A1) and (5) while the driving coefficients in equations (13) and (14) or (15) depend on y and y'. It was stated in the main text that it is better to use the full-saturation quantity as the driving coefficient; therefore, it is valid to use the simpler expressions of equations (A1) and (5) for the comparison here.

The coefficients used in the right-hand side of equation (A1) are in the same ratio as those found to give good response in reference 1 by using equations (13) and (14). The coefficients' sum was set equal to unity so that equations (A1) and (5) would have the same saturation value.

Consider first the comparison of these two equations during a region of satisfactory response. For simplicity, let the input $x = 0$. Let the relay delay for each system be $T_R = 0.01$. The error limit cycle for equation (A1) can be computed using the method presented in reference 1. A plot of the resulting limit cycle is shown in figure 35. The maximum error for this limit cycle is $e = 0.0017$. With the same value of time delay, the chatter error for equation (5) is determined using equation (38) with $k = 0.3$:

$$e_{max_T} = \frac{1}{2}(1)(0.01)^2\left[\frac{0.3 - \frac{1}{2}(0.01)}{0.3 - 0.01}\right]^2 = 0.0000517 \tag{A2}$$

This error is an order of magnitude smaller than the maximum error of 0.0017 found for equation (A1) and it can be concluded that during regions of chatter or satisfactory response a system which switches a single quantity according to $\operatorname{sgn}(e + ke')$ is superior to a system that switches two quantities according to the sign of e and e' separately.

A comparison of these equations for response to discontinuities, such as a step input, shows equation (5) to be superior in this respect also. Equation (A1) is constructed so that no force reversals can occur until the error changes sign, but for equation (5) the driving force reverses at some time before the error passes through zero and hence the velocity at zero error is decreased. In fact, for one particular step amplitude the velocity will be zero when the error becomes zero and the response time will be optimum. This is the value of the step at which the phase-plane trajectory intersects the switching line at the same point at which the switching line intersects the optimum switching curve as given in reference 4. Even if the response of equation (5) is not optimum, it is faster than that given by equation (A1) because maximum torque is applied at all times while equation (A1) applies only one-quarter of the maximum torque for those quarter cycles where the absolute value of the error is decreasing. Also, torque reversals for equation (5) occur before the error passes through zero, as was mentioned above.

APPENDIX B

SEMIGRAPHICAL METHOD FOR FINDING CHATTER ERRORS

In the section "Approximate Expressions for Relay Chatter Errors" a semigraphical method was briefly described for integrating the simplified error differential equation to find the chatter errors. The reader who has not had much contact with the methods of strength of materials will perhaps appreciate the more detailed discussion of the steps involved in finding the error by this method given herein.

Second-Order Time-Delay Imperfection

The differential equations which give rise to chatter errors are

$$\left.\begin{aligned} e'' &= a_1 \quad \text{if} \quad e + ke' < 0 \\ e'' &= -a_2 \quad \text{if} \quad e + ke' > 0 \end{aligned}\right\} \tag{B1}$$

with the stipulation that the device which performs the operation $\operatorname{sgn}(e + ke')$ has a symmetrical time delay T_R. Figure 36 shows the graphical construction of the chatter error and its derivatives for this equation. In order to develop these plots, recall that the chatter errors resulting from equations (B1) are periodic and therefore e and its derivatives must repeat in each cycle. If time is measured from the start of interval T_1, the periodicity requirement on e' is

$$e'(0) = e'(T_1 + T_2) \tag{B2}$$

or

$$\int_0^{T_1+T_2} e''\, d\tau = 0 \tag{B3}$$

Graphically, equations (B2) and (B3) indicate that the periodicity requirement applied to e' is equivalent to requiring that the net area under the e'' curve should be zero. This means that $a_1T_1 = a_2T_2$. Similarly, the periodicity requirement applied to e is

$$\int_0^{T_1+T_2} e' \, d\tau = 0 \tag{B4}$$

That is, the net area under the e' curve must also be zero. In figure 36 an integration constant of $-\frac{1}{2} a_1 T_1$ must be added to e' to satisfy this condition.

The only unknowns remaining are the integration constant for e and the period of the motion. The two equations necessary to find these quantities are the switching criterion $e + ke' = 0$ to be applied at the times indicated by the broken lines in figure 36 which are T_R seconds before the actual switch points. In order to apply this condition in the first interval the error is first expressed by choosing the left side of the interval as the time origin:

$$e = \frac{1}{2} a_1 \tau^2 - \frac{1}{2} a_1 T_1 \tau + C \tag{B5}$$

$$e' = a_1 \tau - \frac{1}{2} a_1 T_1 \tag{B6}$$

The switching criterion is then

$$\left(e + ke'\right)_{\tau=T_1-T_R} = 0 \tag{B7}$$

By substituting equations (B5) and (B6) into equation (B7) one obtains

$$C + \frac{1}{2} a_1 \left(k - T_R\right) T_1 + \frac{1}{2} a_1 T_R^2 - k a_1 T_R = 0 \tag{B8}$$

Choosing the time origin at the beginning of the second interval, the error in this interval is

$$e = -\frac{1}{2} a_2 \tau^2 + \frac{1}{2} a_2 T_2 \tau + C \tag{B9}$$

$$e' = -a_2 \tau + \frac{1}{2} a_2 T_2 \tag{B10}$$

The integration constant C must be the same in both interval T_1 and T_2 (as implied in equations (B5) and (B9)) in order that the periodicity condition imposed on e is not affected.

The switching equation is

$$(e + ke')_{\tau=T_2-T_R} = 0 \tag{B11}$$

which, on substitution of equations (B9) and (B10), becomes

$$C - \frac{1}{2} a_2\left(k - T_R\right)T_2 - \frac{1}{2} a_2 T_R^2 + k a_2 T_R = 0 \tag{B12}$$

Recalling that $a_2T_2 = a_1T_1$, equations (B8) and (B12) are immediately solved for C and T_1 as

$$C = \frac{1}{2}\left(a_1 - a_2\right)T_R\left(k - \frac{1}{2} T_R\right) \tag{B13}$$

and

$$T_1 = \frac{a_1 + a_2}{a_1} T_R\left(\frac{k - \frac{1}{2} T_R}{k - T_R}\right) \tag{B14}$$

To find the peak error in the first interval, the error derivative of equation (B6) is set to zero and the time at peak error is

$$\tau_{m1} = \frac{1}{2} T_1 \tag{B15}$$

Similarly, equation (B10) is set to zero to find the time at peak error in the second interval (remembering, of course, that this time is measured from the start of the second interval):

$$\tau_{m2} = \frac{1}{2} T_2 \tag{B16}$$

If these times are substituted into equations (B5) and (B9), respectively, and m is defined by

$$m = a_1/a_2 \tag{B17}$$

the peak errors are given by equations (43):

$$\left.\begin{aligned} e_{peak_{T_1}} &= -\frac{1}{8}a_1T_R^2\left(\frac{1+m}{m}\right)^2\left(\frac{k-\frac{1}{2}T_R}{k-T_R}\right)^2 - \frac{1}{2}a_1T_R\left(\frac{1-m}{m}\right)\left(k-\frac{1}{2}T_R\right) \\ e_{peak_{T_2}} &= \frac{1}{8}a_1T_R^2\frac{(1+m)^2}{m}\left(\frac{k-\frac{1}{2}T_R}{k-T_R}\right)^2 - \frac{1}{2}a_1T_R\left(\frac{1-m}{m}\right)\left(k-\frac{1}{2}T_R\right) \end{aligned}\right\} \quad (43)$$

W
1
1
0

Third-Order Threshold Imperfection

Although the semigraphical method for finding chatter error for a second-order system is not much of an aid over just straight substitution of initial conditions of the motion, in the third-order case it is a very definite help in that it points the way to a systematic solution of what would be eight simultaneous equations if one were to proceed along the lines of formally matching end conditions. The simplified third-order equations which give rise to chatter oscillations are

$$\left.\begin{aligned} e''' &= N_1 \quad \text{if} \quad e + k_1e' + k_2e'' < 0 \\ e''' &= -N_2 \quad \text{if} \quad e + k_1e' + k_2e'' > 0 \end{aligned}\right\} \quad (B18)$$

where N_1 and N_2 are positive. The chatter occurs because the device which performs the operation $\operatorname{sgn}(e + k_1e' + k_2e'')$ has a threshold of operation ϵ, which is assumed symmetric in the positive and negative directions. The graphical integration of equations (B18) with such an imperfection is shown in figure 24. Notice that again this figure is broken up into its component parts to facilitate integration. Only the repeated plot of e gives a composite figure. The ordinate at any point for the other plots must be taken as the sum of the ordinates of each curve in that plot. The procedure in going from e''' to e'' to e' follows exactly as that in going from e'' to e' to e in the second-order case except that the constant of integration of e' here is found by imposing the condition of periodicity on e. That is, in order to make the integration of e' add up to zero at the right side, a constant of $\frac{N_1T_1}{12}(T_1 - T_2)$ had to be added to e'. Going through the steps, the value at the right side of curve (3), which is the integral of curve (1), is

$$h_3 = \frac{1}{6} N_1 T_1^3 + \frac{1}{3} N_1 T_2^2 + \frac{1}{2} N_1 T_1^2 T_2 \qquad \text{(B19)}$$

Similarly, the value of curve (4), which is the integral of curve (2), at the right side is

$$h_4 = -\frac{1}{4} N_1 T_1 \left(T_1 + T_2\right)^2 \qquad \text{(B20)}$$

Curve (5) is a triangle to be added to curves (3) and (4) such that at the right side

$$h_3 + h_4 + h_5 = 0 \qquad \text{(B21)}$$

Solving equation (B21) one finds that

$$h_5 = \frac{N_1 T_1}{12} \left(T_1 - T_2\right) \left(T_1 + T_2\right) \qquad \text{(B22)}$$

The slope of this triangle is $\frac{N_1 T_1}{12} \left(T_1 - T_2\right)$ which is the integration constant for e', shown by line (6) in figure 24.

As in the second-order case, the only unknowns remaining are the integration constant C_1 for e and the period of the motion. These are found by imposing the switching criterion at the beginning and end of interval T_1.

$$\left(e + k_1 e' + k_2 e''\right)_{\tau=0} = -\epsilon \qquad \text{(B23)}$$

and

$$\left(e + k_1 e' + k_2 e''\right)_{\tau=T_1} = \epsilon \qquad \text{(B24)}$$

where, from curves (3), (4), and (5), e is given in this interval by

$$e = \frac{1}{6} N_1 \tau^3 - \frac{1}{4} N_1 T_1 \tau^2 + \frac{N_1 T_1}{12} \left(T_1 - T_2\right) \tau + C_1 \qquad \text{(B25)}$$

Using equation (B25), equations (B23) and (B24) become

$$C_1 + k_1 \frac{N_1 T_1}{12}\left(T_1 - T_2\right) - \frac{1}{2} k_2 T_1 N_1 = -\epsilon \tag{B26}$$

$$C_1 - \frac{N_1}{12} T_1^2 T_2 + k_1 \frac{N_1 T_1}{12}\left(T_1 - T_2\right) + \frac{1}{2} k_2 T_1 N_1 = \epsilon \tag{B27}$$

Adding equations (B26) and (B27), the integration constant C_1 is found immediately to be

$$C_1 = \frac{N_1 T_1}{24}\left[T_1 T_2 - 2k_1\left(T_1 - T_2\right)\right] \tag{B28}$$

Also, recall that the periodicity condition on e" is

$$\frac{N_1}{N_2} = \frac{T_2}{T_1} \equiv n \tag{B29}$$

If equation (B26) is subtracted from equation (B27) and the result combined with equation (B29), one obtains an equation for T_1:

$$-\frac{n}{12} T_1^3 + k_2 T_1 = \frac{2\epsilon}{N_1} \tag{B30}$$

In this equation n is always less than 1 (one is free to define $N_1 < N_2$ and interpret the results accordingly), ϵ is an imperfection which is made as small as possible for a particular installation, and although N_1 is the smaller driving term it is much greater than ϵ. Therefore the value of T_1 found from equation (B30) will be very small, thus supporting the assumption that the chatter frequency is much higher than the frequency of the controlled process. Since T_1 is small, the first term of equation (B30) may be neglected relative to the second and an explicit expression for T_1 can be given:

$$T_1 = \frac{2\epsilon}{N_1 k_2} \tag{B31}$$

To find the peak values of e in the interval T_1, the derivative e' from equation (B25) is set to zero. The resulting equation can be solved for τ_{cr}, the time from the start of interval T_1 to the peak error:

$$\frac{\tau_{cr}}{T_1} = \frac{1}{2} \pm \sqrt{\frac{1}{4} - \left(\frac{1 - n}{6}\right)} \tag{B32}$$

Notice that if τ_{cr} is to fall within the interval T_1 (the only interval for which the equation applies) then n must be less than 1. This is the reason that all of the equations were developed with $n < 1$. This does not give any restriction on the generality of the results because N_1 can arbitrarily be defined as the smaller driving force, and if it is applied in the negative driving interval a minus sign must be attached to the error and its derivatives as found here.

W
1
1
0

If one develops an equation similar to equation (B32) for the interval T_2, it will be found that n must be greater than 1 in order for the peak error to fall within the interval. Therefore, both error peaks fall in the larger time interval (during the application of driving force N_1 in the convention used here).

When the values of τ_{cr} of equation (B32) are substituted into equation (B25) where C_1 is taken from equation (B28), the resulting expression for the peak errors is surprisingly simple:

$$\frac{e_{peak_\epsilon}}{N_1 T_1^3} = \mp \frac{1}{24}\left(\frac{1 + 2n}{3}\right)^{3/2} - \frac{k_1(1 - n)}{12T_1} \tag{B33}$$

This equation can be put into a more useful form if T_1 is eliminated by using equation (B31):

$$e_{peak_\epsilon} = \mp \frac{1}{3}\left(\frac{1 + 2n}{3}\right)^{3/2} \frac{1}{N_1^2}\left(\frac{\epsilon}{k_2}\right)^3 - \frac{1 - n}{3} \frac{k_1}{N_1}\left(\frac{\epsilon}{k_2}\right)^2 \tag{B34}$$

Also, if equation (B18) is derived from a system of the type given by equations (48) and (49), then

$$N_1 + N_2 = 2N \tag{63}$$

so that equation (B34) is more properly written

$$e_{peak_\epsilon} = \mp \left(\frac{1 + 2n}{3}\right)^{3/2}\left(\frac{1 + n}{2n}\right)^2 \frac{1}{3N^2}\left(\frac{\epsilon}{k_2}\right)^3 - \left(\frac{1 - n^2}{6n}\right)\frac{k_1}{N}\left(\frac{\epsilon}{k_2}\right)^2 \qquad (65)$$

It should be mentioned that the bias term (the last term in equation (65)) is not equal to the integration constant C_1 because part of the expression for C_1 is absorbed into the oscillatory error term.

W
1
1
0

Third-Order Time-Delay Imperfection

If the same method for finding chatter error due to time delay that was used in the second-order case is applied to the third-order case, the resulting equations become very cumbersome. Since the approximations made to arrive at the simplified error differential equation given in equation (B18) required that the imperfections be small, it would be wise to seek a more simplified version of the chatter error due to time delay that takes advantage of the fact that the time delay is small. To do this, it will be assumed from the start that a time delay can be treated as a variable threshold (this in itself is not an approximation). Denoting by F the argument of the switching function, its time derivative is

$$F' = e' + k_1 e'' + k_2 e''' \qquad (68)$$

At the instant before a switch point from $-N_2$ to N_1 (i.e., just before the start of interval T_1) this becomes

$$F' = \frac{N_1 T_1}{12}\left(T_1 - T_2\right) - k_1\left(\frac{1}{2} T_1 N_1\right) - k_2 N_2 \approx -k_2 N_2 \qquad (69)$$

The values of e', e'', and e''' used were taken directly from figure 24. This is valid because the entire development of figure 24 except the evaluation of C_1 and the period applies equally to threshold or time-delay imperfections. That is, the switching equations are not applied until one comes to the point of evaluating T_1 and C_1.

The approximation made above will eliminate the term corresponding to

$$\frac{k - \frac{1}{2} T_R}{k - T_R}$$

which appeared in the second-order case (eqs. (43)). But for small values of T_R, the forthcoming equations will give a good indication of the chatter error. For larger values of T_R the effect of this term can be studied for the case where $N_1 = N_2$. In this case the chatter error can be found by using equation (66) without making the approximation in equation (69).

Using the approximate slope of the switching-function argument given by equation (69), the corresponding equivalent threshold at the start of interval T_1 is

$$\epsilon q_o = -k_2 N_2 T_R \tag{B35}$$

W
1
1
0

Similarly, the equivalent threshold at the end of this interval is

$$\epsilon q_1 = k_2 N_1 T_R \tag{B36}$$

Substituting these equivalent thresholds into equation (B26) and (B27), respectively, one obtains two equations for C_1 and T_1. Eliminating C_1, the equation for T_1 is

$$-\frac{N_1^2}{12N_2} T_1^3 + k_2 N_1 T_1 = k_2 N_2 T_R \left(1 + \frac{N_1}{N_2}\right) \tag{71}$$

Or, again neglecting the cubic terms,

$$T_1 = \left(\frac{1 + n}{n}\right) T_R \tag{B37}$$

The equation for C_1 is

$$C_1 = \frac{N_1 T_1}{24}\left[T_1 T_2 - 2k_1\left(T_1 - T_2\right)\right] - \frac{1}{2} k_2 N_2 T_R (1 - n) \tag{B38}$$

Notice that the first of the two terms on the right-hand side of equation (B38) is identical with C_1 as given by equation (B28). Also, the derivation of τ_{cr} and the accompanying comments apply equally well here

because these considerations were made for T_1 and C_1 in general. Therefore, the error peaks as given in equation (B33) carry over to this case if the addition to C_1 that is given in equation (B38) is added. That is,

$$\frac{e_{peak_T}}{N_1 T_1^3} = \mp \frac{1}{24}\left(\frac{1 + 2n}{3}\right)^{3/2} - \frac{k_1(1 - n)}{12T_1} - \frac{\frac{1}{2} k_2 N_2 T_R(1 - n)}{N_1 T_1^3} \qquad \text{(B39)}$$

W
1
1
0

This additional bias term is due to the unsymmetric equivalent thresholds, and drops out, as does the other bias term, if $n = 1$. Using the value of T_1 given in equation (B37), the peak chatter errors for a small time delay T_R are

$$e_{peak_T} = \mp \frac{1}{24}\left(\frac{1 + 2n}{3}\right)^{3/2}\left(\frac{1 + n}{n}\right)^3 N_1 T_R^3 - \left(\frac{1 - n}{12}\right)\left(\frac{1 + n}{n}\right)^2 k_1 N_1 T_R^2 - \left(\frac{1 - n}{2n}\right) k_2 N_1 T_R \qquad \text{(B40)}$$

Or, for the case where $N_1 + N_2 = 2N$,

$$e_{peak_T} = \mp \left(\frac{1 + 2n}{3}\right)^{3/2}\left(\frac{1 + n}{2n}\right)^2 \frac{1}{3} N T_R^3 - \left(\frac{1 - n^2}{6n}\right) k_1 N T_R^2 - \left(\frac{1 - n}{1 + n}\right) k_2 N T_R$$

(72)

APPENDIX C

CONVERSION OF AIRCRAFT-PITCHING-MOTION EQUATION TO COMPUTER UNITS

Throughout the text, the example used as a third-order controlled process is a simplified equation of the pitching motion of a missile or aircraft. This equation is

$$\frac{d^3\theta}{dt^3} + 2\zeta\omega_a \frac{d^2\theta}{dt^2} + \omega_a{}^2 \frac{d\theta}{dt} = -\omega_a{}^2 v_{ra}\phi \tag{C1}$$

where t is real time, ϕ is a switching function which takes on the values ± 1, θ is the aircraft-flight-path angle measured from level flight, ω_a is the undamped natural frequency of the rapid incidence adjustment mode (the more exact equation is of fourth order with two natural frequencies: the incidence adjustment or high-frequency mode, and the phugoid or low-frequency mode), and v_{ra} is the angular "runaway velocity." The coefficient of the switching function represents the effect of some control surface on the motion, and the surface takes on only two positions, either full up or full down. In order to make the equation third rather than fourth order, perturbation of level flight had to be considered with the change in forward speed neglected. The definition of a "runaway velocity" comes from the observation that, if the control surface is allowed to assume one of its positions for an indefinite length of time, then after the transients die out, the aircraft flight angle will be changing at an angular velocity v_{ra}:

$$\frac{d\theta}{dt} = \pm v_{ra} \tag{C2}$$

In order to study this equation on a differential analog computer, it was decided to scale time and angle so as to use a convenient voltage range and to make the inherent delay of the relays used very small in terms of the natural frequency of the machine equation. Defining y as the dependent machine variable and τ as machine time, the scale factors are

$$y = a_y\theta \qquad \tau = \omega_o t \qquad \Omega = \frac{\omega_a}{\omega_o} \tag{C3}$$

and equation (C1) becomes

$$\frac{\omega_b^3}{a_y}\frac{d^3y}{d\tau^3} + 2\zeta\omega_a\frac{\omega_b^2}{a_y}\frac{d^2y}{d\tau^2} + \omega_a^2\frac{\omega_b}{a_y}\frac{dy}{d\tau} = -\omega_a^2 v_{ra}\phi \qquad (C4)$$

Or, using primes to denote differentiation with respect to τ,

$$y''' + 2\zeta\Omega y'' + \Omega^2 y' = -N\phi \qquad (C5)$$

where

$$N \equiv \frac{\Omega^2 v_{ra} a_y}{\omega_b} \equiv \Omega^2 V_{ra}$$

The parameters N and Ω could be made unity by making the proper adjustments of ω_b and a_y, but it was desired to study the effect of varying ω_a and v_{ra} due to changing aircraft speed and altitude, so that ω_b and a_y were merely adjusted to give convenient machine units.

APPENDIX D

OPTIMUM RESPONSE OF SECOND-ORDER SYSTEM WITH DAMPING

Optimum response of the equation

$$y'' + Dy' = -a\phi(e,e') \tag{124}$$

was discussed briefly in the section "Step Response of Third-Order Contactor System With Two Complex Roots." To find optimum response for this equation for step or ramp inputs, the equation must first be changed into an equation for the error e by substituting $y = x - e$, noting that $x'' = 0$ and $x' = x'_o$ for a ramp input.

$$e'' + De' = Dx'_o + a\phi(e,e') \tag{D1}$$

To find the phase curves for equation (D1), it is first transformed into a differential equation in e' and e by using the identity

$$e'' = e' \frac{de'}{de} \tag{D2}$$

Equation (D1) then becomes

$$e' \frac{de'}{de} + De' = Dx'_o + a\phi(e,e') \tag{D3}$$

or, separating variables (noting that ϕ = Constant over any integration interval)

$$-D\,de = \frac{e'\,de'}{e' - x'_o - \frac{a\phi}{D}}$$

$$= de' + \frac{\left(x'_o + \frac{a\phi}{D}\right)de'}{e' - x'_o - \frac{a\phi}{D}} \tag{D4}$$

Equation (D4) can be integrated directly for $\phi = 1$ or -1 (one cannot integrate over a discontinuity in ϕ, of course). The integration must be broken into two parts in order to avoid the singularity at $e' = x'_o + (a\phi/D)$ so that

$$-D(e - e_o) = e' + \left(x'_o + \frac{a\phi}{D}\right)\log_e\left(e' - x'_o - \frac{a\phi}{D}\right) \qquad e' > x'_o + \frac{a\phi}{D} \qquad \text{(D5a)}$$

$$-D(e - e_o) = e' + \left(x'_o + \frac{a\phi}{D}\right)\log_e\left(-e' + x'_o + \frac{a\phi}{D}\right) \qquad e' < x'_o + \frac{a\phi}{D} \qquad \text{(D5b)}$$

where e_o is the integration constant.

The zero trajectories for $\phi = 1$ and $\phi = -1$ are shown in figure 37(a) for $x'_o > 0$. The solid line is for $\phi = 1$ and the broken line, for $\phi = -1$. Also shown in the same figure are branches on the other side of the singularities at $e' = x'_o \pm (a/D)$. All other trajectories are curves parallel to these and shifted along the e axis according to the integration constant e_o. The equation of the zero trajectory for $\phi = 1$ is found by taking equation (D5b) with e_o evaluated by first setting $e = e' = 0$. The resulting zero trajectory is

$$-De = e' + \lambda_1 \log_e \frac{\lambda_1 - e'}{\lambda_1} \qquad \text{(D6)}$$

where

$$\lambda_1 = \frac{a}{D} + x'_o \qquad -\frac{a}{D} < x'_o < \frac{a}{D}$$

The values of x'_o given are those values for which the system will not diverge. For values of x'_o outside this range, inspection of equation (D1) shows that the system will diverge because the term containing the switching function no longer determines the sign of the right-hand or driving side of the equation.

If the scale factors of the phase-plane axes are changed by λ_1 $\left(\text{i.e., } e = \lambda_1\xi_1 \text{ and } e' = \lambda_1\xi_1'\right)$ the parameter λ_1 can be eliminated in equation (D6) and it becomes

$$-D\xi_1 = \xi_1' + \log_e\left(1 - \xi_1'\right) \tag{D7}$$

Similarly, the zero trajectory for $\phi = -1$ is found by taking equation (D5a) with e_o evaluated by first setting $e = e' = 0$.

$$-De = e' - \lambda_2 \log_e \frac{\lambda_2 + e'}{\lambda_2} \tag{D8}$$

where

$$\lambda_2 = \frac{a}{D} - x'_o \qquad -\frac{a}{D} < x'_o < \frac{a}{D}$$

W
1
1
0

Changing the scale factors in the phase plane by $e = \lambda_2\xi_2$ and $e' = \lambda_2\xi_2'$, equation (D8) becomes

$$-D\xi_2 = \xi_2' - \log_e\left(1 + \xi_2'\right) \tag{D9}$$

Figure 37(b) shows the ingoing branches of the unmodified zero trajectories given by equations (D6) and (D8). Bushaw (ref. 4) shows that the curve made up by these two branches is the optimum switching curve. For points above, ϕ is to be taken as -1, and, for those below, $\phi = 1$. Four types of optimum responses from arbitrary points are shown in the figure. But this switching gives optimum response only for the specific value of x'_o for which it was plotted. Figure 37(c) shows the ingoing branches of equations (D7) and (D9) in which the parameters λ_1 and λ_2, which depend on x'_o, have been eliminated. In order to plot both branches in the same figure, it was necessary to take different scale factors for the positive and negative axes as shown. Since these curves do not depend on x'_o, operation in this distorted phase plane gives optimum response for any ramp input in the range $-a/D < x'_o < a/D$.

The procedure for providing optimum response for an arbitrary ramp input is first to form the "normalized" switching curve shown in figure 37(c). The error and error derivative fed into this function must then be modified by the scale factor λ_1 or λ_2, depending upon the location of the state point. Since the choice of scale factor is not important in the first and third quadrants, one may switch the scale factor from λ_1 to λ_2 according to sgn e or sgn e', whichever is more convenient. This scheme also includes step inputs, of course, as a degenerate case where $\lambda_1 = \lambda_2 = a/D$.

REFERENCES

1. Flügge-Lotz, I., Taylor, C. F., and Lindberg, H. E.: Investigation of a Nonlinear Control System. NACA Rep. 1391, 1959. (Supersedes NACA TN 3826.)

2. MacColl, L. A.: Fundamental Theory of Servomechanisms. D. Van Nostrand Co., Inc., 1945, pp. 79-87.

3. Flügge-Lotz, I.: Discontinuous Automatic Control. Princeton Univ. Press (Princeton, New Jersey), 1953.

4. Bushaw, D. W.: Differential Equations With a Discontinuous Forcing Term. Rep. 469, Contract N-onr-26302, Office of Naval Res. and Exp. Towing Tank, Stevens Inst. of Tech., Jan. 1953.

5. Flügge-Lotz, I., and Klotter, K.: On the Motions of an Oscillating System Under the Influence of Flip-Flop Controls. NACA TM 1237, 1949.

6. Kochenburger, R. J.: Frequency-Response Methods for Analyzing and Synthesizing Contactor Servomechanisms. Trans. AIEE, vol. 69, no. 8, Aug. 1950, pp. 270-284.

7. Flügge-Lotz, I., and Wunch, W. S.: Mechanical Reproduction of an Arbitrary Function of Time. Tech. Rep. 19, Pts. I and II, Contract N6-onr-251, Task Order II, Office of Nav. Res. and Div. of Eng. Mech., Stanford Univ., 1952. (Excerpts appear in article by Flügge-Lotz, I., and Wunch, W. S.: On a Nonlinear Transfer System. Jour. Appl. Phys., vol. 26, no. 4, Apr. 1955, pp. 484-488.)

8. Tsien, H. S.: Engineering Cybernetics. McGraw-Hill Book Co., Inc., 1954.

9. Bogner, I., and Kazda, L. F.: An Investigation of the Switching Criteria for Higher Order Contactor Servomechanisms. Trans. AIEE, vol. 73, no. 13, July 1954, pp. 118-126.

10. Rose, Nicholas J.: Theoretical Aspects of Limit Control. Rep. 459, Contract N-onr-26302, Office of Naval Res. and Exp. Towing Tank, Stevens Inst. of Tech., Nov. 1953.

11. Schmidt, Stanley F., and Triplett, William C.: Use of Nonlinearities to Compensate for the Effects of a Rate-Limited Servo on the Response of an Automatically Controlled Aircraft. NACA TN 3378, 1955.

TABLE I.- COMPARISON OF EXPERIMENTAL AND THEORETICAL SECOND-ORDER SYMMETRICAL CHATTER-ERROR AMPLITUDES FOR EQUATION (45)

[D = 0.5; a = 40; x = 0]

T_R	k = 0.5		k = 0.25	
	Theoretical e_{max_T}	Experimental e_{max_T}	Theoretical e_{max_T}	Experimental e_{max_T}
0.025	0.013	0.013	0.013	0.013
.035	.026	.023	.029	.026
.045	.045	.045	.050	.047
.055	.070	.072	.080	.081
.065	.098	.095	.120	.120
.090	.203	.180	.266	.24
.115	.348	.32	.535	.47
.165	.843	.70		
.215	1.75	1.31		
.265	3.43	2.16		
.315	6.73	3.18		

W 1 1 0

TABLE II.- COMPARISON OF EXPERIMENTAL AND THEORETICAL THIRD-ORDER SYMMETRICAL CHATTER-ERROR AMPLITUDES FOR TWO EXAMPLES

T_R	$\frac{1}{3} NT_R^3$	Exp. A (a)	Exp. B (b)
0.035	0.00057	0.002	0.002
.055	.0022	.010	.006
.065	.0037	.032	.014
.090	.0097	Diverge	.050
.115	.0203	Diverge	.045

[a]Experiment A: x = 0; $y''' = 40\ \mathrm{sgn}(e + 0.50e' + 0.10e'')$.

[b]Experiment B: x = 0; $y''' + 2\zeta\Omega y'' + \Omega^2 y' = 40\ \mathrm{sgn}(e + 0.50e' + 0.10e'')$; $\zeta = 0.6$; $\Omega^2 = 2.79$.

TABLE III.- COMPARISON OF EXPERIMENTAL AND THEORETICAL CHATTER BIAS ERRORS FOR THIRD-ORDER SYSTEM OF EQUATION (49)

$$\left[e'''(\tau) + 2\zeta\Omega e''(\tau) + \Omega^2 e'(\tau) = N_1 \quad \text{if} \quad \left(e + k_1 e' + k_2 e''\right)_{\tau - T_R} < 0;\right.$$

$$e'''(\tau) + 2\zeta\Omega e''(\tau) + \Omega^2 e'(\tau) = -N_2 \quad \text{if} \quad \left(e + k_1 e' + k_2 e''\right)_{\tau - T_R} > 0;$$

$$\left.\Omega^2 = 2.79;\ \zeta = 0.6;\ N_1 = 40;\ n = N_1/N_2\right]$$

Values of parameters				Theoretical chatter bias error, B (a)	Experimental chatter bias error, B_{ex}	$B - B_{ex}$
k_1	k_2	n	T_R			
0.50	0.10	0.50	0.055	0.066	0.063	0.003
.50	.10	.25	.055	.106	.105	.001
.20	.10	.25	.055	.092	.092	0
.50	.50	.25	.055	.436	.43	.006
.527	.10	.25	.065	.132	.135	-.003
.527	.10	.50	.115	.167	.18	-.013
.527	.10	.25	.115	.282	.39	-.108

$$^{a}\text{Error}\quad B = \frac{k_1}{12}\left(\frac{n+1}{n}\right)\left(1 - n^2\right)N_1 T_R^{\,2} + \frac{1}{2}\,k_2(1 - n)N_2 T_R.$$

TABLE IV.- COMPARISON OF LOW-FREQUENCY-ERROR AMPLITUDES FOUND IN ANALOG-COMPUTER SIMULATION WITH THOSE GIVEN BY EQUATION (87) FOR SECOND-ORDER SYSTEM WITH $x = A \sin \omega\tau$

[$y'' + y' = a\,\mathrm{sgn}(e + ke')$; the following parameter values are defined as "normal:"

$a = 40$ volts $\quad k = 0.24$
$A = 20$ volts $\quad \sum_n T_{1i} = 0.5$
$\omega = 1$]

W
1
1
0

Run	Values of parameters (a)	Theoretical error amplitude, Q (b)	Experimental error amplitude, Q_{ex}	$Q - Q_{ex}$	Error difference, percent
1	Normal	0.234	0.27	-0.036	-15
2	$\sum_n T_{1i} = 0.10$	.468	.49	-.022	-5
3	$\omega^2 = 0.6$	.1415	.16	-.018	-13
4	$\omega^2 = 0.2$	.0477	.05	-.002	-4
5	$k = 0.5$	.447	.50	-.053	-12
6	$k = 0.167$	.164	.19	-.026	-16
7	$A = 10$	.117	.13	-.023	-20

[a]All parameters are normal but one listed.

[b]Error amplitude $Q = \dfrac{kA\omega^2 \sum_n T_{1i}}{\sqrt{1 + k^2\omega^2}}$.

TABLE V.- COMPARISON OF LOW-FREQUENCY-ERROR AMPLITUDES FOUND IN ANALOG-COMPUTER SIMULATION WITH THOSE GIVEN THEORETICALLY FOR A THIRD-ORDER SYSTEM WITH INPUT

$$x = A \sin \omega\tau$$

[The following parameter values are defined as "normal:"

$\Omega^2 = 2.79$, $\zeta = 0.6$, $N = 47$, $\omega = 0.815$, $A = 20$

$k_1 = 0.527$

$k_2 = 0.079$ for table V(a)

$k_2 = 0.10$ for tables V(b) and V(c)

$\sum_n T_{1i} = 0.052$

$\sum_m T_{2i} = 0.292$]

(a) System $y''' + 2\zeta\Omega y'' + \Omega^2 y' = N \operatorname{sgn}\left(e + k_1\tilde{e}' + k_2 e''\right)$ with only x' filtering; theoretical errors given by equation (97)

Run	Values of parameters (a)	Theoretical error amplitude, Q (b)	Experimental error amplitude, Q_{ex}	$Q - Q_{ex}$	Error difference, percent
1	Normal	0.350	0.35	0	0
2	$\sum_n T_{1i} = 0.102$	.686	.65	.036	5
3	$k_1 = 1.05$	.570	.54	.03	5
4	$k_1 = 0.263$	.188	.184	.004	2
5	$\omega = 0.407$	.0898	.08	.0098	11
6	$\omega = 0.628$	.211	.206	.005	2
7	$A = 10$	.175	.17	.005	3
8	$k_2 = 0.213$	.380	.362	.018	5
9	$k_2 = 0.588$	.488	.436	.052	11

[a]All parameters are normal but one listed.

[b]Error amplitude $Q = \dfrac{Ak_1\omega^2 \sum_n T_{1i}}{\sqrt{\left(1 - k_2\omega^2\right)^2 + k_1^2\omega^2}}$.

TABLE V.- COMPARISON OF LOW-FREQUENCY-ERROR AMPLITUDES FOUND IN ANALOG-COMPUTER SIMULATION WITH THOSE GIVEN THEORETICALLY FOR A THIRD-ORDER SYSTEM WITH INPUT $x = A \sin \omega\tau$ - Continued

(b) System $y''' + 2\zeta\Omega y'' + \Omega^2 y' = N \operatorname{sgn}\left(e + k_1 e' + k_2 \tilde{e}''\right)$ with only x'' filtering; theoretical errors given by equation (98)

Run	Values of parameters (a)	Theoretical error amplitude, Q (b)	Experimental error amplitude, Q_{ex}	$Q - Q_{ex}$	Error difference, percent
1	Normal	0.308	0.294	0.014	4.5
2	$\sum_m T_{2i} = 0.192$	.203	.194	.009	4.3
3	$\sum_m T_{2i} = 0.392$	.413	.388	.025	6.0
4	$\omega = 0.407$	.0383	.0375	.0008	2.0
5	$\omega = 0.628$	.141	.143	-.002	-1.4
6	$k_1 = 1.05$	.250	.264	-.014	-5.6
7	$k_1 = 0.263$	.330	.295	.035	10.6
8	$k_2 = 0.25$	.844	.77	.074	8.8
9	$k_2 = 0.50$	1.995	1.74	.255	12.8
10	A = 10	.154	.153	.001	.6
11	Normal	.308	.296	.012	3.9

[a] All parameters are normal but one listed.

[b] Error amplitude $Q = \dfrac{Ak_2\omega^3 \sum_m T_{2i}}{\sqrt{\left(1 - k_2\omega^2\right)^2 + k_1^2\omega^2}}$.

TABLE V.- COMPARISON OF LOW-FREQUENCY-ERROR AMPLITUDES FOUND IN ANALOG-COMPUTER SIMULATION WITH THOSE GIVEN THEORETICALLY FOR A THIRD-ORDER SYSTEM WITH INPUT

$x = A \sin \omega\tau$ - Concluded

(c) System $y''' + 2\zeta\Omega y'' + \Omega^2 y' = N \operatorname{sgn}\left(e + k_1\tilde{e}' + k_2\tilde{e}''\right)$ with both x' and x'' filtering; theoretical errors given by equation (102)

Run	Values of parameters (a)	Theoretical error amplitude, Q (b)	Experimental error amplitude, Q_{ex}	$Q - Q_{ex}$	Error difference, percent
1	Normal	0.496	0.53	-0.034	-6.8
2	$\sum_m T_{2i} = 0.192$	.422	.455	-.033	-7.8
3	$\sum_m T_{2i} = 0.392$	.589	.61	-.021	-3.6
4	$\sum_n T_{1i} = 0.152$	1.105	1.12	-.015	-1.5
5	$\omega = 0.407$	.103	.107	-.004	-3.9
6	$\omega = 0.628$	.265	.276	-.011	-4.1
7	$k_1 = 1.05$	.654	.666	-.012	-1.8
8	$k_1 = 0.263$	.368	.38	-.012	-3.3
9	$k_2 = 0.25$	.974	.91	.064	6.6
10	$k_2 = 0.50$	2.21	1.92	.29	13.1
11	Normal	.496	.53	-.034	-6.8
12	A = 10	.248	.26	-.012	-4.8

[a] All parameters are normal but one listed.

[b] Error amplitude $Q = \dfrac{A\omega\sqrt{k_1^2\alpha_1^2 + k_2^2\alpha_2^2\omega^2 + k_1k_2\omega\alpha_1\alpha_2(\alpha_2 - \alpha_1)}}{\sqrt{\left(1 - k_2\omega^2\right)^2 + k_1^2\omega^2}}$.

TABLE VI.- COMPARISON OF EXPERIMENTAL AND THEORETICAL BREAKDOWN FREQUENCY FOR THIRD-ORDER SYSTEM OF EQUATION (47) WITH $x = A \sin \omega\tau$

Experiment	Ω^2	ζ	N	A	Experimental ω_c^2	ω_c^2, real root of $\omega_c^6 + \left(4\Omega^2 - 2\right)\Omega^2\omega_c^4 + \Omega^4\omega_c^2 = \pm \frac{N^2}{A}$
1	2.79	0.3	47	20	2.52	2.15
2	[a]1.35	.3	47	20	2.62	2.42
3	2.79	[a]0	47	20	4.00	3.97
4	2.79	.3	[a]80	20	3.66	3.64
5	2.79	.3	47	[a]10	4.47	4.01

[a]Only quantity different from those for experiment 1.

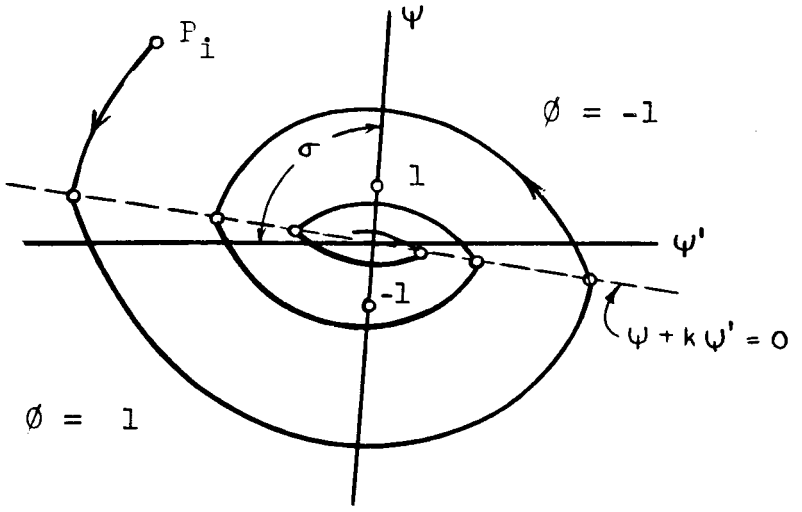

(a) $k > 0$.

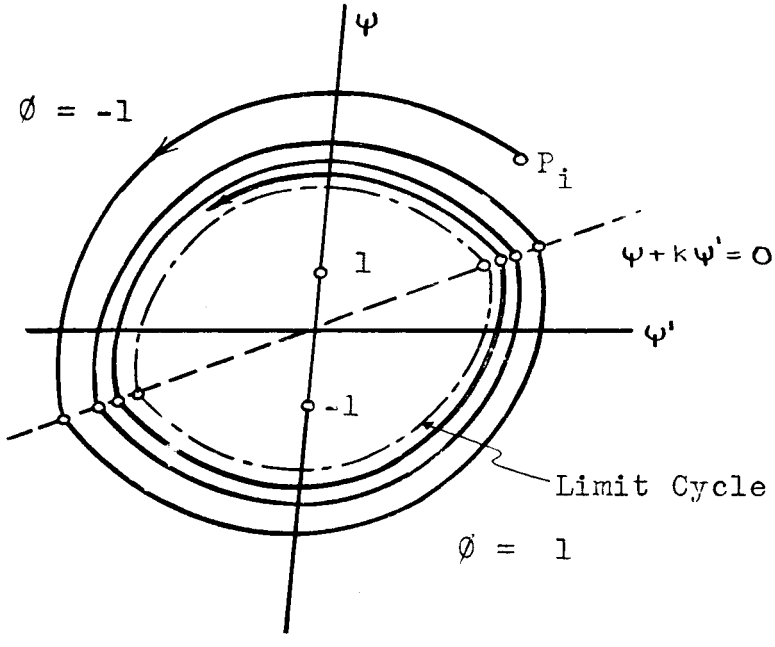

(b) $k < 0$.

Figure 1. Transient response in phase plane for equation (1).

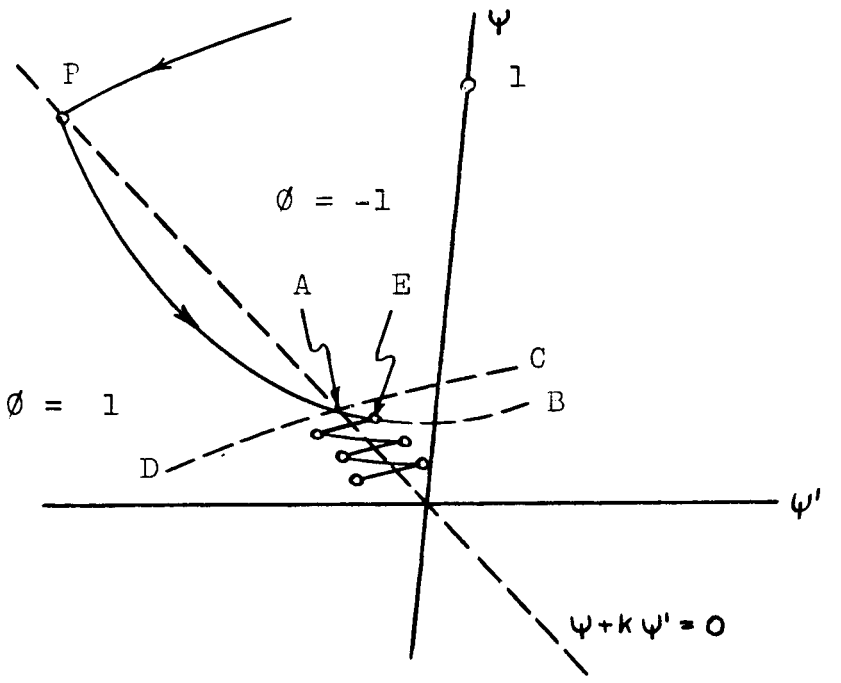

Figure 2.- Motion after end point A (see eq. (1) with $k > 0$).

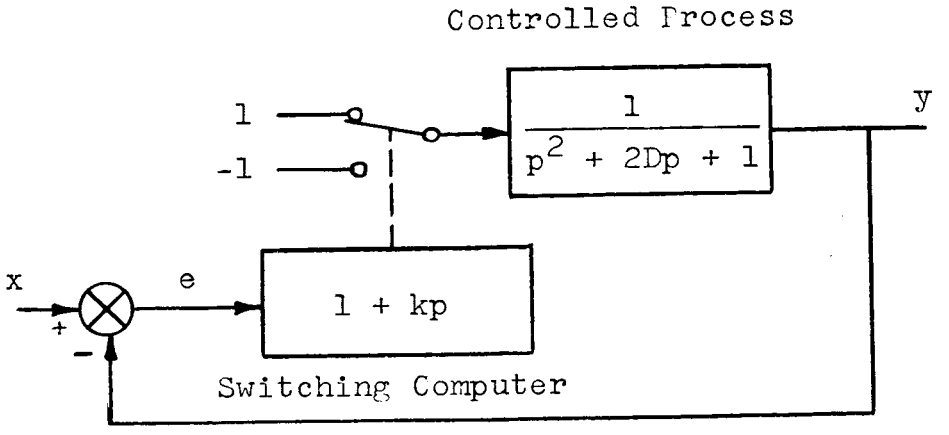

Figure 3.- Second-order followup system.

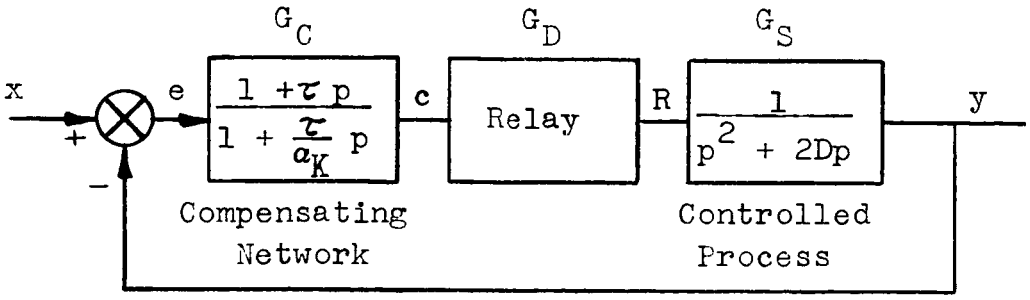

Figure 4.- Series transfer functions used by Kochenburger.

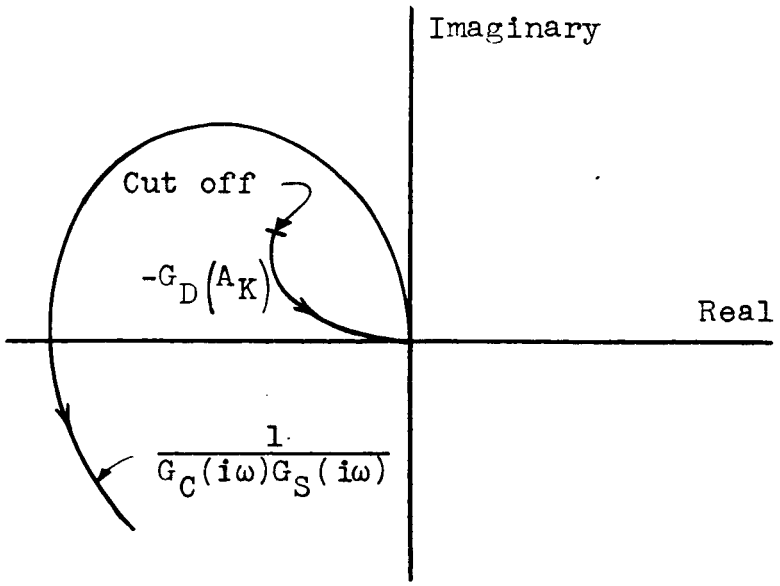

Figure 5.- Frequency response in complex plane. Arrows drawn in direction of increasing ω and a.

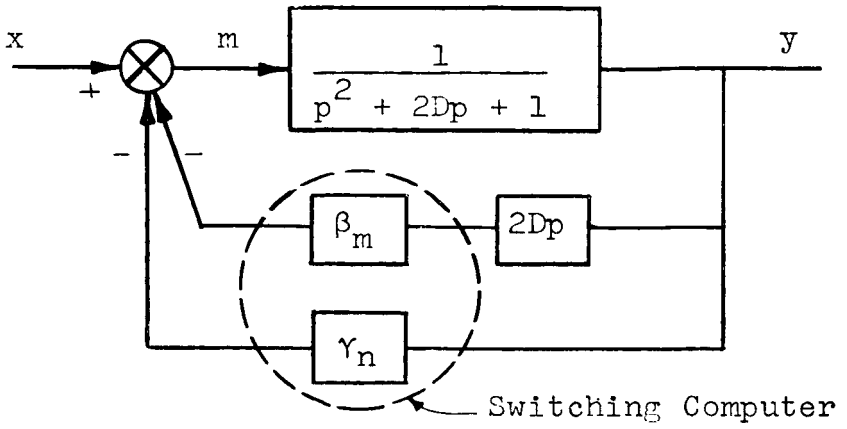

Figure 6.- Varied-coefficient scheme.

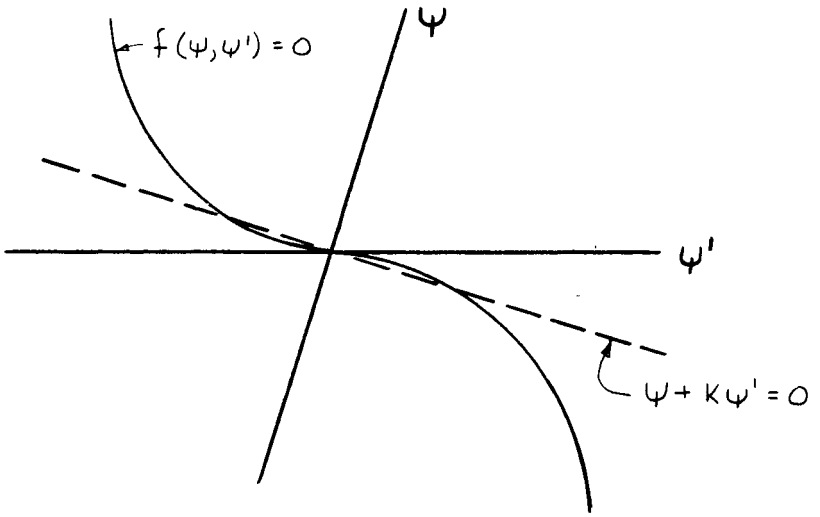

Figure 7.- Response near origin where a more complicated switching function can be replaced by a straight line.

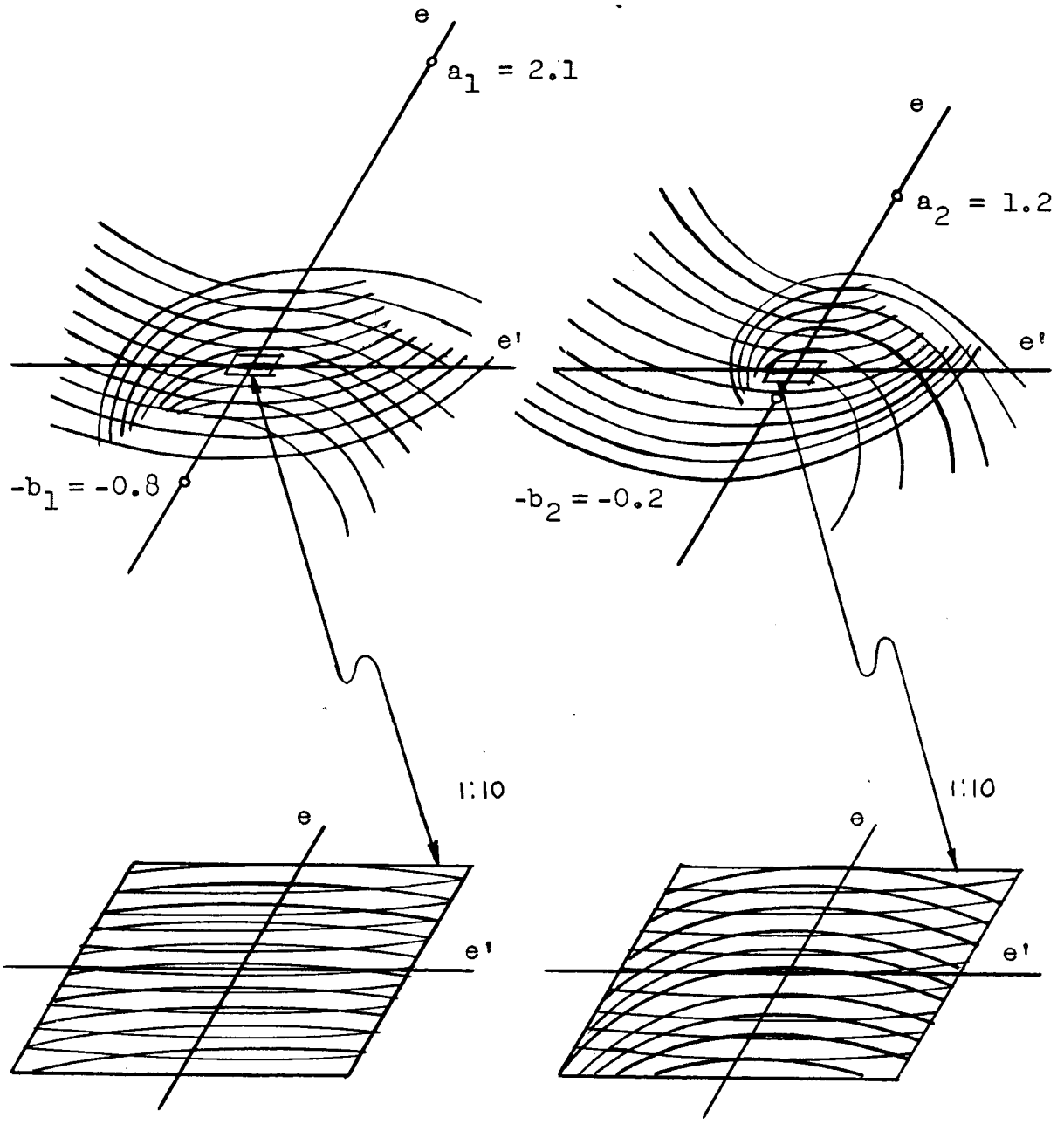

Figure 8.- Phase-plane meshwork near origin for various values of a and b.

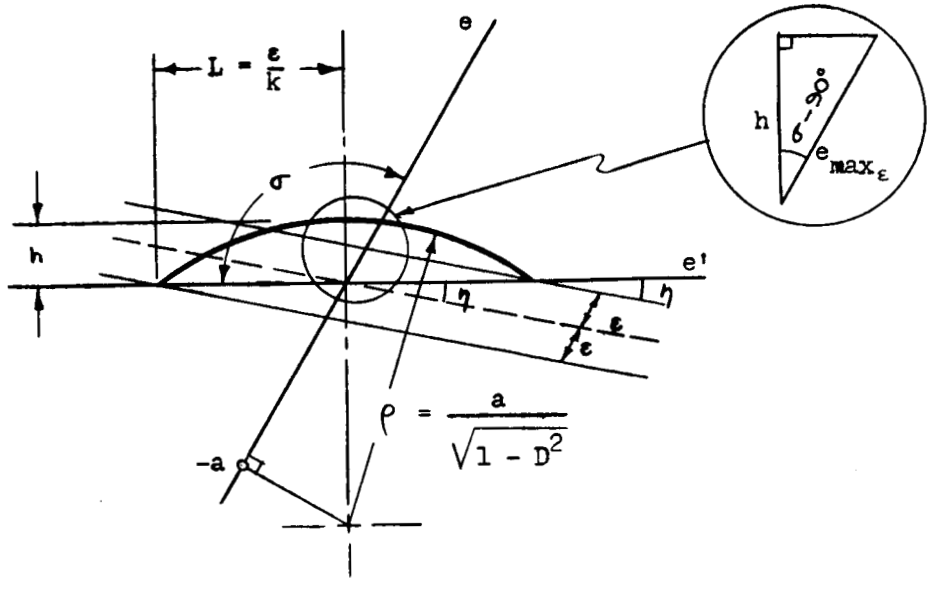

(a) Threshold imperfections; $e_{max_\epsilon} \approx \frac{1}{2a}\left(\frac{\epsilon}{k}\right)^2$.

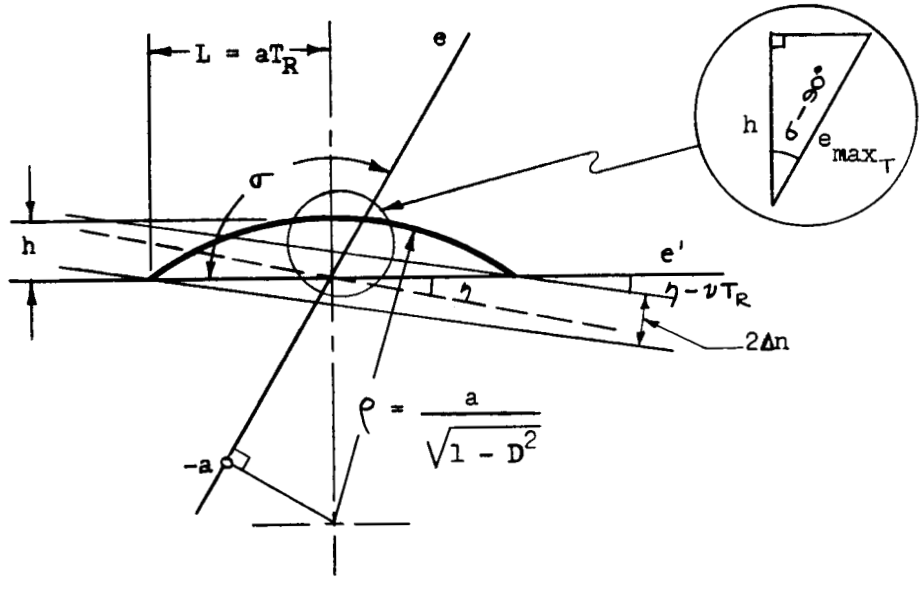

(b) Time-delay imperfections; $e_{max_T} \approx \frac{aT_R^2}{2}$.

Figure 9.- Approximations of one-half of the error limit cycles resulting from threshold and time-delay imperfections of the type of equation (18). Figure not drawn to scale.

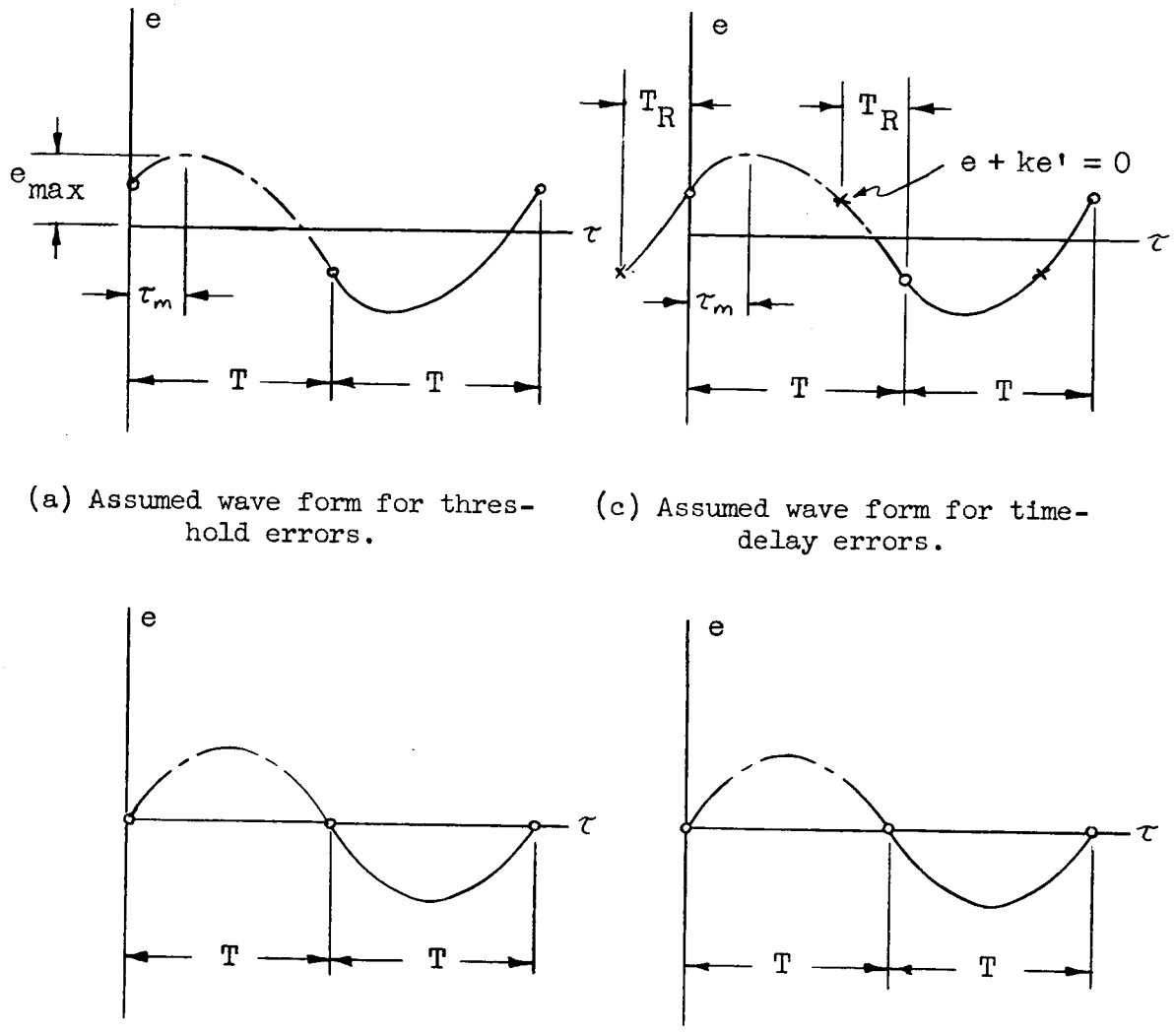

(a) Assumed wave form for threshold errors.

(c) Assumed wave form for time-delay errors.

(b) Actual wave form for threshold errors.

(d) Actual wave form for time-delay errors.

Figure 10.- Symmetrical chatter-error wave forms for a second-order system.

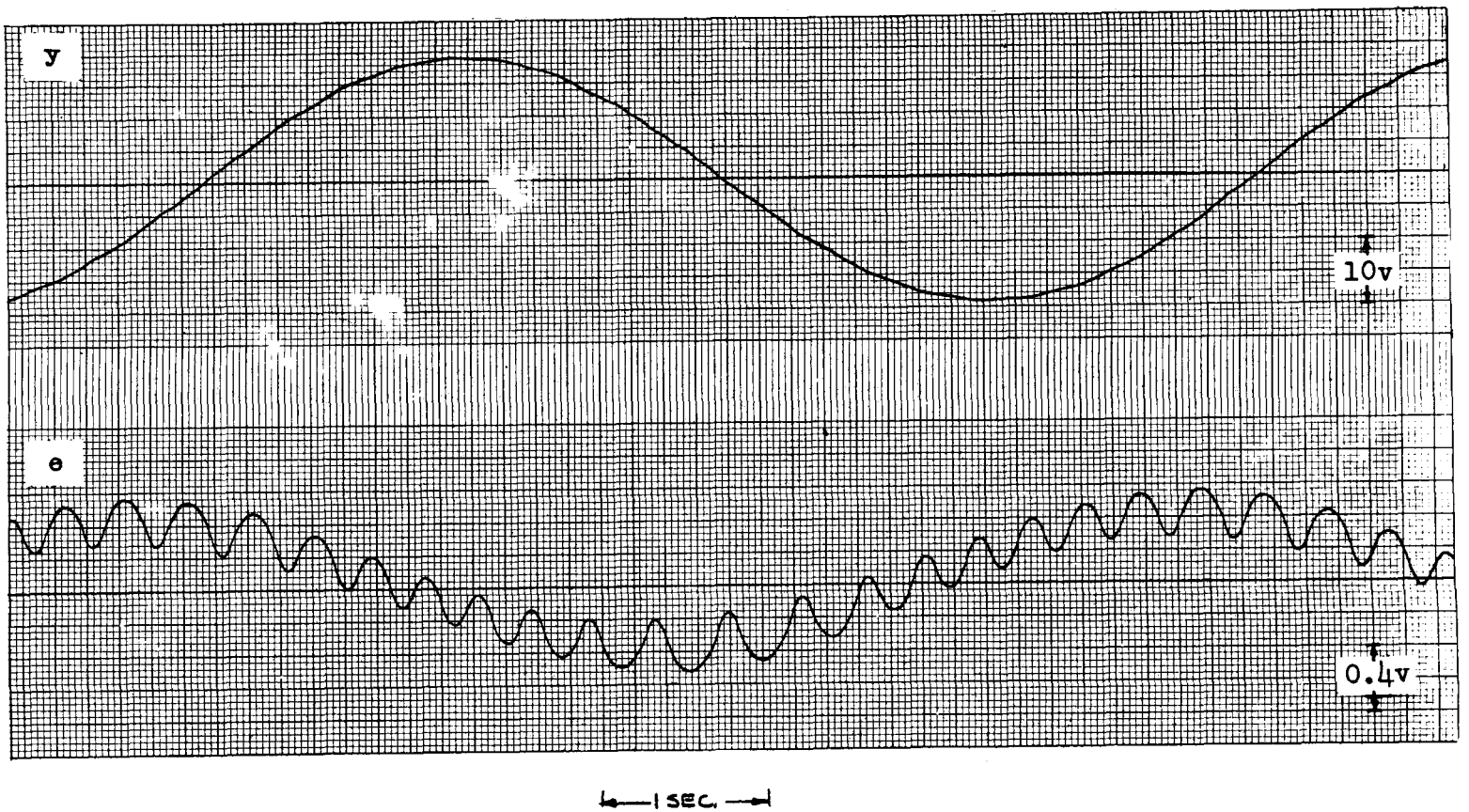

Figure 11.- Response of second-order system of equation (45) with $D = 0.5$, $a = 40$ volts, $k = 0.25$, and $T_R = 0.065$ to an input $x = 19 \sin \tau$.

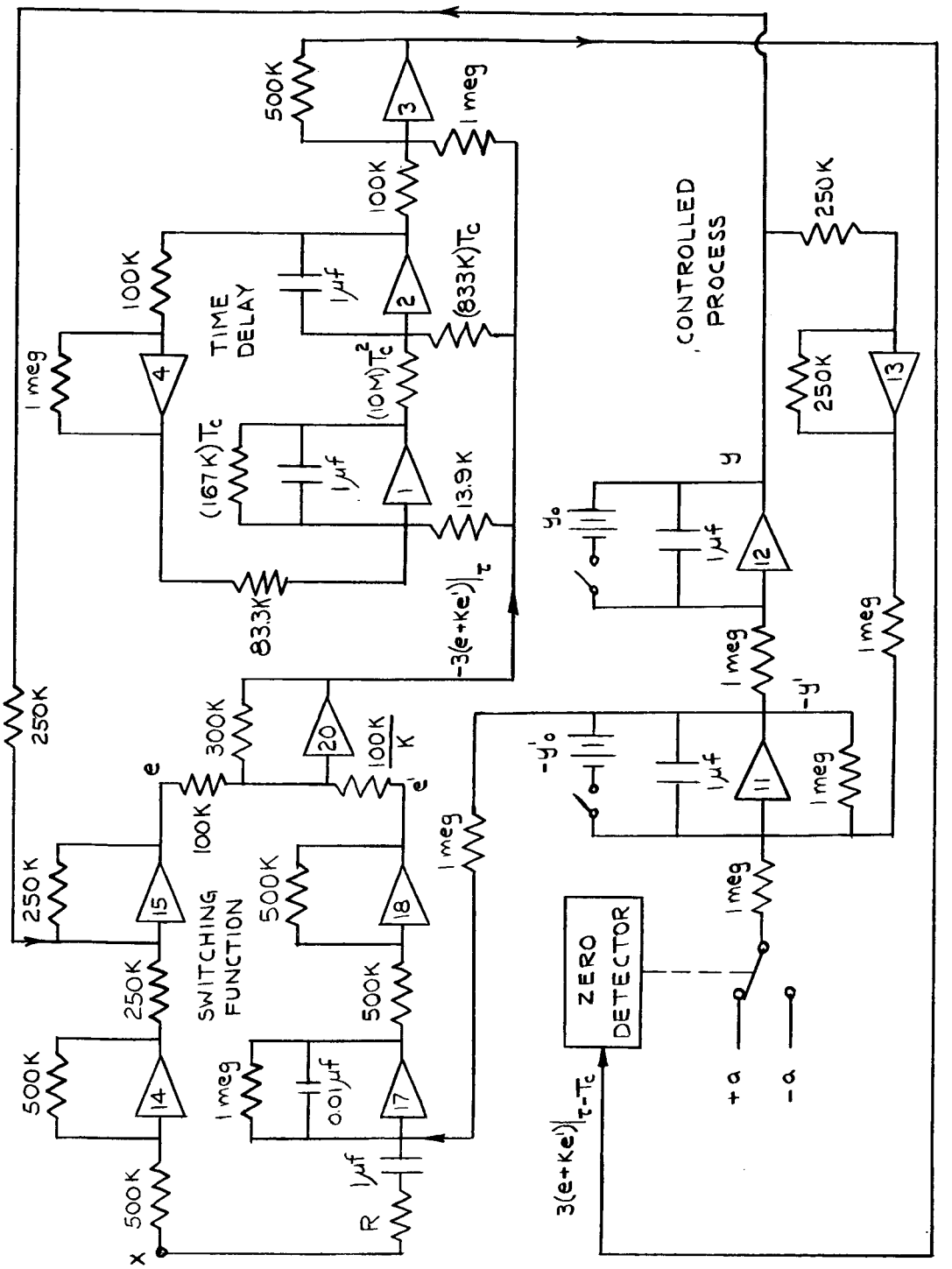

Figure 12.- Analog-computer circuit for second-order system with an artificial relay time delay. y_o and y'_o are initial values.

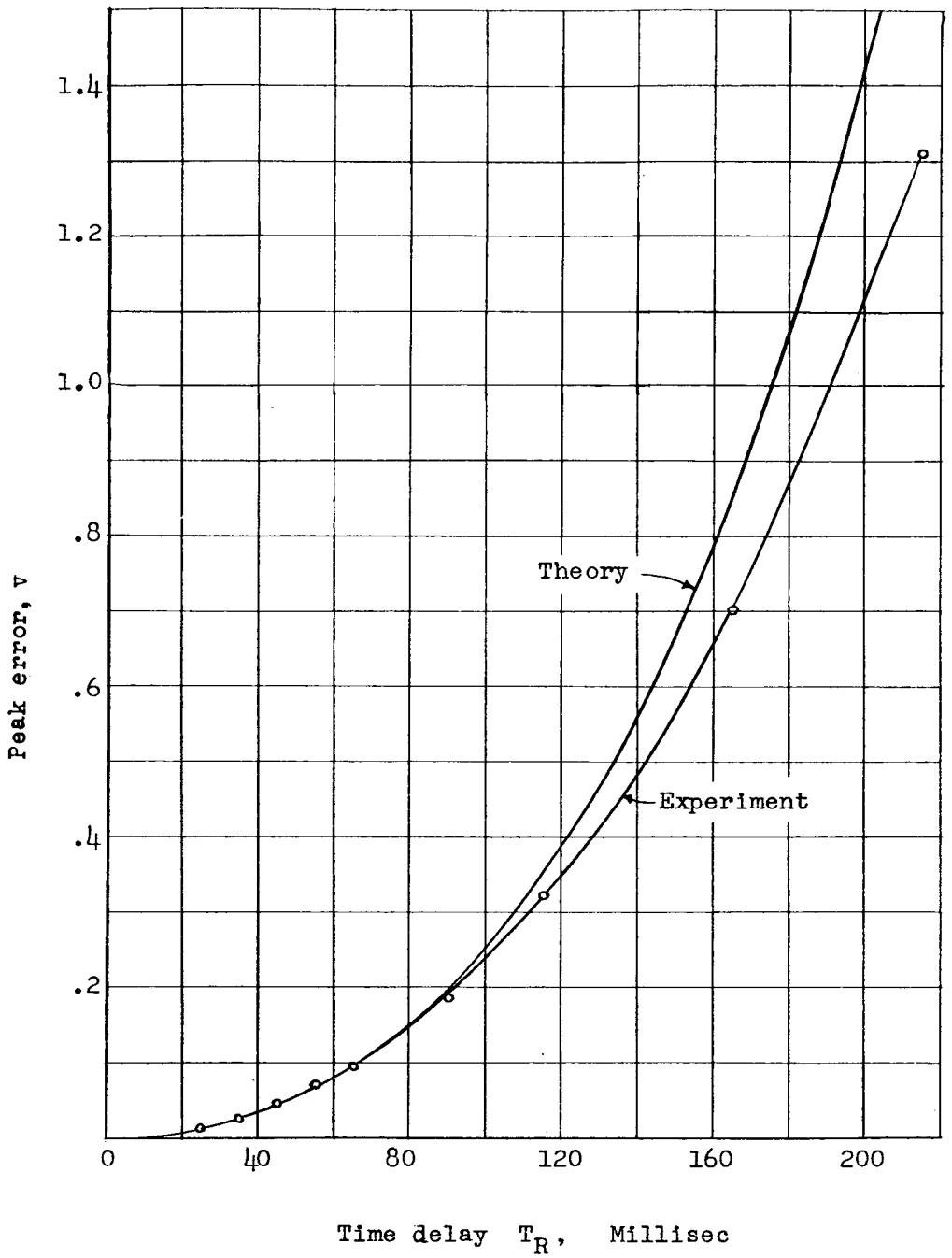

Figure 13.- Comparison of theoretical and experimental chatter error for a second-order system. $e_{max_T} = \frac{1}{2} a T_R^2 \left(\frac{k - \frac{1}{2}T_R}{k - T_R} \right)^2$; $k = 0.5$.

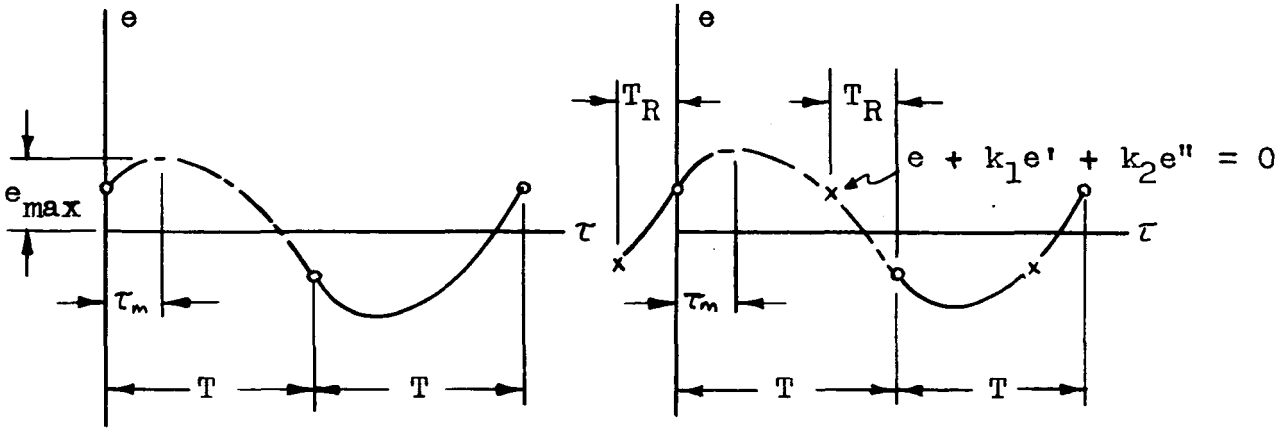

(a) Assumed wave form for threshold errors.

(c) Assumed wave form for time-delay errors.

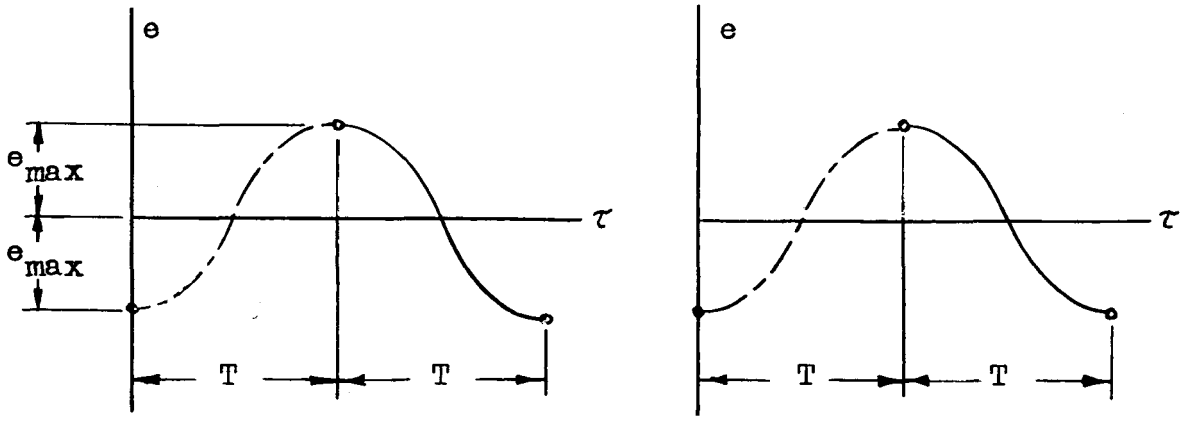

(b) Actual wave form for threshold errors.

(d) Actual wave form for time-delay errors.

Figure 14.- Symmetrical chatter-error wave forms for third-order systems.

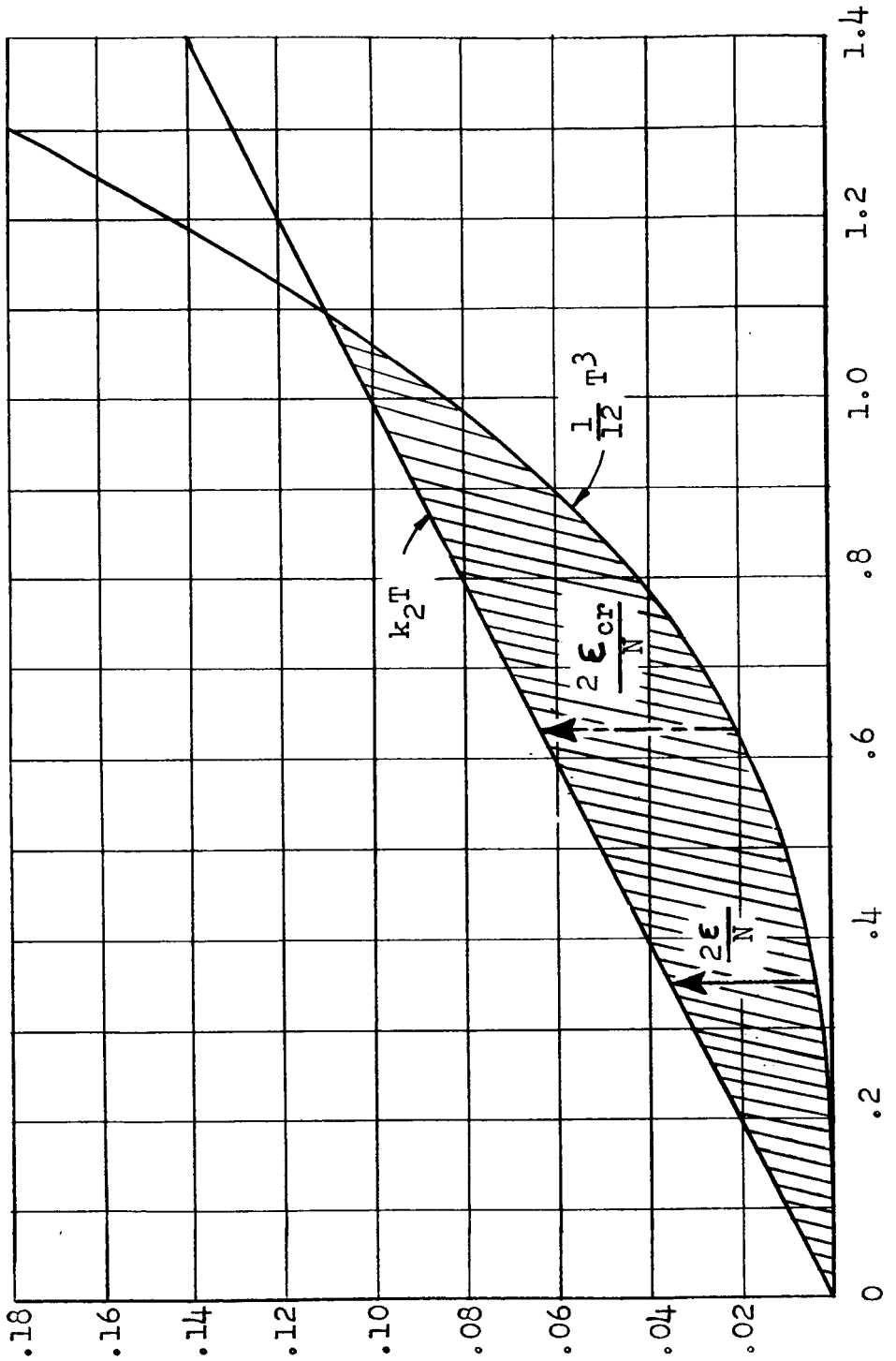

Figure 15.- Plot of terms on left-hand side of equation (54).

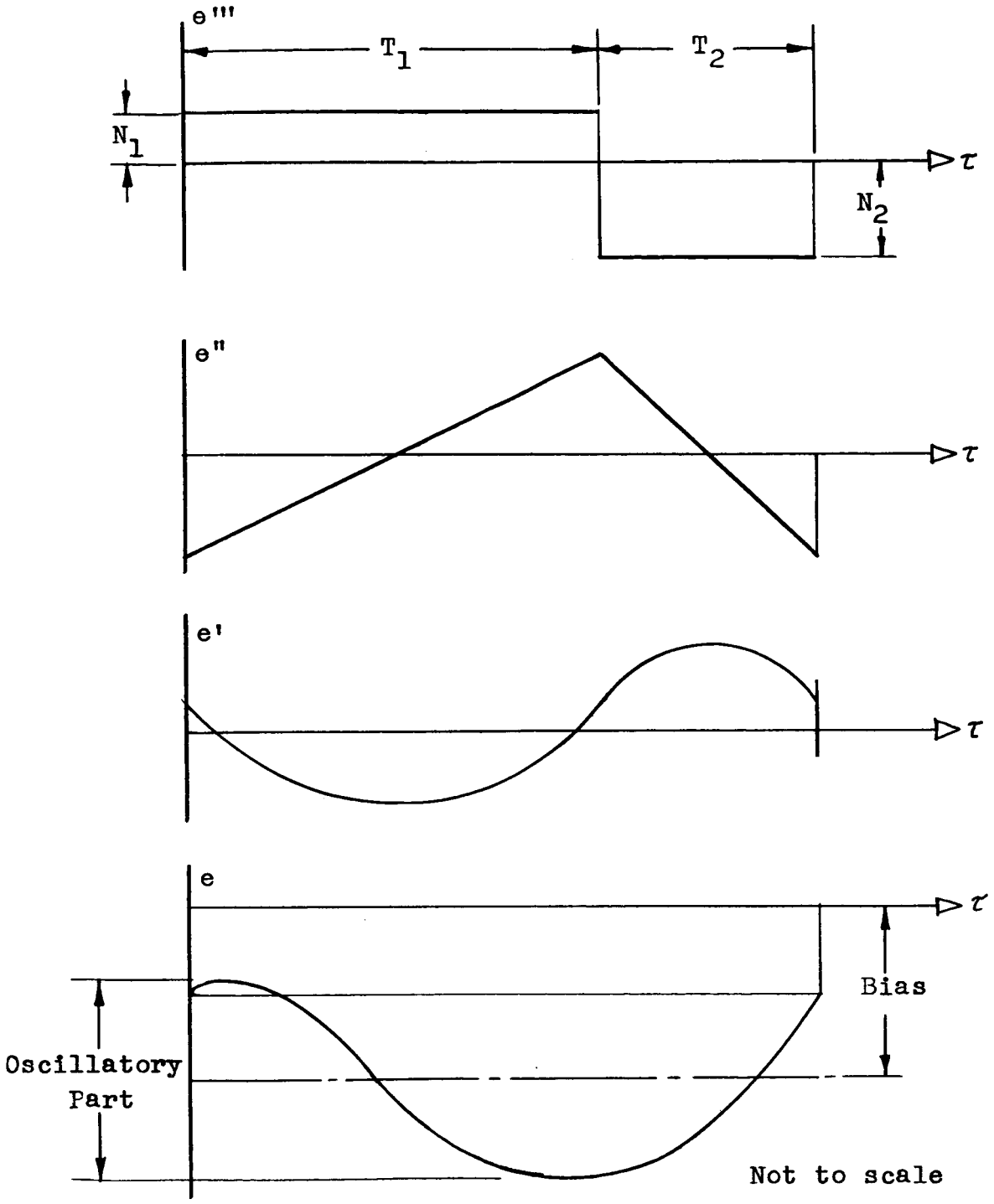

Figure 16.- Sketch of one cycle of chatter error for a third-order system.

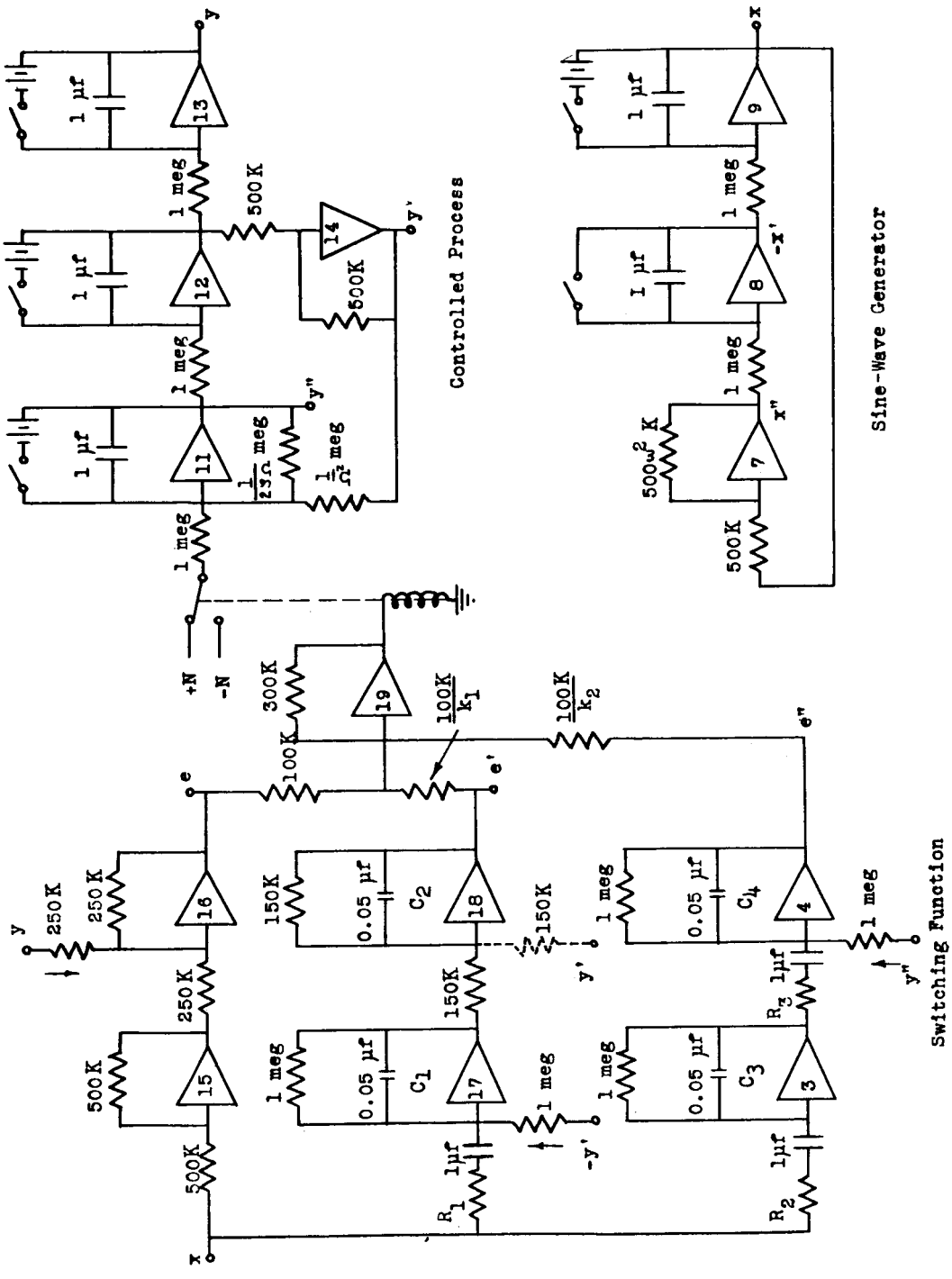

Figure 17.- Computer circuit diagram for third-order systems of equations (47) and (88).

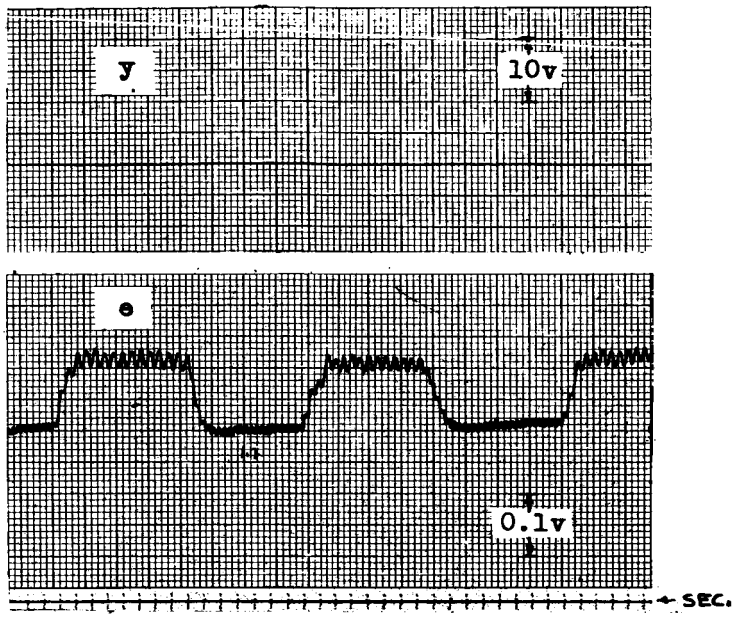

Figure 18.- Bias error for third-order system of equation (47) with $\Omega^2 = 2.79$, $\zeta = 0.6$, $N_1 = 40$, $N_2 = 10$, $k_1 = 0.50$, $k_2 = 0.10$, and $T_R = 0.055$.

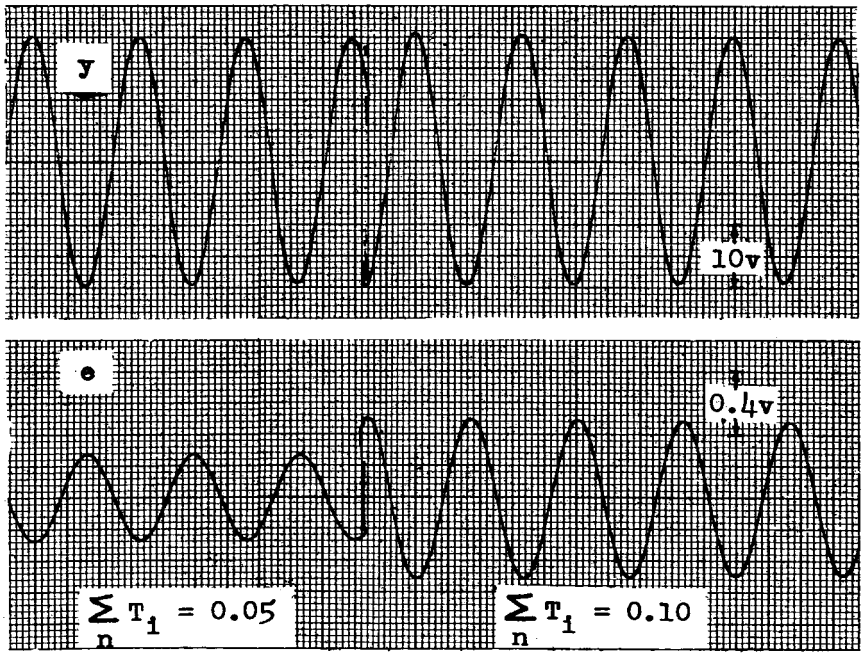

Figure 19.- Response of second-order system $y'' + y' = 40\ \mathrm{sgn}(e + 0.24e')$ to input $x = 20 \sin \tau$.

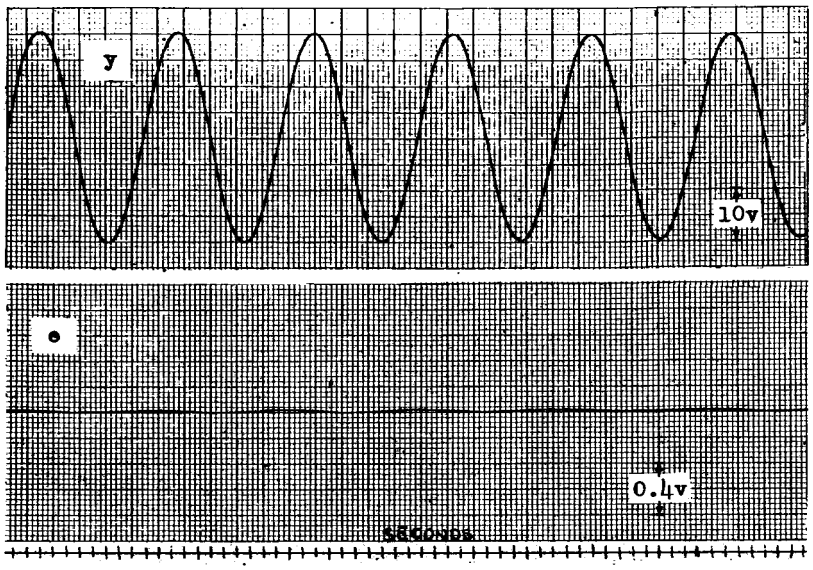

(a) No filtering on x' or x".

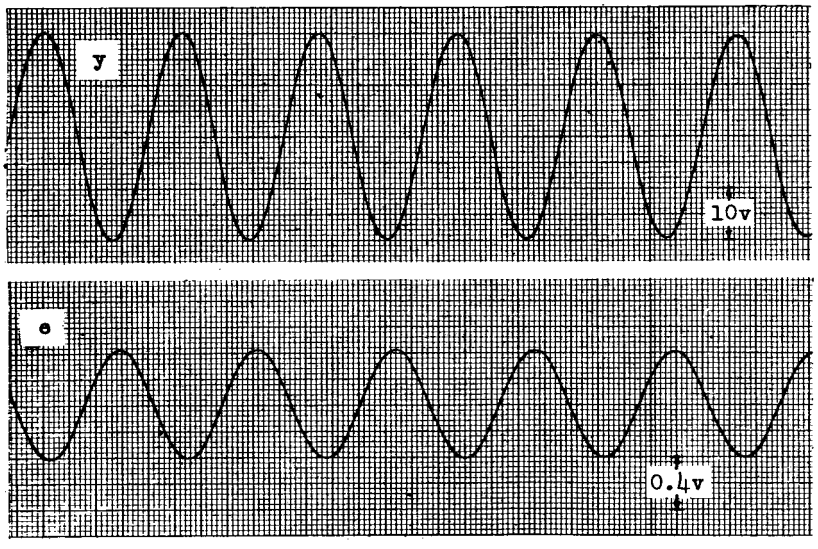

(b) $\sum_{n} T_{1i} = 0.10.$

Figure 20.- Response of third-order system of table V(a) to $x = 20 \sin 0.63\tau$.

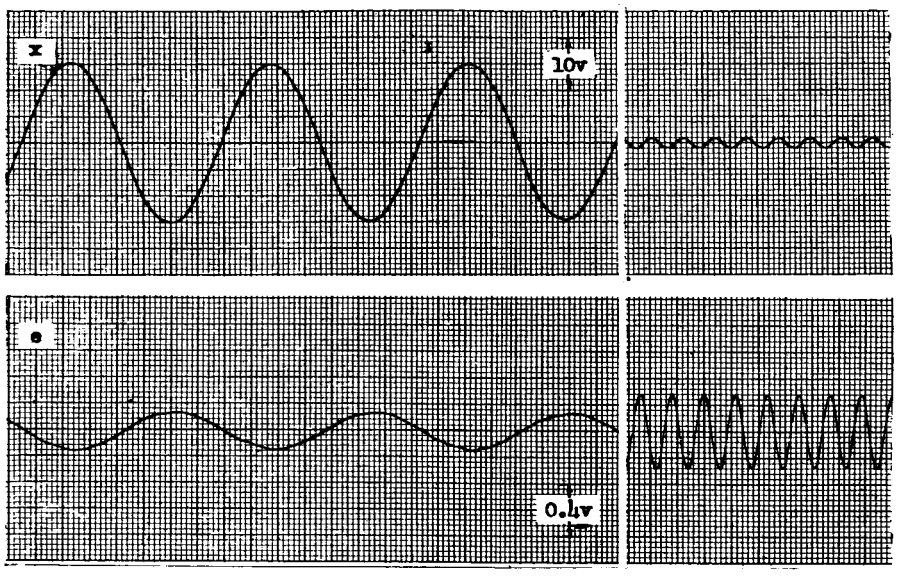

(a) $x = 15.0 \cos(0.446\tau)$. (b) $x = 1.00 \cos(2.83\tau)$.

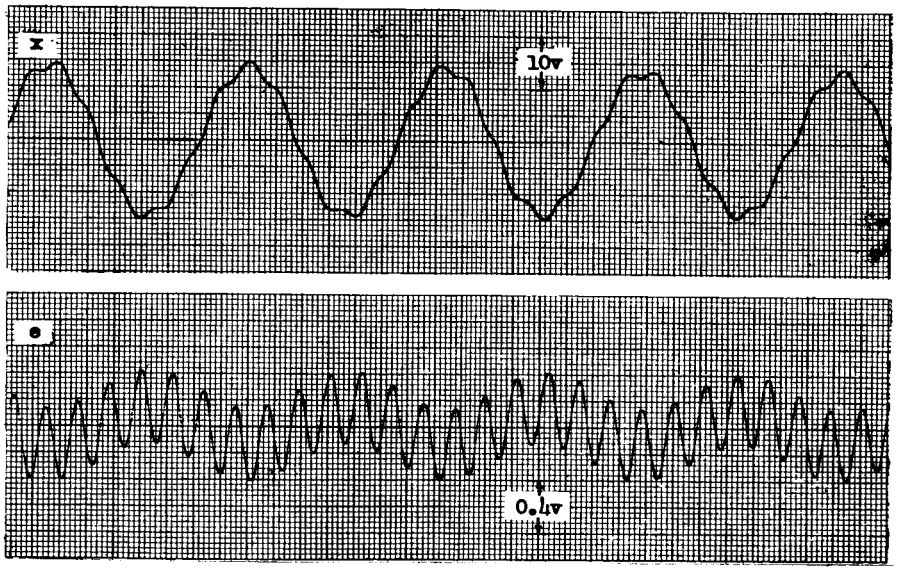

(c) $x = 15.0 \cos(0.446\tau) + 1.00 \cos(2.83\tau)$.

Figure 21.- Response of third-order system of table V(a) with $k_1 = 0.10$ and $\sum_n T_{1i} = 0.10$ to sum of two sinusoids.

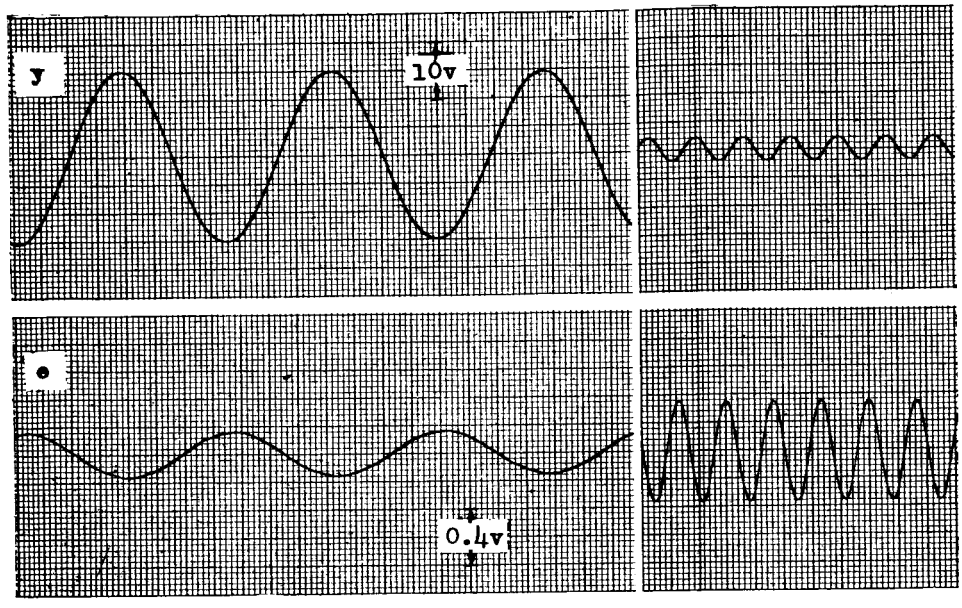

(d) $x = 15.0 \sin(0.446\tau)$.

(e) $x = 2.0 \sin(2\tau)$.

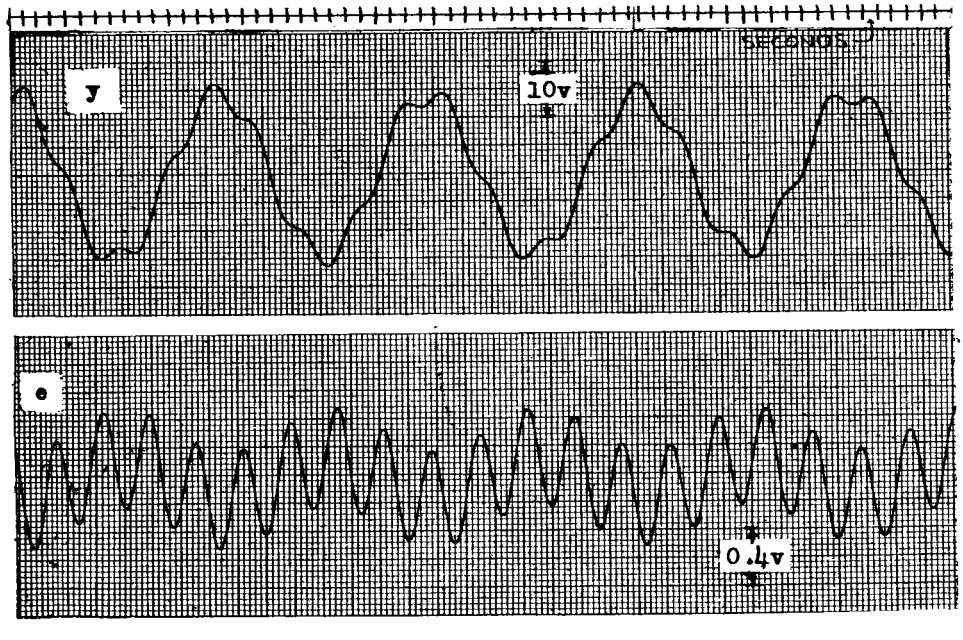

(f) $x = 15.0 \sin(0.446\tau) + 2.0 \sin(2\tau)$.

Figure 21.- Concluded.

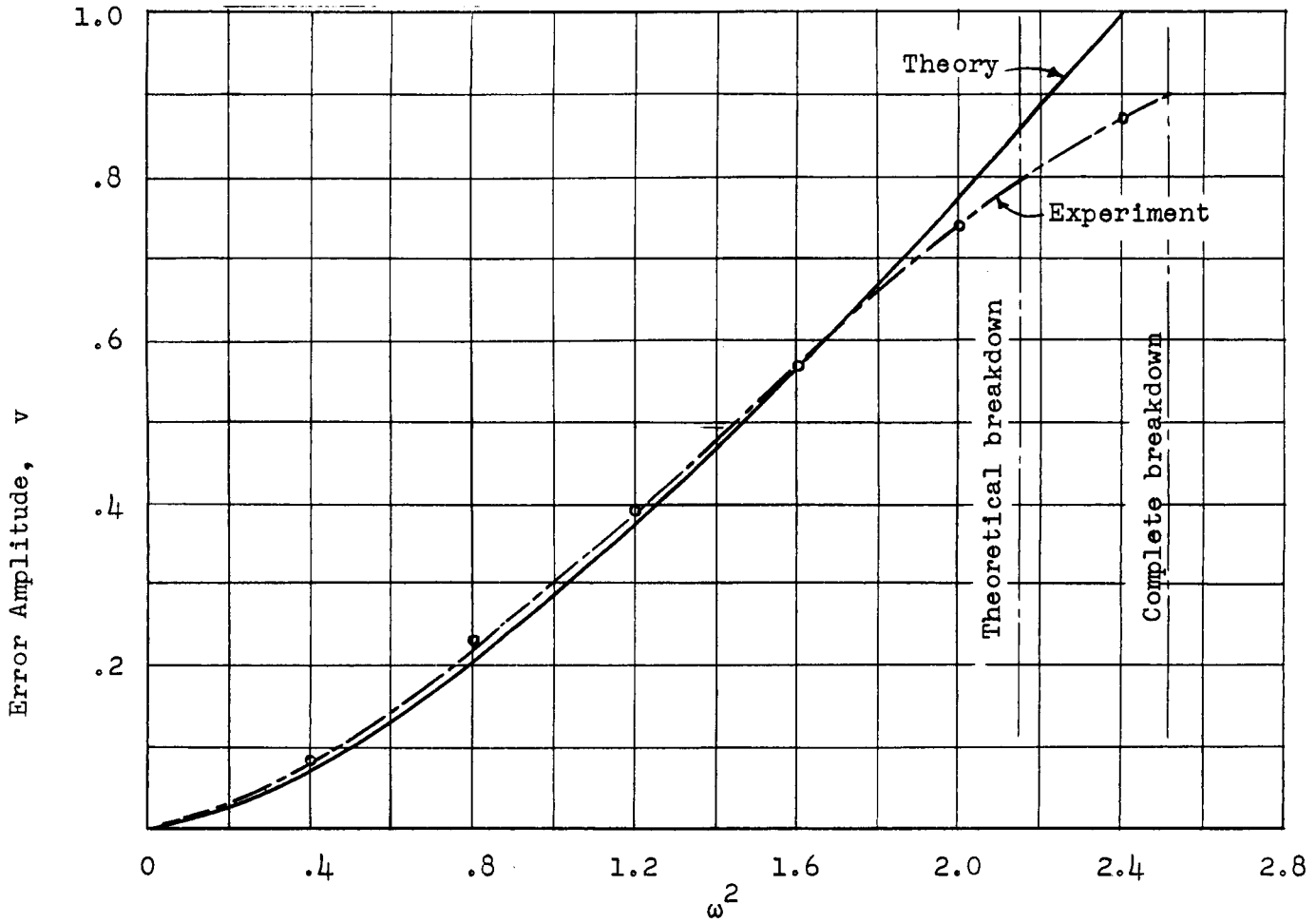

Figure 22.- Theoretical and experimental error of third-order system of equation (47) near breakdown frequency. $x = A \sin \omega\tau$; $\sum_n T_{1i} = 0$; $\sum_m T_{2i} = 0.15$; $\Omega^2 = 2.79$; $\zeta = 0.3$; $N = 47$; $k_1 = 0.527$; $k_2 = 0.10$; $A = 20$.

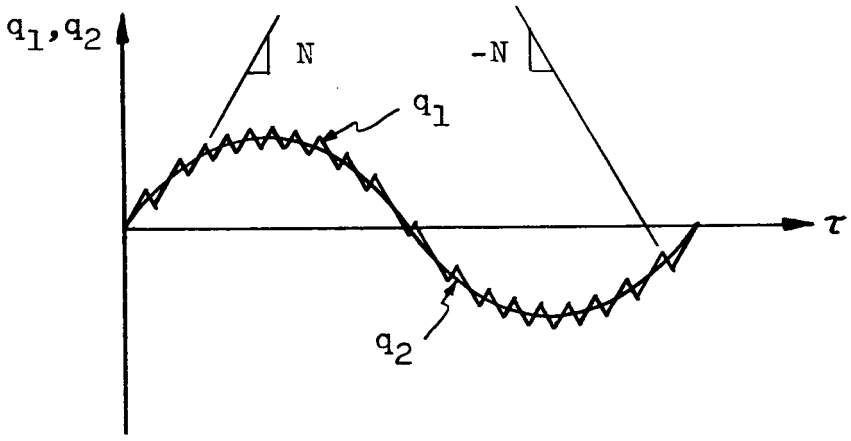

Figure 23.- Comparison curves for breakdown study.

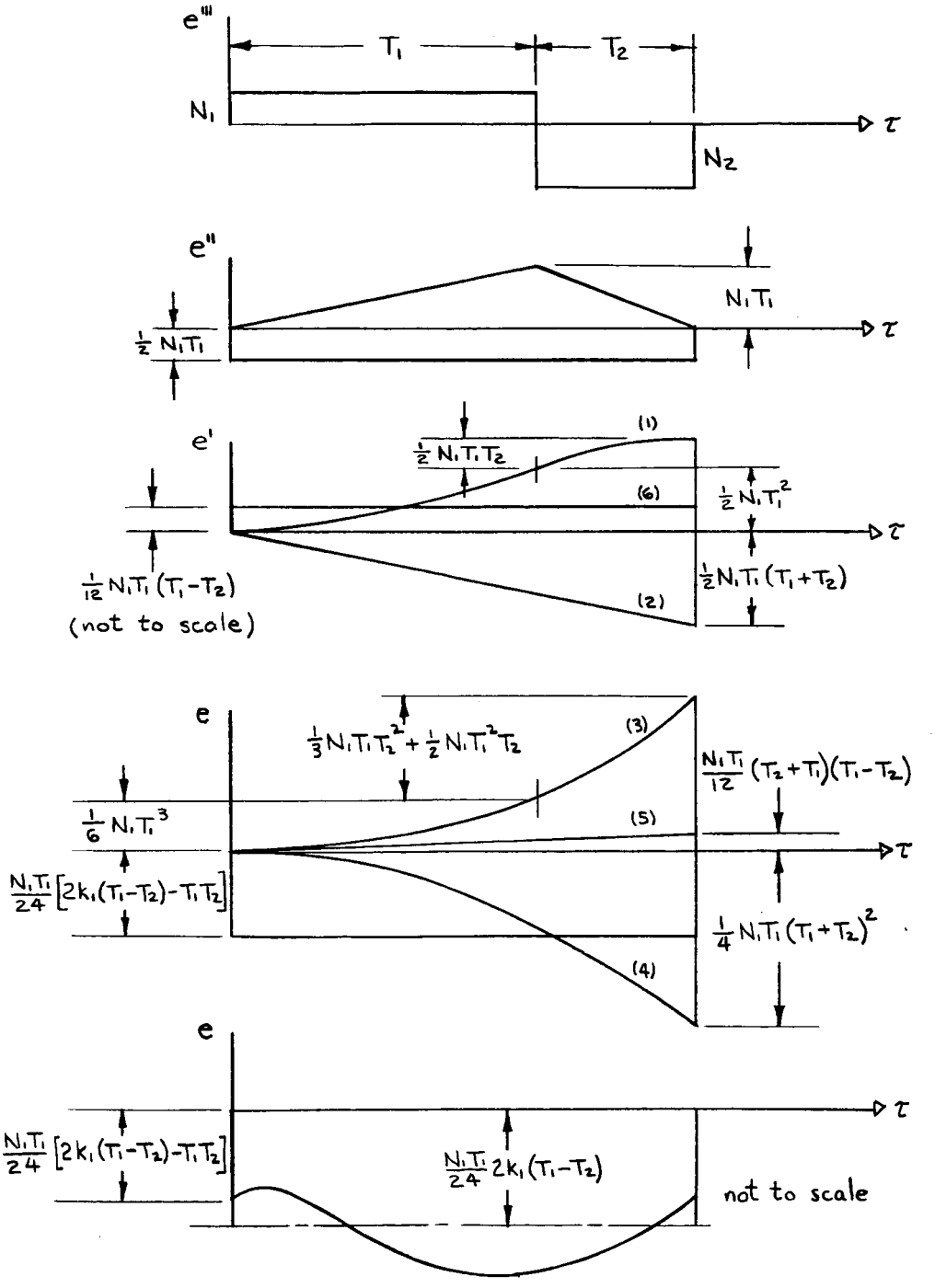

Figure 24.- Graphical construction of chatter error due to relay imperfection for third-order system. For explanation of numbers in parentheses see text.

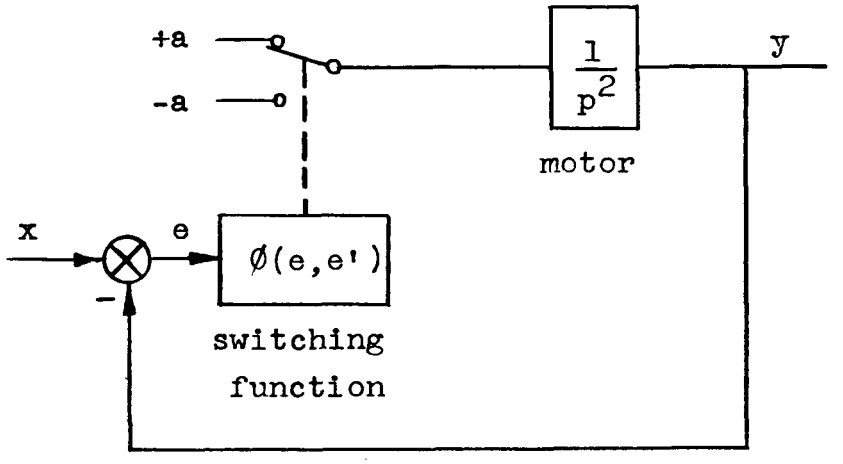

Figure 25.- Simple second-order example of optimum switching.

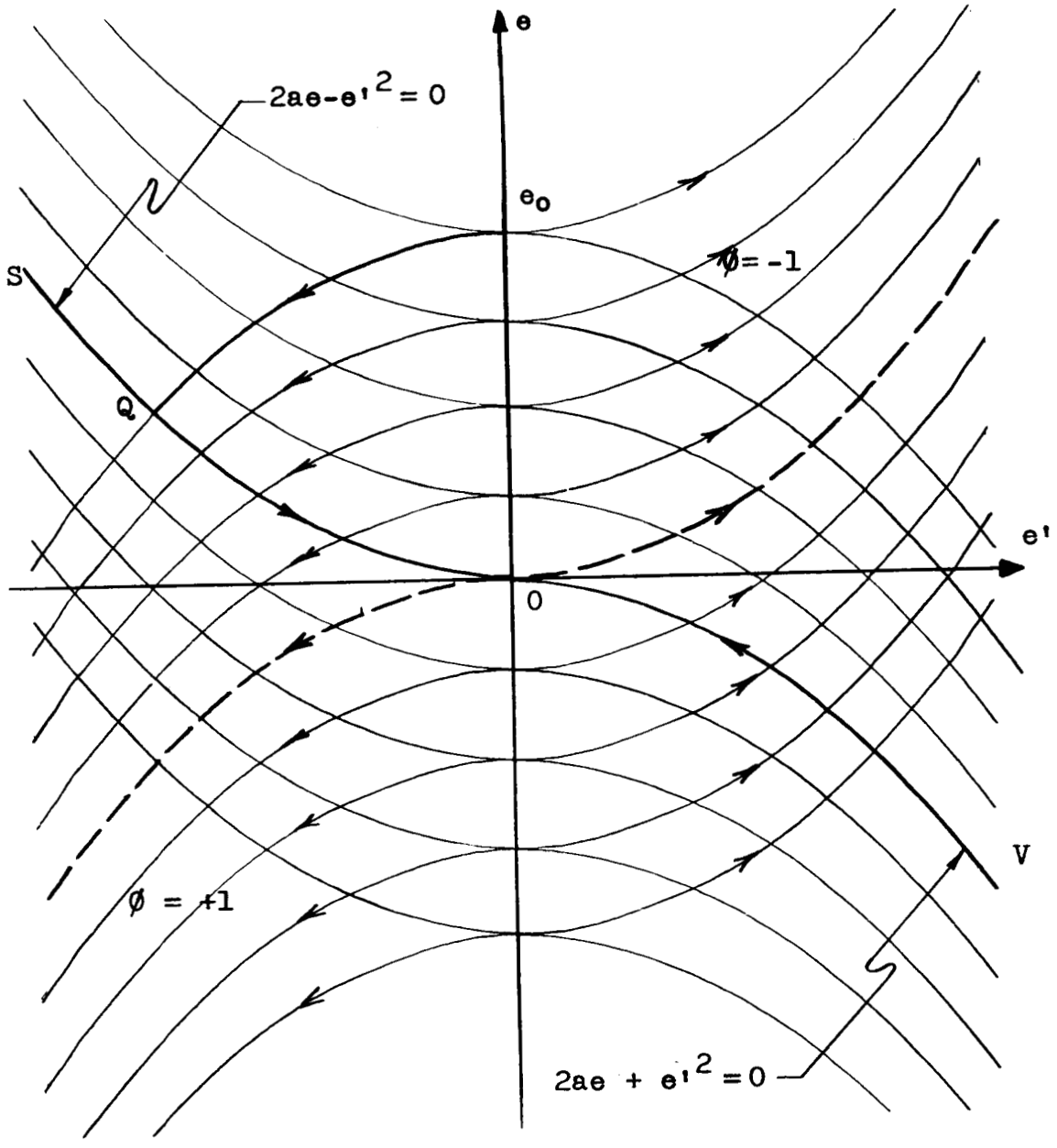

Figure 26.- Optimum switching for simple second-order system of figure 25.

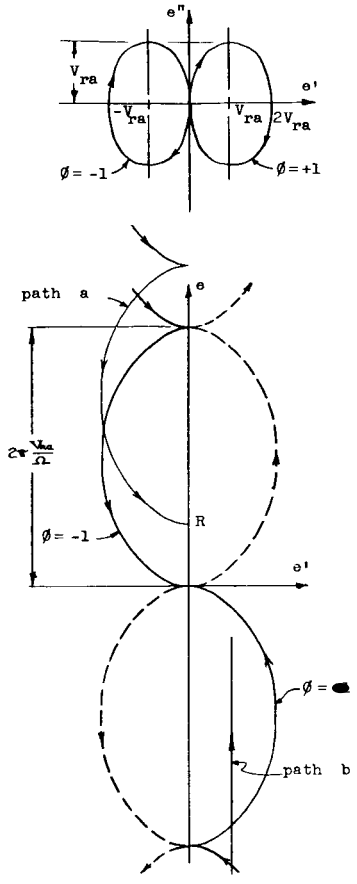

Figure 27.- Zero trajectory for third-order system of equation (130).

Equations of zero trajectory:

$$\left(\frac{e''}{\Omega}\right)^2 = V_{ra}^2 \sin^2 \Omega\tau$$

$$\left(e' \mp V_{ra}\right)^2 = V_{ra}^2 \cos^2 \Omega\tau$$

$$\left(\frac{e''}{\Omega}\right)^2 + \left(e' \mp V_{ra}\right)^2 = V_{ra}^2$$

Compare equations of zero trajectory

$$e = \phi\left(V_{ra}\tau - \frac{V_{ra}}{\Omega} \sin \Omega\tau\right)$$

$$\frac{e'}{\Omega} = \phi\left(\frac{V_{ra}}{\Omega} - \frac{V_{ra}}{\Omega} \cos \Omega\tau\right)$$

with parametric equations of cycloid

$$y = v_o t - r \sin \frac{v_o t}{r}$$

$$x = r - r \cos \frac{v_o t}{r}$$

where $r \rightarrow \frac{V_{ra}}{\Omega}$ and $v_o \rightarrow V_{ra}$.

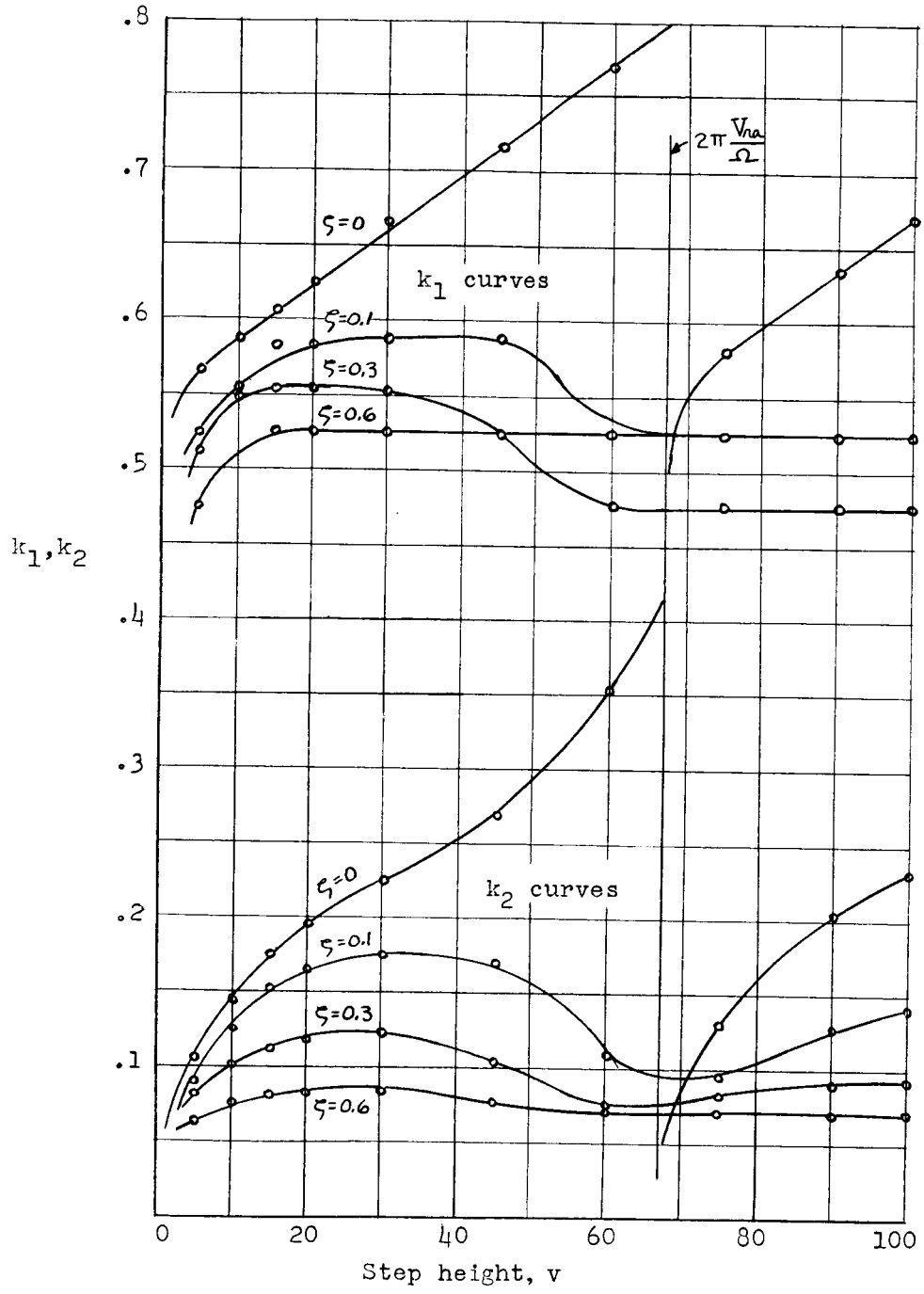

(a) $\Omega^2 = 2.79$; $\Omega^2 V_{ra} = 47.3$ volts.

Figure 28.- Linear switching-function coefficients of equation (47) that give optimum response to step inputs.

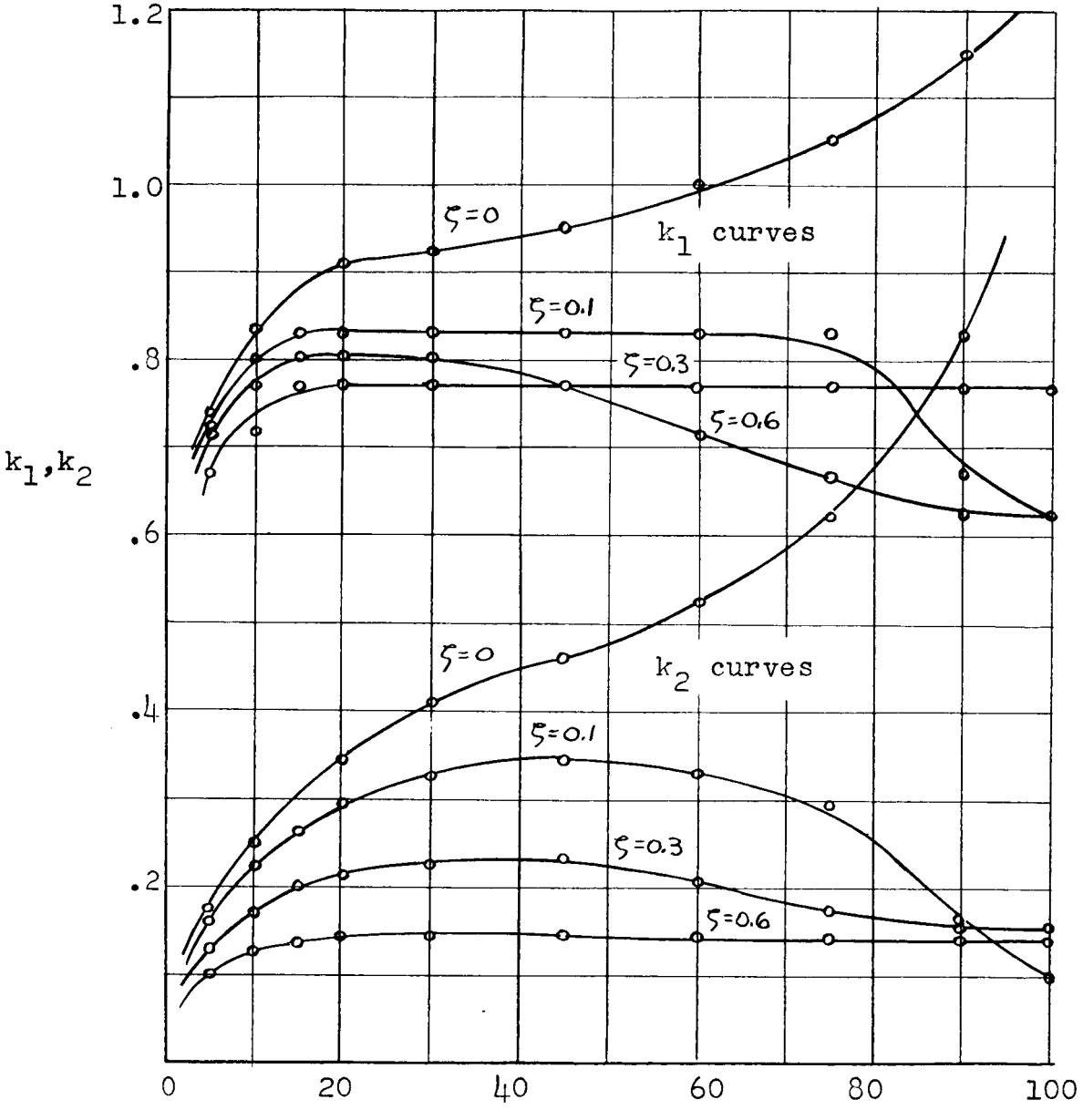

(b) $\Omega^2 = 1.35$; $\Omega^2 V_{ra} = 23.2$ volts.

Figure 28.- Concluded.

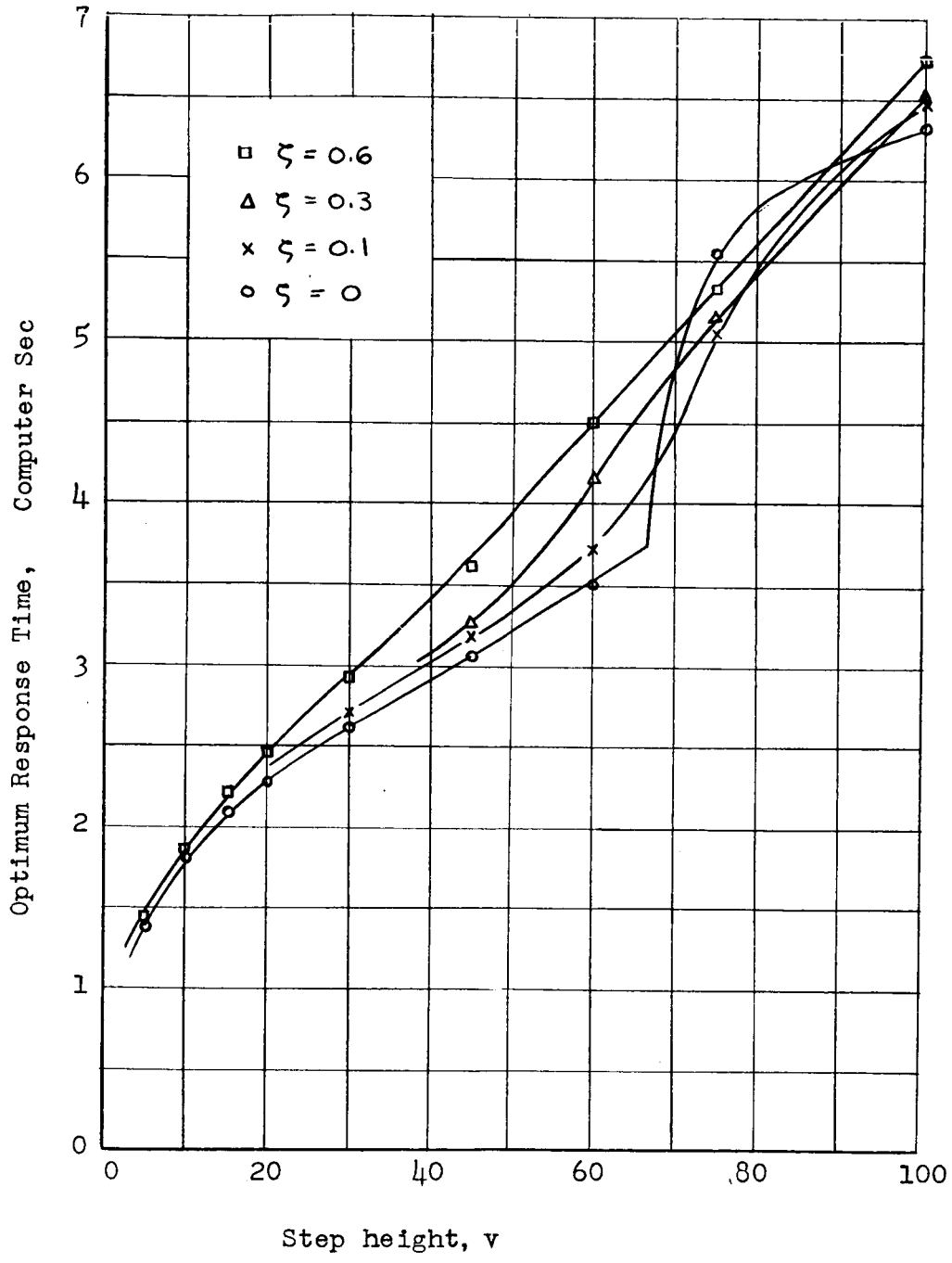

(a) $\Omega^2 = 2.79$; $\Omega^2 V_{ra} = 47.3$ volts.

Figure 29.- Optimum response times of equation (127) for step responses starting from rest.

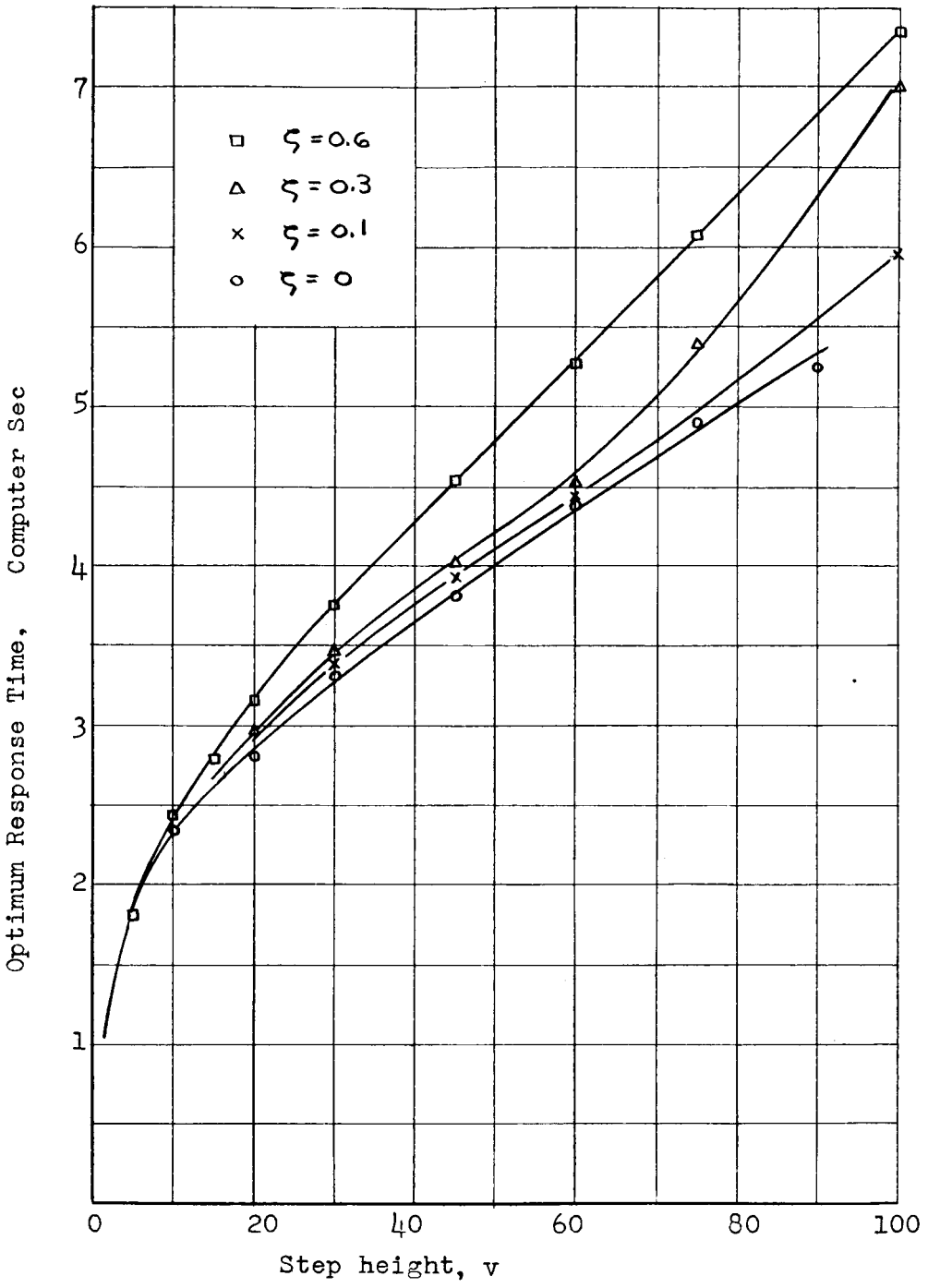

(b) $\Omega^2 = 1.35$; $\Omega^2 V_{ra} = 23.2$ volts.

Figure 29.- Concluded.

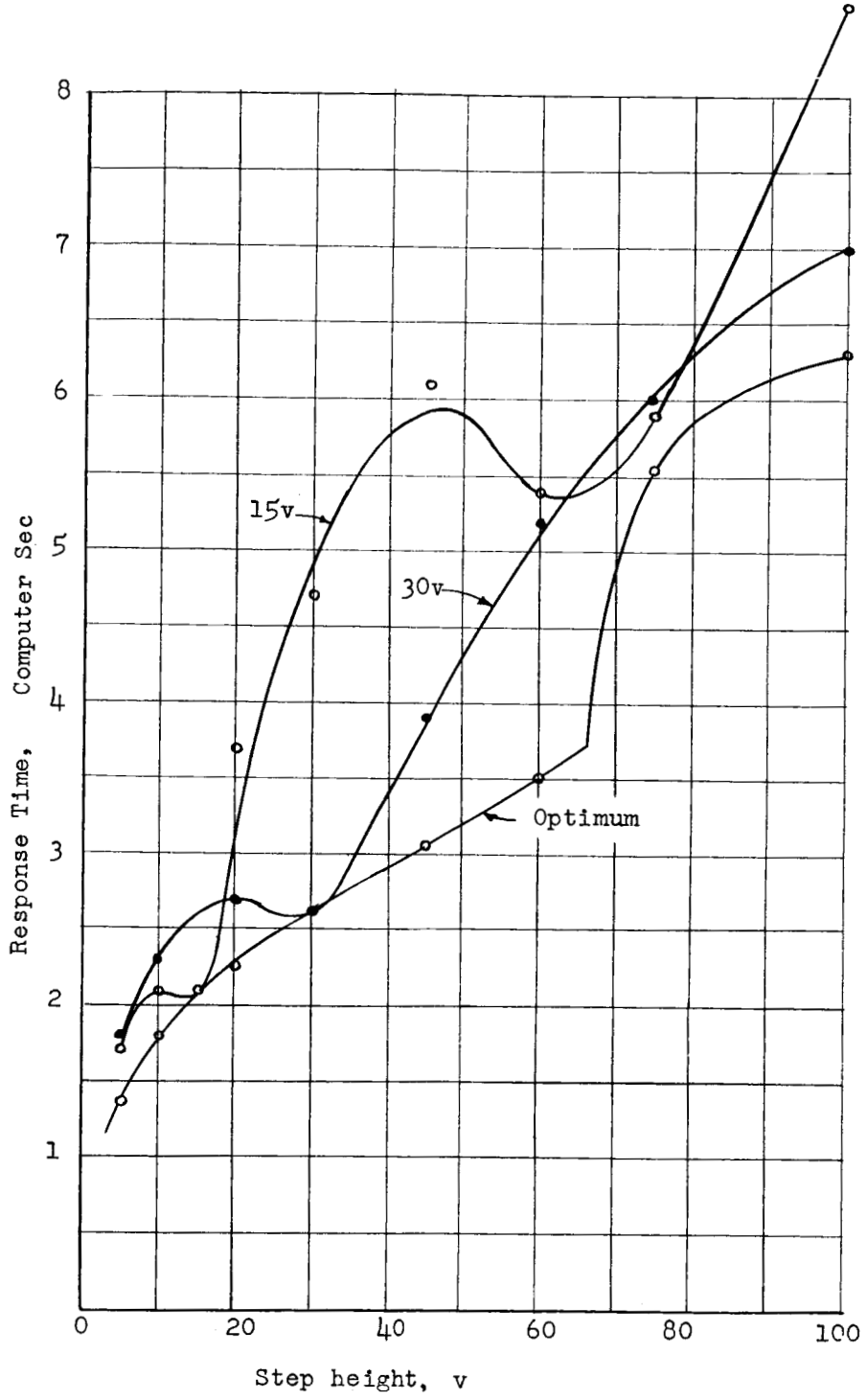

(a) $\zeta = 0$; $\Omega^2 = 2.79$; $\Omega^2 V_{ra} = 47.3$ volts.

Figure 30.- Comparison of optimum and linear switching response times for equation (127).

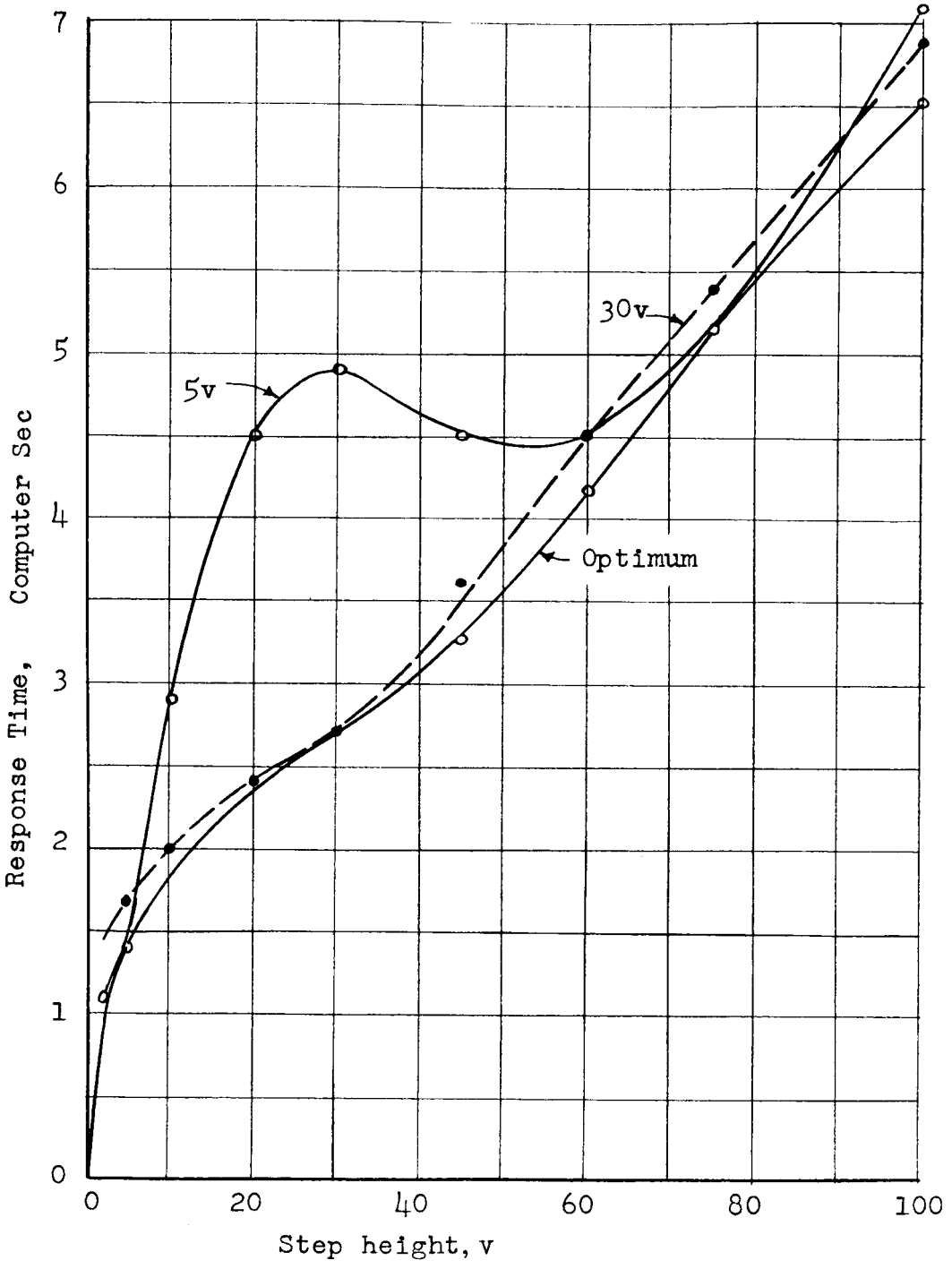

(b) $\zeta = 0.3$; $\Omega^2 = 2.79$; $\Omega^2 V_{ra} = 47.3$ volts.

Figure 30.- Concluded.

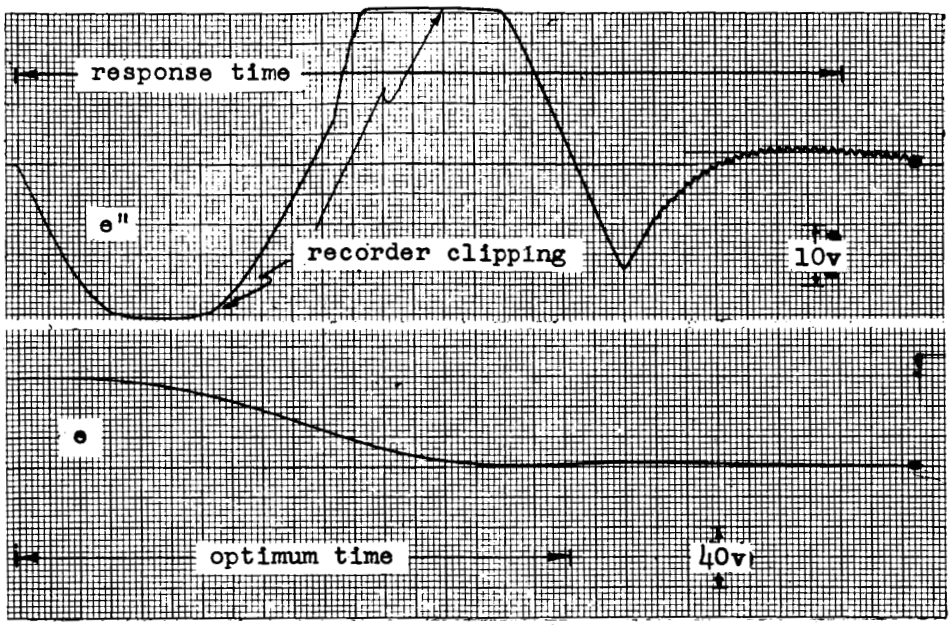

(a) Response to 60-volt step.

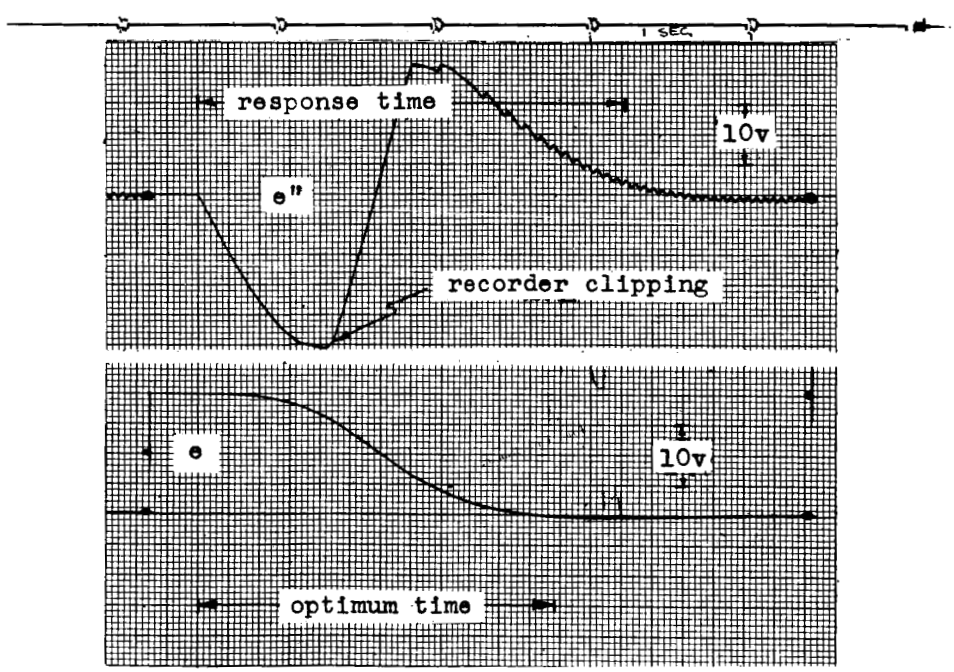

(b) Response to 20-volt step.

Figure 31.- Response to step inputs of a system described by equation (47) with $\zeta = 0$ and k_1 and k_2 optimized for a 30-volt step.

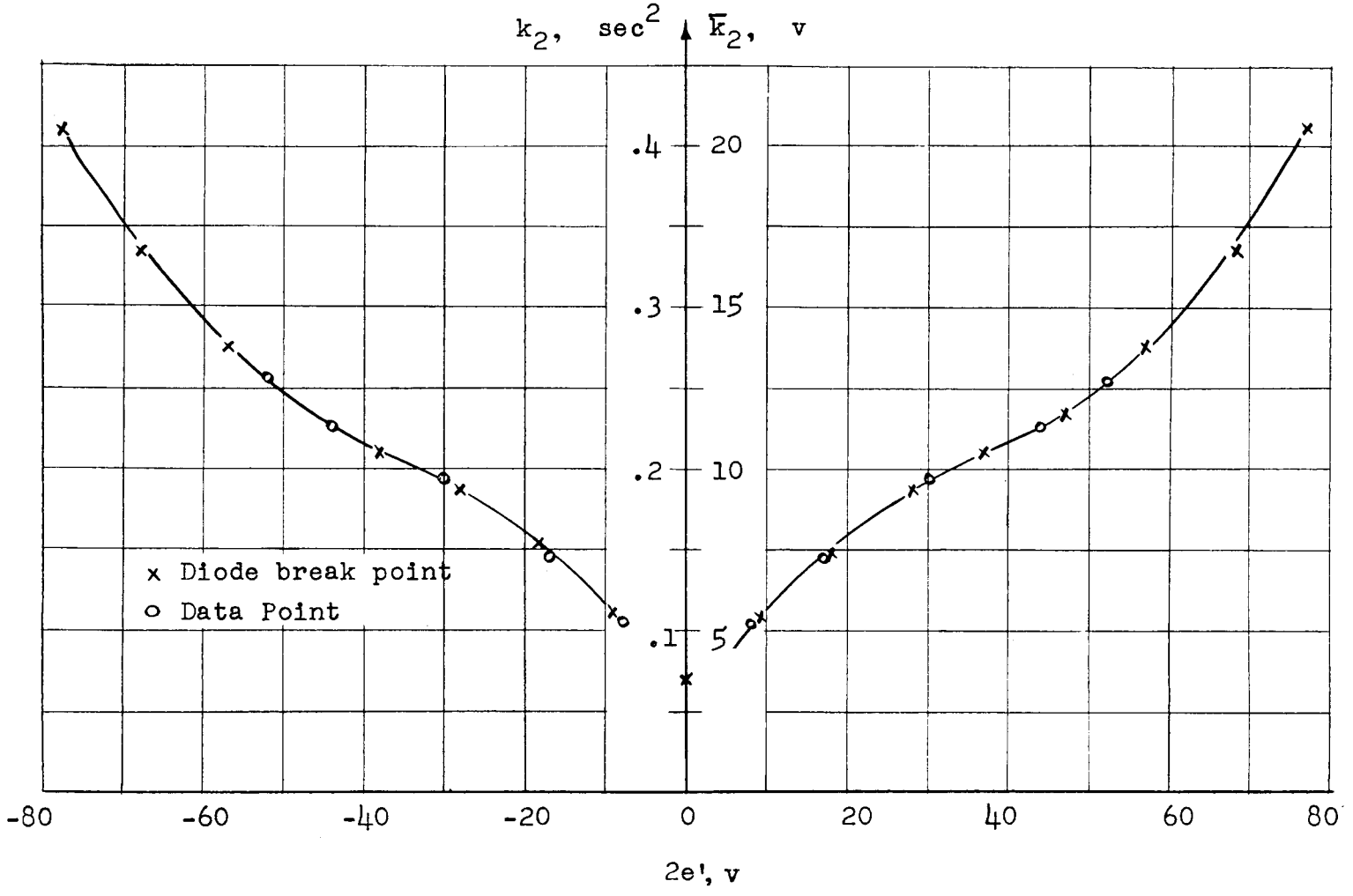

Figure 32.- Switching coefficient k_2 as a function of e' to give optimum response. $\Omega^2 = 2.79$; $\Omega^2 V_{ra} = 47.3$ volts.

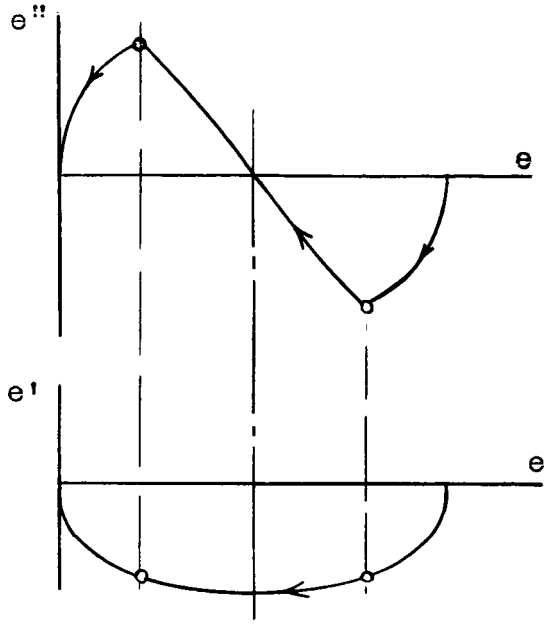

Figure 33.- Sketch of two views of optimum step-response trajectory for equation (130).

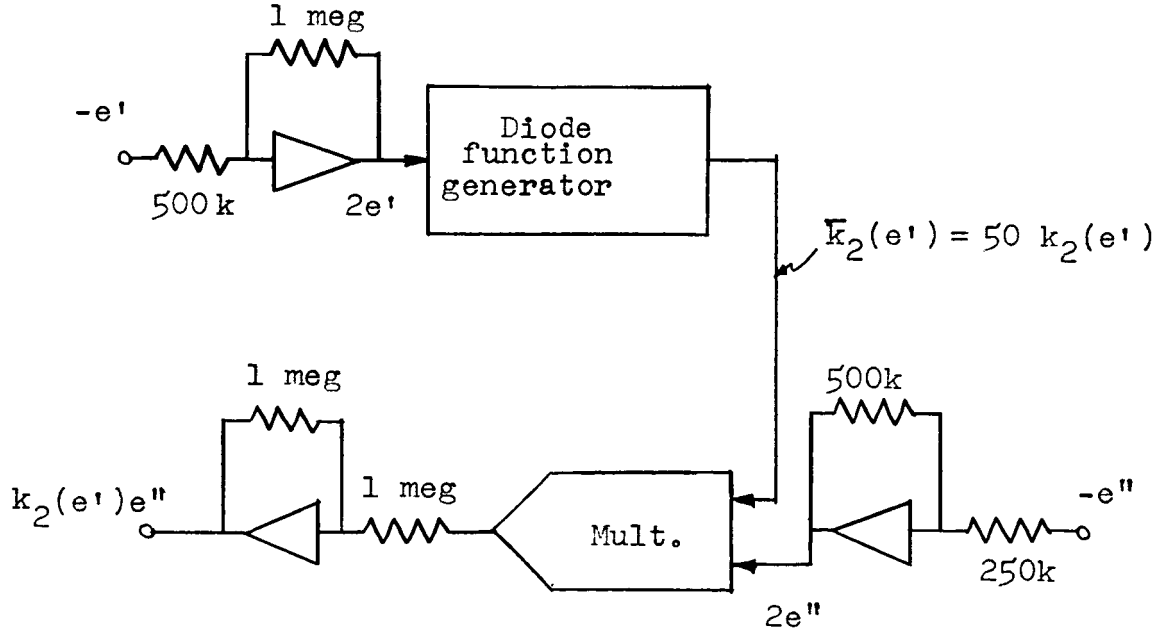

Figure 34.- Schematic diagram of circuit which forms $k_2(e')$ to give quasi-optimum response.

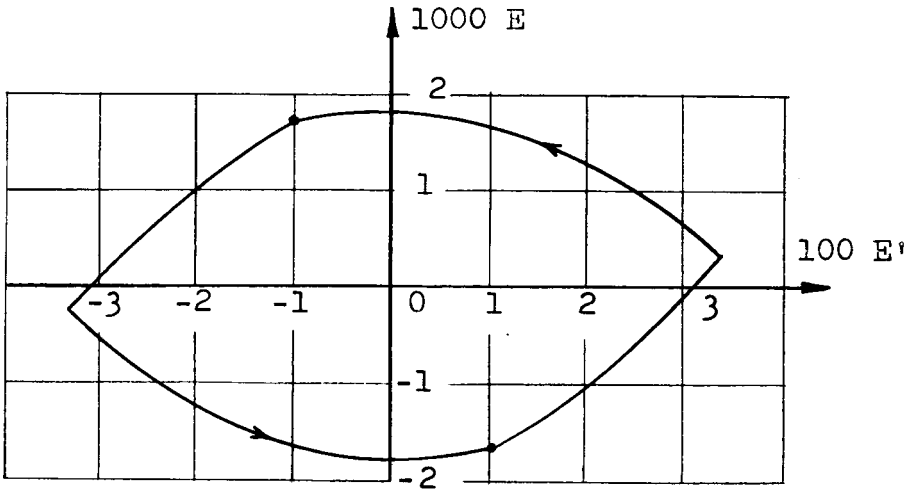

Figure 35.- Chatter error limit cycle for equation (A1) with $T_R = 0.01$.

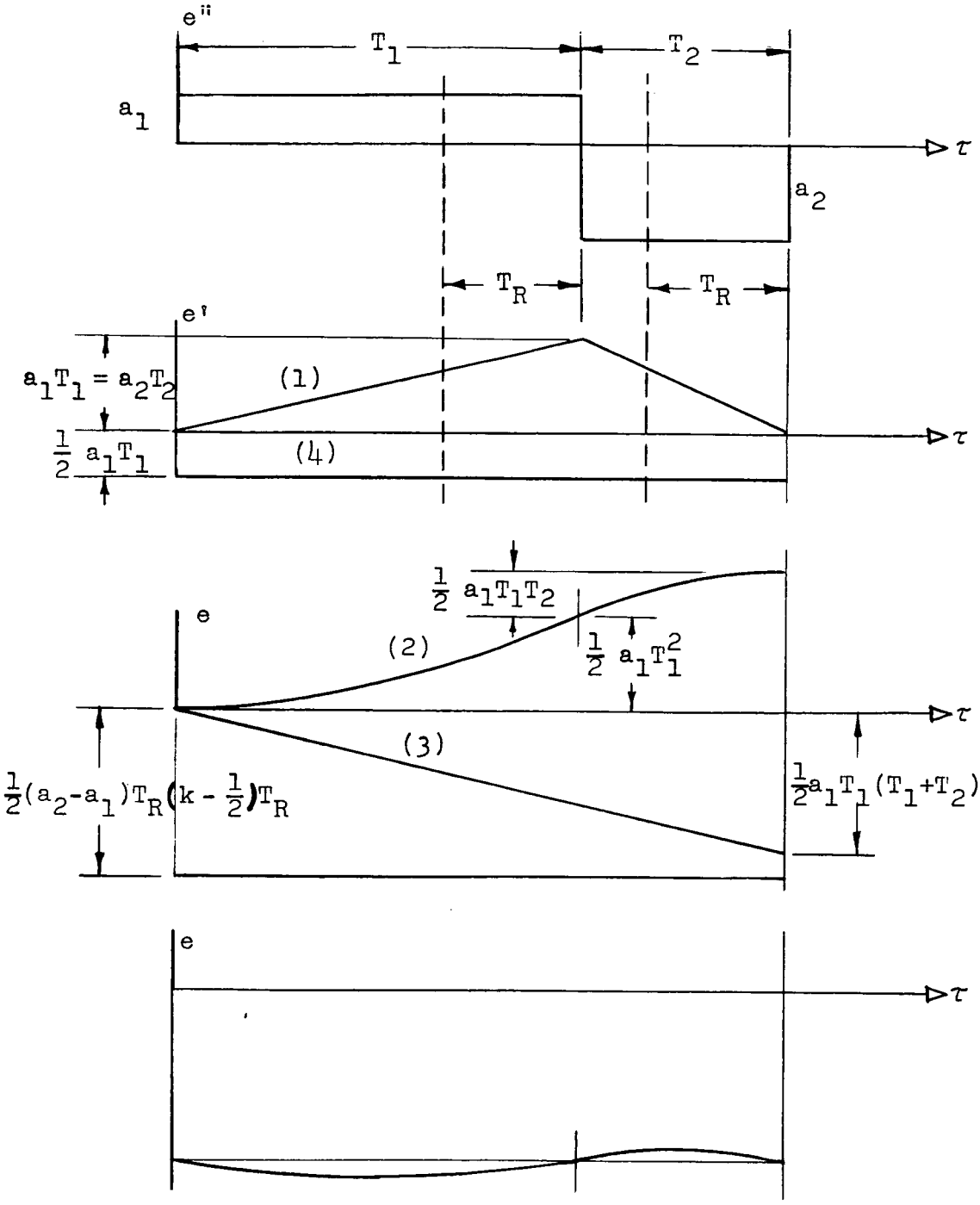

Figure 36.- Graphical construction of chatter error due to time delays for second-order systems. For explanation of numbers in parentheses see text.

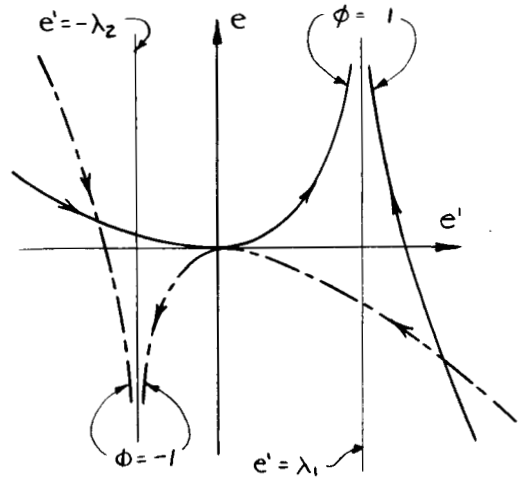

(a) Zero trajectories for $\phi = 1$ and -1 for $x'_0 > 0$.

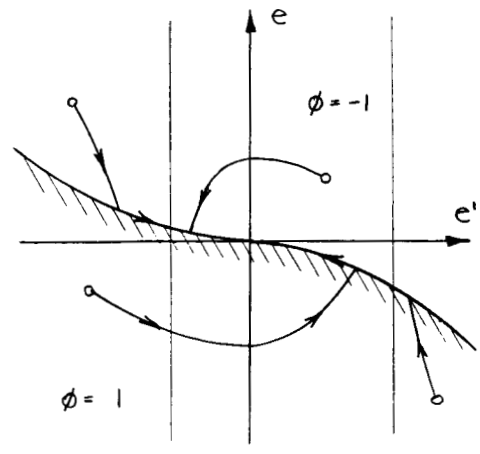

(b) Ingoing branches of unmodified zero trajectories of equations (D6) and (D8).

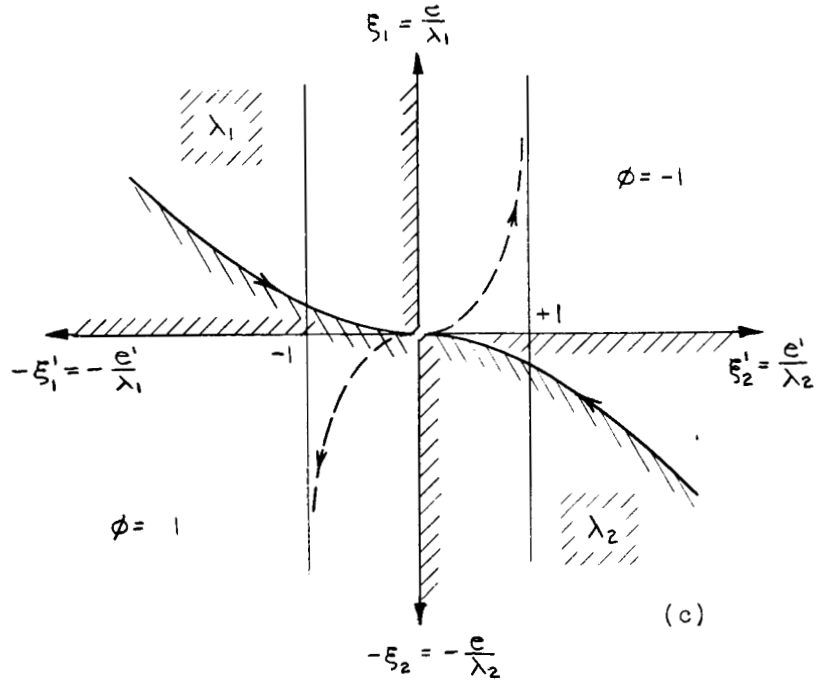

(c) Ingoing branches of modified zero trajectories of equations (D7) and (D9).

Figure 37.- Optimum switching lines for second-order system with damping.